ISSN 2303-4521

Periodicals of

Engineering and Natural Sciences

VOL. 4 NO. 1
(2016)

Published by International University of Sarajevo

Periodicals of Engineering and Natural Sciences (PEN)

Periodicals of Engineering and Natural Sciences (ISSN: 2303-4521) is an international open access single-blind review journal published online.

Publication frequency: Semiyearly (1. January - June; 2. July - December).

Publication Fees: No fee required (no article submission charges or processing charges).

Digital Object Identifier DOI: 10.21533/pen

Editorial Office

Mailing Address

Hrasnicka cesta 15
71000 Sarajevo
Bosnia

Principal Contact

Benjamin Durakovic
Managing Editor
International University of Sarajevo
Hrasnicka cesta 15
71000 Sarajevo
Bosnia
Phone: +387 33 957 229
Email: pen@ius.edu.ba

Available online at:

http://pen.ius.edu.ba

Editorial Team

DOI: 10.21533/pen

Publication Frequency

Expected frequency of publication is twice per year:
1. January - June;
2. July - December.

Journal items can be published collectively, as part of an issue with its own Table of Contents. Alternatively, individual items can be published as soon as they are ready, by adding them to the "current" volume's Table of Contents.

Open Access Policy

This journal provides immediate open access to its content on the principle that making research freely available to the public supports a greater global exchange of knowledge.

Journal Ethics and Malpractice Statement

PEN Journal is committed to ensure and uphold standards of ethical behavior at all stages of the publication process, whereby such values also rely on editors, reviewers, contributors and authors who are expected to behave ethically. The standards are based on Committee on Publication Ethics' (COPE) code of conduct, and provide guidelines for best practices in order to meet these requirements. The following ethical guidelines are only intended to give a summary of our key expectations of editors, peer-reviewers, and authors but if you have any questions or concerns please also feel free to contact the Editor of the Journal.

1. Ethical Expectations

Editors' responsibilities

- To carry out their duties in a fair, objective and consistent manner, without discrimination on grounds of gender, sexual orientation, religious or political beliefs, ethnic or geographical origin of the authors.
- To take care that each article undergoes the proper peer-review process.
- To promote consistent ethical policies of PEN journal, and to ensure the confidentiality of the reviewing process.
- To uphold integrity in their work as editors of the journal, doing away with any personal interest, so that articles are considered and accepted solely on their academic merit and without commercial influence.
- To work with authors, reviewers, and the Editorial Board members to ensure the implementation of journals' ethics and publishing policies.
- To adopt and follow reasonable procedures in the event of complaints of an ethical or conflict nature, in accordance with the policies and procedures. To handle process of complaints and giving authors an opportunity to respond any complaints. All complaints should be investigated and the documentation associated with any such complaints should be retained.

Reviewers' responsibilities

- To act objectively, fairly and in a timely manner in reviewing submitted manuscript with the aim of improving its quality such as pointing out relevant published work, which is not cited, etc.
- To alert PEN in case of any competing interest that could affect the impartiality of their reviewing, or any potential conflict of interest that includes any relationship between reviewer and author, or any content that is substantially similar to that under review.
- To conduct themselves fairly and impartially.
- To keep the confidentiality of the review process and to not retain or copy the manuscript.

DOI: 10.21533/pen

Authors' responsibilities

- To ensure that their work submitted to the journal is original and authored by them and has not been previously published nor under consideration or accepted for publication elsewhere.
- To ensure that original ideas, data, findings and materials taken from other sources (including their own published writing) are properly documented and cited. Any content reproduced from other sources author should have permission.
- To ensure that their data is their won, true and not manipulated. Thus, authors are responsible to maintain accurate records and to provide access to their data associated with their manuscript.
- To ensure their work does not violate any rights of others, including privacy rights and intellectual property rights. In addition, authors should ensure that any studies involving human or animal subject are in accordance with local lows and requirements.
- To declare any real or apparent conflicting or competing interest at any stage during the publication process that could be considered or viewed as exerting an undue influence on his/her duties.
- To alert PEN in case if a significant error in their publication is identified and correct any errors prior or subsequent to publication of their work.
- To adhere to all research ethics guidelines of their discipline, and to ensure that authorship and/or co-authorship of the paper was accurately represented.

PEN responsibilities

- The journal and the publisher shall ensure that good practice is maintained to the standards outlined above.
- To deal with research misconduct allegations appropriately when it is occurred. The journal and the publisher shall undertake reasonable actions to identify and prevent the publication of papers where research misconduct has occurred.
- To maintain the editorial independence of journal editors.
- To support journal editors in ethical and academic matters.
- To ensure critical and objective assessment of all articles by reviewers and referees. To keep an accurate and transparent record, including publishing corrections and retractions when necessary.
- The following commonly recognized procedure for dealing with unethical behavior is adopted.

2. Procedures for Dealing With Unethical Behavior

Identification of unethical behavior

- Misconduct and unethical behavior may be identified and brought to the attention of the editor and publisher at any time, by anyone.
- Misconduct and unethical behavior may include, but need not be limited to, examples as outlined above.
- For an investigation sufficient information and evidence should be provided. All allegations should be taken seriously and treated in the same way, until a successful decision or conclusion is reached.

Investigation

- An initial decision should be taken by the editor, who should consult with or seek advice from the publisher, if appropriate.
- Evidence should be gathered, while avoiding spreading any allegations beyond those who need to know.

Minor breaches

- Minor misconduct might be dealt with without the need to consult more widely. In any event, the author should be given the opportunity to respond to any allegations.

DOI: 10.21533/pen

Serious breaches

- Serious misconduct might require that the employers of the accused be notified. The editor, in consultation with the publisher should make the decision whether or not to involve the employers, either by examining the available evidence themselves or by further consultation with a limited number of experts.

Outcomes (in increasing order of severity; may be applied separately or in conjunction)

- Informing or educating the author or reviewer where there appears to be a misunderstanding or misapplication of acceptable standards.
- A more strongly worded letter to the author or reviewer covering the misconduct and as a warning to future behavior.
- Publication of a formal notice detailing the misconduct.
- Publication of an editorial detailing the misconduct.
- A formal letter to the head of the author's or reviewer's department or funding agency.
- Formal retraction or withdrawal of a publication from the journal, in conjunction with informing the head of the author or reviewer's department, Abstracting & Indexing services and the readership of the publication.
- Imposition of a formal embargo on contributions from an individual for a defined period.
- Reporting the case and outcome to a professional organization or higher authority for further investigation and action.

Originality and Plagiarism Policy

Authors by submitting their manuscript to PEN declare that their work is original and authored by them, their work submitted to PEN has not been previously published, original ideas, data, findings and materials taken from other sources (including their own published writing) are properly documented and cited, their work does not violate any rights of others, including privacy rights and intellectual property rights, their data is their won, true and not manipulated. Plagiarism in whole or in part without proper citation is not tolerated by the Journal. Manuscripts submitted to the journal will be checked for originality using anti-plagiarism software.

DOI: 10.21533/pen

ISSN 2303-4521

PERIODICALS OF ENGINEERING AND NATURAL SCIENCES
Vol. 4 No. 1 (2016)
Available online at: http://pen.ius.edu.ba

Solid State Welding and Application in Aeronautical Industry

Enes Akca*, Ali Gursel

International University of Sarajevo Faculty of Engineering and Natural Sciences
Sarajevo, Bosnia and Herzegovina

enesakca@hotmail.com.tr, eakca@ius.edu.ba

Abstract

In this study solid state welding andapplication in aeronautic industryhave been researched. The solid state welding technicisused in the industrial production fields such as aircraft, nucleer, space industry, aeronautic industry, ect., actually solid state welding is a process by which similar and dissmilar metals can be bonded together. Hence a material can be created as not heavy but strong strength. Beside, advantages and disasvantages of solid state welding have been discussed. Also the diffusion welding and friction welding which belong to the solid state welding is obsevered in aeronautic industry.

Keywords: solid state welding, aeronautic industry,diffusion welding, dissimilar materials

1 Introduction

Welding is a metal joining process which produces coalescence of metals by heating them to suitable temperatures with or without the application of pressure or by the application of pressure alone, and with or without the use of filler material. Basically, welding is used for making permanent joints. It is used in the manufacture of automobile bodies, aircraft frames, railway wagons, machine frames, structural works, tanks, furniture, boilers, general repair work and ship building.

Advantages of Solid State Welding:

- Strong and tight joining,
- Cost effectiveness,
- Simplicity of welded structures design,
- Welding processes may be mechanized and automated.

Disadvantages of Solid State Welding:

- Internal stresses, distortions and changes of micro-structure in the weld region,
- Harmful effects: light, ultra violate radiation, fumes, high temperature,

Also there are many kinds of welding processes;

- Arc welding;
  - Carbon arc welding,
  - Shieled metal arc welding (SMAW),
  - Submerged arc welding (SAW),
  - Metal inert gas welding (MIG,GTAW),
  - Tungsten inert gas welding (TIG, GTAW),
  - Electroslag welding (ESW),
  - Plasma arc welding (PAW),
- Resistance Welding (RW);
  - Spot welding (RSW),
  - Flash Welding (FW),
  - Resistance butt welding (UW),
  - Seam welding (RSEW),

DOI: 10.21533/pen.v4i1.46

- Gas Welding (GW);
    - Oxyacetylene welding (OAW),
    - Oxyhydrogen welding (OHW),
    - Pressure gas welding (PGW),
- Solid state welding (SSW);
    - Forge welding (FOW),
    - Cold roll welding (CRW),
    - Friction welding (FRW),
    - Explosive welding (EXW),
    - Diffusion welding (DFW),
    - Ultrasonic welding,
- Thermit welding (TW),
- Electron beam welding (EBW),
- Laser welding (LW),

Solid-state welding describes a group of joining techniques which produces coalescence at temperatures below the melting point of the parent materials without the addition of third material. External pressure and relative movement may or may not be used to enhance the joining process.

This group of joining techniques includes e.g. friction (stir) welding, cold pressure welding,diffusion welding, explosion welding,electromagnetic pulse welding, , and ultrasonicwelding. In all of these joining methods, propercontrol of the process parameters (time, temperature, and pressure individually or in combination) results in the coalescence of the parent materials without melting or only negligible melting at the interface. Technically, solid-state welding methods are not welding processes in the traditional sense since the materials do not reach their melting point, but can be rather compared with the traditional forging techniques [1].

Solid-state welding offers specific advantages since the base metal do not (or only marginally) melt and re-solidify [1].The parent metals essentially retain their original properties; heat-affected zone problems - which generally develop when there is base metal melting - are significantly diminished. Also the formation of intermetallic phases at the interface which can be brittle and may yield corrosion concerns is largely eliminated or minimized. Furthermore, when dissimilar metals are joined, their thermal expansion and conductivity characteristics have much less influence on the resulting joint performance than with fusion welding processes.

Solid state welding in the aeronautics industry is experiencing exciting developments. The widespread application of computers and the improved knowledge and design of new materials are shaping the way welding is implemented and process and product are being designed.

This article focuses on the application of solid state welding in aeronautical industry, and on the trends in the industry that can be expected from progress at a fundamental level. It describes the following processes: friction welding and diffusion welding.

2 Solid State Welding (SSW)

Solid State Welding is a welding process, in which two work pieces are joined under a pressure providing an intimate contact between them and at a temperature essentially below the melting point of the parent material. Bonding of the materials is a result of diffusion of their interface atoms [2].

Advantages of Solid State Welding:

- Weld (bonding) is free from microstructure defects (pores, non-metallic inclusions, segregation of alloying elements),
- Mechanical properties of the weld are similar to those of the parent metals,
- No consumable materials (filler material, fluxes, shielding gases) are required,
- Dissimilar metals may be joined (steel - aluminum alloy steel - copper alloy).

Disadvantages of Solid State Welding:

- Thorough surface preparation is required (degreasing, oxides removal, brushing/sanding),
- Expensive equipment.

2.1 Forge Welding (FOW)

Forge Welding is a Solid State Welding process, in which the components are heated to about 1800°F (1000°C) and then forged (hammered). Prior to Forge Welding, the parts are scarfed in order to prevent entrapment of oxides in the joint. Forge Welding is used in general blacksmith shops and for manufacturing metal art pieces and welded tubes [2, 3].

Advantages of Forge Welding:

- Good quality weld may be obtained,
- Parts of intricate shape may be welded,
- No filler material is required.

Disadvantages of Forge Welding:

- Only low carbon steel may be welded,
- High level of the operators skill is required,
- Slow welding process,
- Weld may be contaminated by the coke used in heating furnace.

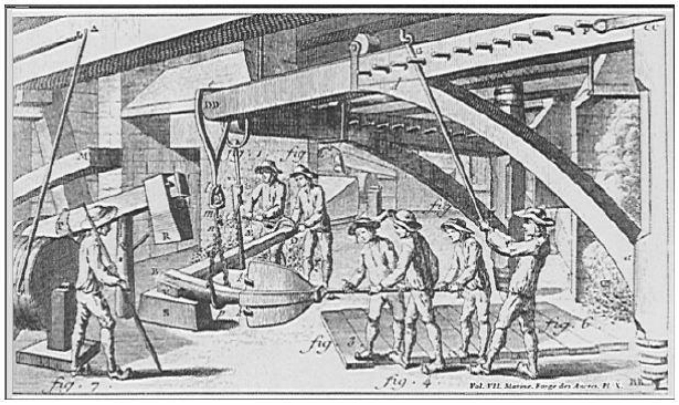

Figure 1: Woodcut showing a large ship's anchor being forged in 18th century France. The arm and the shaft of the anchor are being forge-welded together in this view.

2.2 Cold Roll Welding (CRW)

Cold Welding is a Solid State Welding process, in which two work pieces are joined together at room temperature and under a pressure, causing a substantial deformation of the welded parts and providing an intimate contact between the welded surfaces [3].

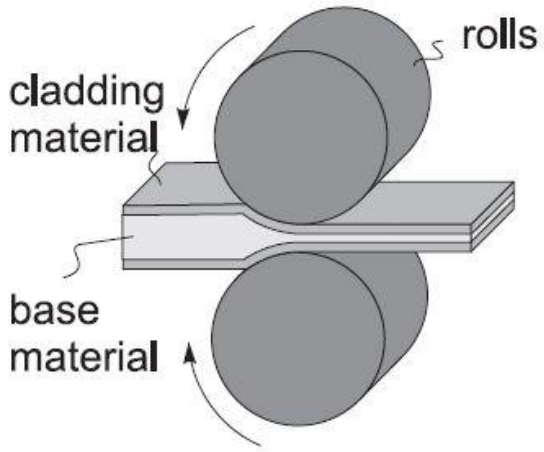

Figure 2: Cold welding (also cladding) process

As a result of the deformation, the oxide film covering the welded parts breaks up, and clean metal surfaces reveal. Intimate contact between these pure surfaces provides a strong and defectless bonding.Aluminum alloys, Copper alloys, low carbon steels, Nickel alloys, and other ductile metals may be welded by Cold Welding.

Cold Welding is widely used for manufacturing bi-metal steel - aluminum alloy strips, for cladding of aluminum alloy strips by other aluminum alloys or pure aluminum (Corrosion protection coatings). Bi-metal strips are produced by Rolling technology. Presses are also used for Cold Welding. Cold Welding may be easily automated [3, 4].

2.3 Diffusion Welding (DFW)

Diffusion Welding is a Solid State Welding process, in which pressure applied to two work pieces with carefully cleaned surfaces and at an elevated temperature below the melting point of the metals. Bonding of the materials is a result of mutual diffusion of their interface atoms [5, 6].

In order to keep the bonded surfaces clean from oxides and other air contaminations, the process is often conducted in vacuum. No appreciable deformation of the work pieces occurs in Diffusion Welding.Diffusion Welding is often referred more commonly as Solid State Welding (SSW). Diffusion Welding is able to bond dissimilar metals, which are difficult to weld by other welding processes:

- Steel to tungsten,
- Steel to niobium,
- Stainless steel to titanium,
- Gold to copper alloys.

Diffusion Welding is used in aerospace androcketry industries, electronics, nuclearapplications, manufacturing composite materials.

Advantages of Diffusion Welding:

- Dissimilar materials may be welded (Metals, Ceramics, Graphite, glass),
- Welds of high quality are obtained (no pores, inclusions, chemical segregation, distortions),
- No limitation in the work pieces thickness.

Disadvantages of Diffusion Welding:

- Time consuming process with low productivity,
- Very thorough surface preparation is required prior to welding process,
- The mating surfaces must be precisely fitted to each other,
- Relatively high initial investments in equipment.

2.4 Explosion Welding (EXW)

Explosive Welding is a Solid State Welding process, in which welded parts (plates) are metallurgically bonded as a result of oblique impact pressure exerted on them by a controlled detonation of an explosive charge.

One of the welded parts (base plate) is rested on an anvil, the second part (flyer plate) is located above the base plate with an angled or constant interface clearance.Explosive charge is placed on the flyer plate. Detonation starts at an edge of the plate and propagates at high velocity along the plate.The maximum detonation velocity is about 120% of the material sonic velocity.The slags (oxides, nitrides and other contaminants) are expelled by the jet created just ahead of the bonding front.Most of the commercial metals and alloys may be bonded (welded) by Explosive Welding.Dissimilar metals may be joined by Explosive Welding:

- Copper to steel,
- Nickel to steel,
- Aluminum to steel,
- Tungsten to steel,
- Titanium to steel,
- Copper to aluminum.

Advantages of Explosive Welding

- Large surfaces may be welded,
- High quality bonding: high strength, no distortions, no porosity, no change of the metal microstructure,
- Low cost and simple process,
- Surface preparation is not required.

Disadvantages of Explosive Welding:

- Brittle materials (low ductility and low impact toughness) cannot be processed,
- Only simple shape parts may be bonded: plates, cylinders,
- Thickness of flyer plate is limited - less than 2.5” (63 mm),
- Safety and security aspects of storage and using explosives.

Explosive Welding is used for manufacturing clad tubes and pipes, pressure vessels, aerospace structures, heat exchangers, bi-metal sliding bearings, ship structures, weld transitions, corrosion resistant chemical process tanks [5].

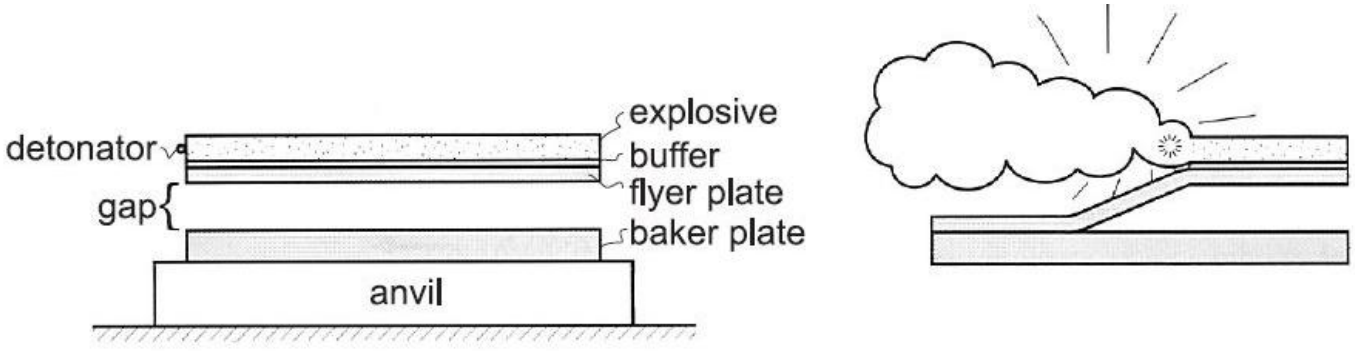

Figure 3: Explosive welding showing the initial setup and the process of explosive welding with the propagating shock wave.

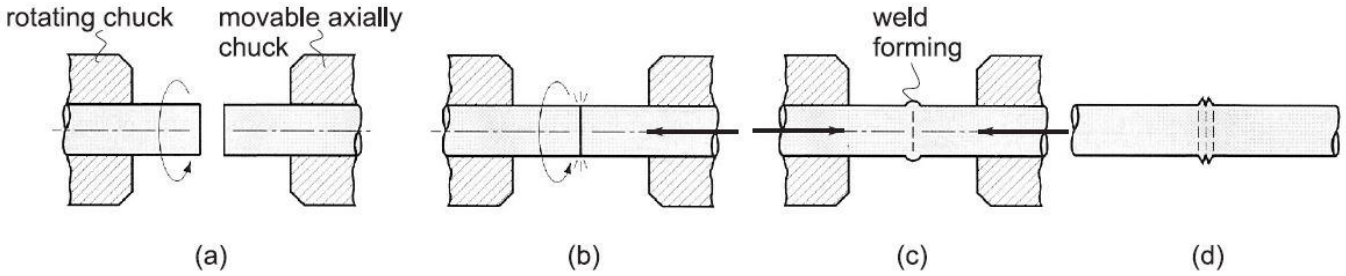

Figure 4: Friction welding: (a) no contact, (b) parts brought into contact to generate friction heat, (c) rotation stops and axial pressure applied, (d) final product showing the flash.

2.5 Friction Welding (FRW)

Friction welding is a solid-state welding process in which coalescence is achieved by frictional heat combined with pressure. The heat is generated by the friction between the two components surfaces, usually by rotation of one part relative to the other. Then the parts are driven toward each other with sufficient force to form a metallurgical bond. The sequence is portrayed in the figure for the typical application of this operation, welding of two cylindrical parts.

The axial compression force upsets the parts, and the material displaced produces a flash. The flash must be subsequently trimmed to provide a smooth surface in the weld region. No filler metal, flux, or shielding gases are required.

Machines used for friction welding have the appearance of an engine lathe. They require a powered spindle to turn one part at high speed and a means of applying an axial force between the rotating part and the non-rotating part.

With its short cycle times, the process is suitable for mass production. It is applied in the welding of various shafts and tubular parts of similar or dissimilar metals. One typical application of friction welding is to coalesce medium-carbon steel shanks to carbide tips in producing twist drills.

2.6 Ultrasonic Welding (USW)

Ultrasonic Welding is a Solid State Welding process, in which two work pieces are bonded as a result of a pressure exerted to the welded parts combined with application of high frequency acoustic vibration (ultrasonic).

Ultrasonic vibration causes friction between the parts, which results in a closer contact between the two surfaces with simultaneous local heating of the contact area. Interatomic bonds, formed under these conditions, provide strong joint.Ultrasonic cycle takes about 1 sec. The frequency of acoustic vibrations is in the range 20 to 70 KHz. Thickness of the welded parts is limited by the power of the ultrasonic generator.Ultrasonic Welding is used mainly for bonding small work pieces in electronics, for manufacturing communication devices, medical tools, watches, in automotive industry.

Advantages of Ultrasonic Welding:

- Dissimilar metals may be joined,
- Very low deformation of the work pieces surfaces,
- High quality weld is obtained,
- The process may be integrated into automated production lines,
- Moderate operator skill level is enough.

Disadvantages of Ultrasonic Welding:

- Only small and thin parts may be welded,
- Work pieces and equipment components may fatigue at the reciprocating loads provided by ultrasonic vibration,
- Work pieces may bond to the anvil.

3 Solid State Welding Processes for Aeronautics

The nature of welding in the aeronautical industry is characterized by low unit production, high unit cost, extreme reliability, and severe operating conditions [7]. These characteristics point towards the more expensive and more concentrated heat sources such as plasma arc, laser beam and electron beam welding as the processes of choice for welding of critical components. But mostly diffusion welding and friction welding techniques are used in the industry, and it has been growing permanently[8].

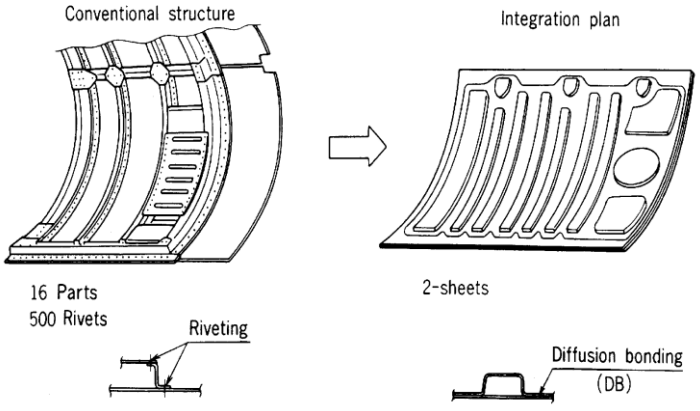

Figure 5: Conventional structure and integrated plan for door panel using SPF/DFW

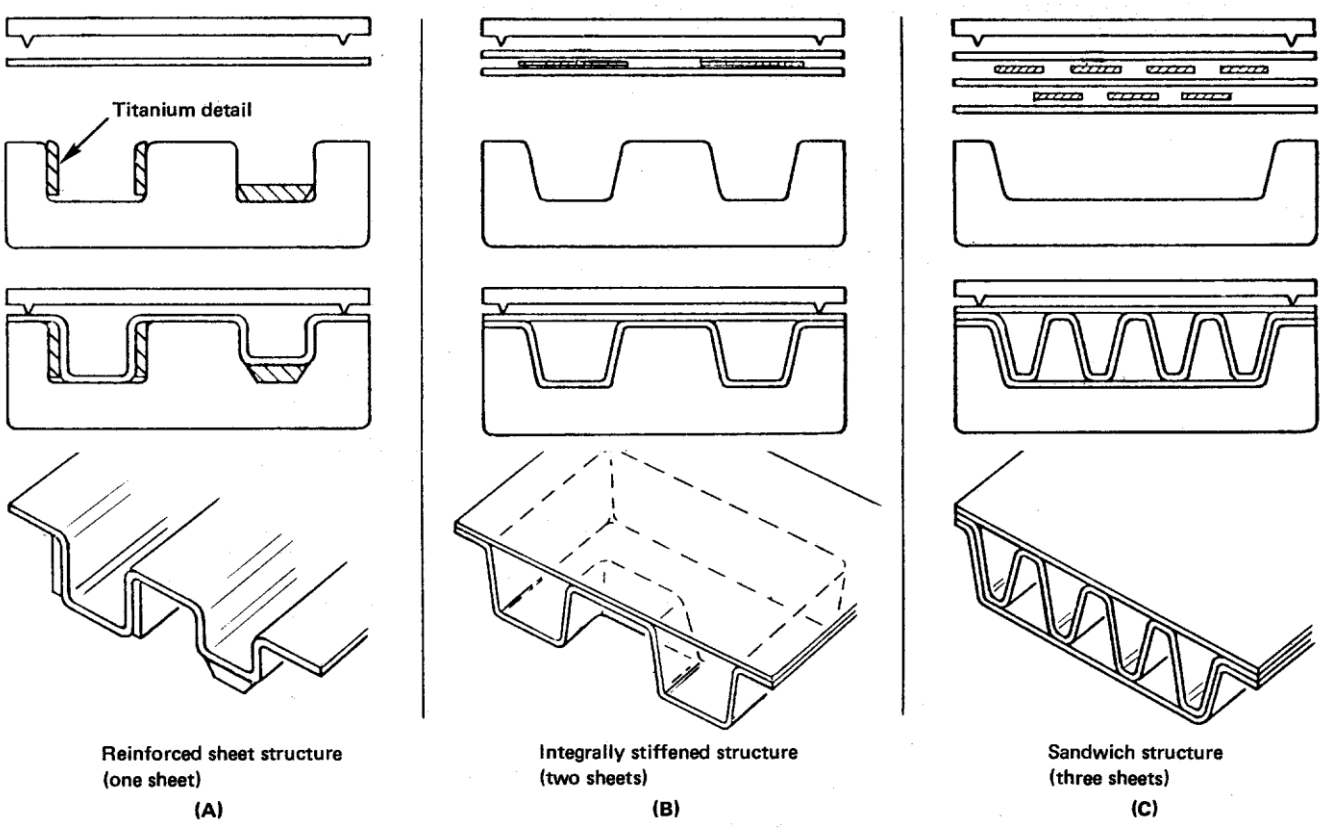

Figure 6: Manufacturing of reinforced structures in titanium by a combination of SPF and DFW32

3.1 Diffusion welding in Aeronautics Industry

It is a solid-state welding process that produces a weld by the application of pressure at elevated temperature with no macroscopic deformation or relative motion of the pieces [9]. The aeronautic industry is the major user of DFW25. This process has proven particularly useful when combined with the superplastic forming (SPF) of titanium alloys. In this case, complicated geometries can be obtained in just one manufacturing step as shown in Figure 6. The quality and low cost of the joint enables in some cases the substitution of riveted aluminum components with SPF/DFW titanium replacements. Figure 5 shows a possible improvement for the door panel of an aircraft fuselage [10, 11]. The conventional fabrication consisted of 16 parts held together by 500 fasteners. It was proposed to replace that design by a 2-sheet assembly, integrally stiffened produced by SPF/DFW. Figure 8 shows an exit hatch for the British Aerospace Bae 125/800. The application of SPF/DFW reduces the original riveted aluminum design from 76 detail parts and 1000 fasteners to a titanium version with only 14 details and 90 fasteners with a total cost savings of 30%. Figure 7 shows a wing access panel for the Airbus A310 and A320 in which switching from riveted aluminum to SPF/DFW titanium achieved a weight saving in excess of 40%. The success of SPF/DFW with titanium stimulated much research with the goal of accomplishing a similar process with aluminum[11, 12, 13].

The fundamental difference between DFW of titanium and aluminum is that titanium can dissolve its oxides, and aluminum cannot [13]. Therefore, the residual oxide at the interface of aluminum joint dramatically reduces the strength of the diffusion weld. This problem has prevented the SPF/DFW of aluminum from being generally adopted [14, 15].

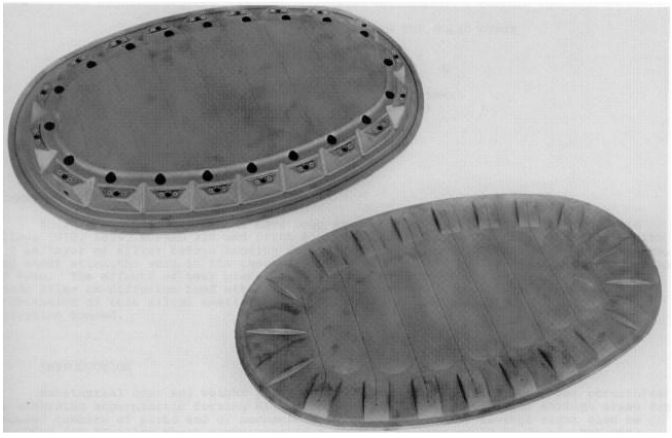

Figure 7: Wing access panel for the airbus A310/A320 made of titanium SPF/DFW33

Figure 8: Exit hatch for the BAe 125/800 made of titanium SPF/DFW33

3.2 Friction welding in Aeronautics Industry

In this process, the joining of the metals is achieved through mechanical deformation. Since there is no melting, defects associated with melting-solidification phenomena are not present and unions as strong as the base material can be made [15, 16]. This process can join components with a relatively simple cross section. It is used for the joining of aluminum landing gear components [17]. Linear friction (fretting) welding was considered by General Electric and Pratt & Whitney as an alternative for the manufacture and repair of high temperature alloy blisks for jet engines [18, 19]. Although little was disclosed about these processes, they do not seem to have evolved into commercial applications [20, 21].

4 Conclusion

Welding processes and solid state welding processes have been researched, and the application of diffusion welding and friction welding which belong to solid state welding have been investigated, in the aeronautic industry.

Weight reduction and improved damage tolerance characteristics were the prime drivers to develop new family of materials for the aeronautical industry, like Fiber/Metal Laminated (FML) or Metal Matrix Composites (MMC). Those advanced materials cannot be welded by conventional techniques because the high temperatures involved would destroy their properties. For such materials, diffusion welding is an attractive solution because it is a solid state joining technique, which is normally carried out at a temperature much lower than the melting point of the material.

The range of applications for this type of welding on aeronautic industry is vast and includes: structural aircraft sections, blades of aircraft engines, electronic components, helicopters rotor parts, space shuttle fuselage, exhaust components for gas turbines [22].

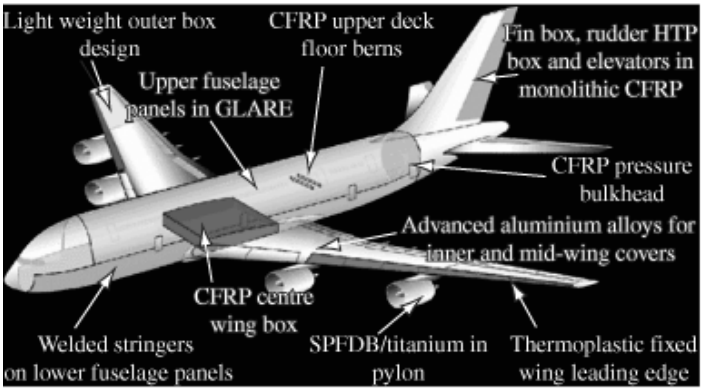

Figure 9: The components of an airplane

In the near future, Airbus planes (A318 and A3XX) will feature fuselage stringers laser welded to the airplane skin. Looking further into the future, it is likely that friction welding will be applied on airplane structural components, since it can reliably join alloys of the series 2xxx and 7xxx [23, 24].

Also, it is reasonable to expect that the amount and criticality of EBW of titanium in future military aircraft will increase. The use of castings in aircraft is increasing; this will surely bring up new challenges that had not been present with wrought alloys. Besides that, diffusion welding is getting more and more useful in aeronautic industry.

References

1. European Aluminium Association, Version 2015.

2. H.Kreye, “Melting Phenomena in Solid State Welding Processes“, welding research supplement, 1977.
3. Valery Marinoc,“ Manufacturing Technology“.
4. D. Kopeliovich,“ Solid State Welding (SSW)“.
5. D. Kopeliovich,“ Classification of Welding Processes“.
6. G.S.Hoppin and T.F.Berry,“ Activated Diffusion Bonding“, welding research supplement, 1970.
7. Shaw, C.B. “Welding Research for Aerospace in USA, in International Congress on Welding Research“, Boston, MA, 1984.
8. A.P.Costa, E.C.Botelho, M.L.Costa, N.E.Narite, and J.R. Tarpani,“ A Review of Welding Techonologies for Thermoplastic Composites in Aerospace Applications“, Brazil, 2012.
9. Dunkerton, S.B. and C.J. Dawes,“The Application of Diffusion Bonding and Laser Welding in the Fabrication of Aerospace Structures, in Advanced Joining of Aerospace Metallic Materials“, Oberammergau, Germany: Advisory Group for Aerospace Research & Development (NATO), 1985.
10. Williamson, J.R.“Diffusion Bonding in Superplastic Forming/Diffusion Bonding, in Welding Technology for the Aerospace Industry“ Las Vegas, NV: American Welding Society, 1980.
11. Stephen, D. and S.J. Swadling,“Diffusion Bonding in the Manufacture of Aircraft Structure, in Advanced Joining of Aerospace Metallic Materials“, Oberammergau, Germany: Advisory Group for Aerospace Research & Development (NATO), 1985.
12. Patricio F. Mendez,“ New Trends in Welding in the aeronautic industry“, Massachusetts Institute of Technology, USA.
13. Institude Superior Tecnico,“Diffusion Welding in Aeronautic Industry“, 2007.
14. Rose F., "A Rapid Method for Diffusion Bonding Aerospace Structures," SAE Technical Paper 650780, 1965.
15. Muser C., "Diffusion Bonded Structures for Application to Air Transport Aircraft," SAE Technical Paper 680331, 1968.
16. Viliam Sinka,“The Present and Future Prospects of Friction Stir Welding in Aeronautics“, Brazil, 2014.
17. Irving, B., “Sparks Begin to fly in Nonconventional Friction Welding and Surfacing“, Welding Journal, 1993.
18. Y.Chen, C. Liu, and G. Liu,“ Study on the joining of Titanium and Aluminum Dissimilar Alloys by Friction Stir Welding“, Jiujiang University, China, 2011.
19. M.Aonuma and K.Nakata,“ Dissmilar Metal Joining of 2024 and 7075 Aluminium Alloys to Titanium Alloys by Friction Stir Welding“, Tokyo Metropolitan Industrial Technology Research Institude, Japan, 2011.
20. Rathod, M. and Karale, T., "Friction Stir Welding of Aluminium-Alloys," SAE Technical Paper 2014-28-0015, 2014.
21. T. Pan,"Friction Stir Spot Welding (FSSW) - A Literature Review," SAE Technical Paper 2007-01-1702, 2007.
22. Cary H.B., “Modern Welding Technology“, Prentice Hall, 1998.
23. Eagar T.W., “Energy Sources Used for Fusion Welding“ in ASM Handbook, 1993.
24. W.D. Brewer, R.K. Bird, and T.A. Wallace, “Titanium Alloys and Processing for High Speed Aircraft“, Nasa Langley Research Center, Hampton Virginia 23681-0001.
25. E. Akca and A. Gursel,“The importance of interlayers in diffusion welding – A review“ *Periodicals of Engineering and Natural Sciences*, vol 3, no 2, pp. 12-16, 2015.

ISSN 2303-4521
PERIODICALS OF ENGINEERING AND NATURAL SCIENCES
Vol. 4 No. 1 (2016)
Available online at: http://pen.ius.edu.ba

The Application of CFD to IUS Buildings Analysis

Enes Akca

International University of Sarajevo, Faculty of Engineering and Natural Sciences, Mechanical Engineering Program
Sarajevo, Bosnia and Herzegovina

enesacka@hotmail.com.tr, eakca@ius.edu.ba

Abstract

In this study, wind characteristics and energy potential of IUS Campus region is investigated. Assessment of the site is carried out by using turbulent flow models. Commercial software STAR CCM+ was used to solve turbulent flow equations. STAR CCM+ is a computational fluid dynamics (CFD) software package that solves Navier-Stokes equations that define fluid flow, by using numerical techniques.

Keywords: computational fluid dynamics,wall y^+,heat transfer coefficient, stream lines

1 Introduction

Computational Fluid Dynamics (CFD) can play an important role in building design. For all aspects and stages of building design, CFD can be used to provide more accurate and rapid predictions of building performance with regard to air flow, pressure, temperature, and similar parameters.

Computational Fluid Dynamics (CFD) can play an important role in building design. For all aspects and stages of building design, CFD can be used to provide more accurate and rapid predictions of building performance with regard to air flow, pressure, temperature, and similar parameters.

Computational fluid dynamics (CFD) is used in science andengineering for numerical simulation of steady or unsteady flowfields. At Fraunhofer IBP we provide CFD competences in terms ofmodelling, simulation and analysis of complexphenomena relatedto indoor environmental quality. CFD enables in depth analysisof thermodynamic systems in all relevant application domainslike buildings and construction, as well as theautomotive andaviation sector. The CFD simulations consider heat transfer modesof convection, radiation and conduction incombination with multi-physics approaches. The CFD results are used to evaluate thermalcomfort of humans, quality of trading goods, ventilation efficiencyin buildings or thermal management strategies in vehicles.

Also the purpose of the case study is to compute flow around A and B buildings of IUS campus using CDF. The main focus of the case study is how heat is transferred by the forced convection which is natural wind. The computation is used to compute a heat transfer coefficient at the buildings wall for the winter season. For that purpose, velocity field, heat transfer coefficient distribution along the buildings, pressure distribution, wall y+, turbulent kinetic energy, and temperature distribution will be shown in scalar, vector and graph forms. The temperature of outside the buildings is declared as -2℃, and the wind flows at 21℃ with the velocity 5 m/s.

Figure 1describes the wind direction in the region in the winter season as defined. The wind direction

DOI: 10.21533/pen.v4i1.49

is based on real observations from the weather station at Sarajevo/Butmir [1].

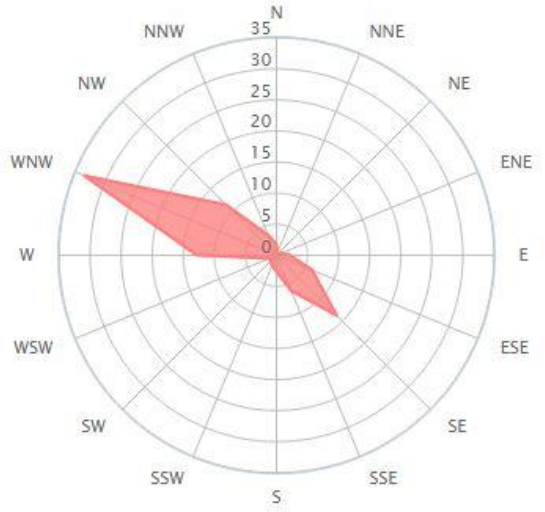

Figure 1: Direction of wind

2 Star CCM+

STAR-CCM+ is one of the most modern in comparison with competitors software package designed to solve the problems of continuum mechanics. It is characterized by extraordinary ease of use.

STAR-CCM+ includes the latest numerical algorithms such as advanced solvers,raspredelennny (segregated solver) and connected (coupled solver), moreover, it is created using the most advanced programming techniques. All this allows STAR-CCM+ provideunprecedented accuracy, reliability and flexibility in solving problems of computational continuum mechanics.Powerful new tools for building grids: from restoring the integrity of the surface (surface wrapping) to create grids of polyhedral cells. Using these new tools for building grids can reduce the clock time for solving the problem.A large set of physical models: laminar and turbulent flow of Newtonian and non-Newtonian fluids, multiphase flow, cavitation, radiation, combustion, development of boundary layer flows with high Mach numbers, the conjugate heat transfer, as well as new models for the calculation of heat exchangers and fans.

3 Theoretical Background

The flow module determines the velocity and pressure fields by solving the three-dimensional momentum equations and the pressure correction equations, respectively. These equations are guided by the laws of conservation of mass and momentum, which lead to the use of the Navier-Stokes equations to iteratively resolve the flow solutions. The following sections describe the governing flow equations[2].

Applying the mass, momentum and energy conservation, the continuity equation, momentum equation and energy equation can bederived as follows.

3.1 Continuity Equation

$$\frac{d\rho}{dt} + \rho\frac{\partial U_i}{\partial x_i} = 0$$

Momentum Equation

$$\underbrace{\rho\frac{\partial U_j}{\partial t}}_{I\ II} + \underbrace{\rho U_i\frac{\partial U_j}{\partial x_i}}_{III\ \ IV} = \underbrace{-\frac{\partial P}{\partial x_j}}_{V} \underbrace{-\frac{\partial \tau_{ij}}{\partial x_i}}_{IV} + \underbrace{\rho g_j}_{V}$$

Where

$$\tau_{ij} = -\mu\left(\frac{\partial U_j}{\partial x_i} + \frac{\partial U_i}{\partial x_j}\right) + \frac{2}{3}\delta_{ij}\mu\frac{\partial U_k}{\partial x_k}$$

I : Local change with time

II : Momentum convection

III : Surface force

IV : Molecular-dependent momentum exchange (diffusion)

V : Mass force

3.2 Energy Equation

$$\underbrace{\rho C_\mu\frac{\partial T}{\partial t}}_{I} + \underbrace{\rho C_\mu U_i\frac{\partial T}{\partial x_i}}_{II} = \underbrace{-P\frac{\partial U_i}{\partial x_i}}_{III} + \underbrace{\lambda\frac{\partial^2 T}{\partial x_i^2}}_{IV} \underbrace{-\tau_{ij}\frac{\partial U_j}{\partial x_i}}_{V}$$

I : Local energy change with time

II : Convective term

III : Pressure work

IV : Heat flux (diffusion)

V : Irreversible transfer of mechanical energy into heat

If the fluid is compressible, the continuity equation and momentum equation can besimplified as follows.

Continuity Equation

$$\frac{\partial U_i}{\partial x_i} = 0$$

Momentum Equation

$$\rho \frac{\partial U_j}{\partial t} + \rho U_i \frac{\partial U_j}{\partial x_i} = -\frac{\partial P}{\partial x_j} - \mu \frac{\partial^2 U_j}{\partial x_i^2} + \rho g_j$$

3.3 General Form of Navier-Stokes Equation

To simplify the Navier-Stokes equations, they can be rewritten as the general form.

$$\frac{\partial(\rho\Phi)}{\partial t} + \frac{\partial}{\partial x_i}\left(\rho U_i \Phi - \Gamma_\Phi \frac{\partial \Phi}{\partial x_i}\right) = q_\Phi$$

When Φ=1, U_j, T, and they can be respectively get as continuity equation, momentum equation and energy equation.

3.4 Finite Volume Method

The Navier-Stokes equations are analytical equations. Human can understand and solve them, but if we want to solve them by computer, we have to transfer them into discretized form. This process is discretization. The typical discretization methods are finite difference, finite element and finite volume methods. Here we introduce finite volume method, because finite volume methods are generally used in CFD [3].

The Approach of Finite Volume Method

Integrate the general form of Navier-Stokes equation over a control volume and apply Gauss Theory,

$$\int_V \frac{\partial}{\partial x_i} \Phi dV = \int_S \Phi \cdot n_i dS$$

The integral form of Navier-Stoke equation can written as

$$\int_V \frac{\partial(\rho\Phi)}{\partial t} dV \int_S \left(\rho U_i \Phi - \Gamma \frac{\partial \Phi}{\partial x_i}\right) \cdot n_i dS = \int_V q_\Phi dV$$

3.5 *k* - εTurbulentModel

In the *k* - *ε*turbulent model, the notation of *k* is the kinetic energy and ε is the turbulence dissipation rate. The turbulent dynamic viscosity is expressed as

$$\frac{\mu_t}{\mu} = 20$$

$$\mu_t = C_\mu \rho \frac{k^2}{\varepsilon}$$

$$\varepsilon = \frac{C_\mu \rho k^2}{20 \cdot \mu} \quad , \quad \frac{\sqrt{k}}{V_b} = 10\% = 0.1$$

In the above equations, $V_b$is the bulk velocity, ρ is the fluid density, $\mu$and $\mu_t$are the laminar and turbulent dynamic viscosities respectively. The turbulence model constant used in the aboveequations are C_μ= 0.09[4].

4 Computational Details

A 3-D finite-volume approach is adopted by the software STAR CCM+because of its capability of conserving solution quantities. The software solves the conservation equations for continuity, momentum, and energy as well as the equations for turbulent kinetic energy and its dissipation rate. The two-equation *k* - ε turbulence model is used.

A three-dimensional model of the IUS buildings in the shape of a rectangular prism was developed. The physical dimensions were set to be 48 m wide by 51 long by 20 m tall.

RANS solver is used to solve the governing equations of continuity and momentum in a viscous flow around the buildings model. The Navier-Stokes Equations (NSE) are solved with a segregated, algebraic multigrid solver using Gauss-Seidel iterations.

In this study case, for the three-dimensional case, implicit unsteady simulations were carried out at step intervals of 0.01 seconds for 200 time steps which is equivalent to 2seconds.A description of the conditions and assumptions is given in the following sections.

4.1 Computationaldomain

Generally, the size of the entire computational domain depends on the targeted area and theboundary conditions. For a single building, the distance from the top of the building to the top

ofthe computational domain should be about20H, where H is thebuilding height and is defined as 20m. For the laterals boundary, 20H is required between the buildings and the computational domain.In the figure 2, the computational domain and dimensions are shown, and dimensions' units are in cm.

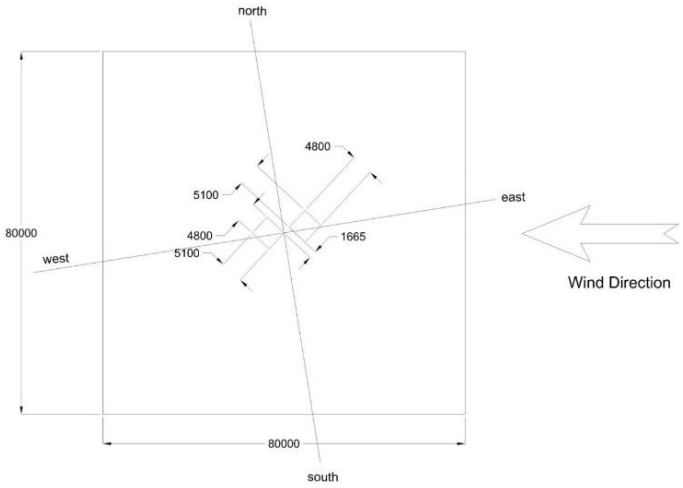

Figure 2: The Computational domain and dimensions.

4.2 Computational Grids

The hexahedra cell has been chosen for meshing purpose. Also prism layer mesher and surface remesher options were used. All computational domains of this study were undertaken for generating mesh by means of relative cell size. The base size value is defined as 5m. Boundary growth rate is selected as very slow, and default growth rate is as medium. Also the mesh values in the buildings are selected relative size is 1m. Thus, relative maximum cell size of 5m and relative minimum size of 1m were used as limits for generating local mesh of all domains and the buildings. Meshing of this computational domain was carried out with 1,243,390 cells and 3737529 faces, covering the whole volume of the domain.

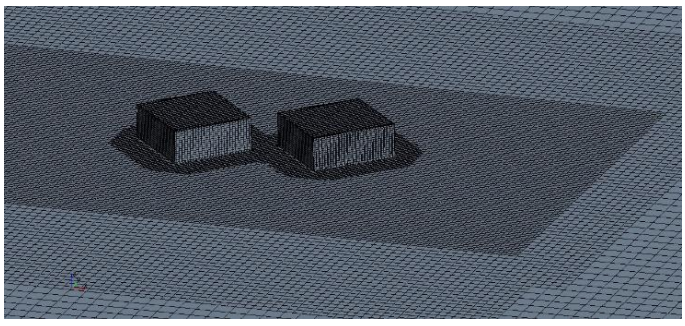

Figure 3: computational grids of the buildings.

4.3 Turbulence Models

The CFD program was set to use a standard k-ε model for turbulence. The required input variables were the turbulent kinetic energy, *k*, and the turbulent dissipation rate, ε.The inlet flow velocity was taken to be 5 m/s.This inlet flow velocity can be directly inserted into equations in section 2.5, to result in a turbulent kinetic energy value, *k*, of 0.25 J/kg. Also, the turbulent dissipation rate, ε, can be calculated using the equation in the section 2.5, and the result is calculated as, ε, of 17 m^2/s^3.

4.4 Initial Conditions

Initial conditions describe the state of the system at the initial instant of time through the values of a solution variable, and have to be defined in the whole domain: $f0 = f(t0)$. If the equations to be solved include high-order time derivatives, the initial condition include also the specification of the correspondingly lower derivatives of solution variables at the initial instant of time. The initial parameters are set as calculated before, shown in table 1.

Table 1: Initial conditions.

Pressure	Static Temperature	Turbulent Dissipation Rate	Turbulent Kinetic Energy	Velocity
101,325 Pa	-2℃	17 m^2/s^3	0.25 J/kg	5 m/s

4.5 BoundaryConditions

A boundary condition describes the state of a system, expressed through conditions on the solution variables holding on all boundaries of the system.

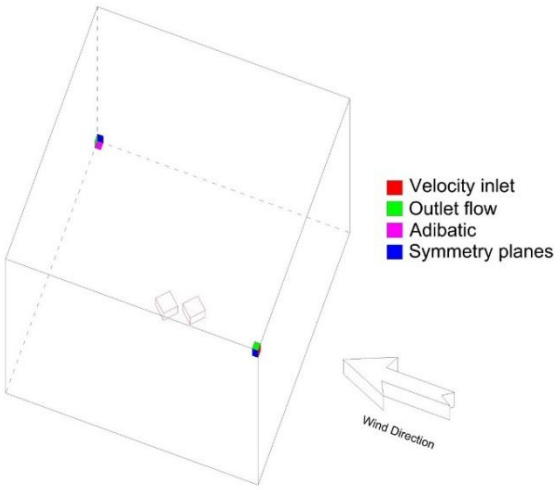

Figure 4: Boundaries of all faces

In figure 4, each surface is described as boundary conditions, and their types of boundaries are defined. Also the physical values of boundaries are given in table 2. Heat transfer coefficient and thermal resistance were as constant typical values [5].

Table 2: Boundary conditions and physical values.

Velocity inlet	Outlet flow	Adiabatic	Symmetry planes	Building Boundaries
Mag. : 5 m/s	Flow- Split Outlet	No Heat Transfer		Environment
Temp. : -2 ℃				Amb.Tem.: 21℃
Turb. Diss. Rate: 17 m^2/s^3				HeatTransfer Coefficient: 2.18 W/m^2-K
Turb.Kinetic Energy : 0.25 J/kg				Thermal Resistance: 0.13 m^2-K/W

Asymmetry plane boundary represents an imaginary plane ofsymmetry in the simulation. The solution that is obtained with asymmetry plane boundary is identical to the solution that would be obtained by mirroring the mesh about thesymmetry plane.

5 Results

The results are shown in figures below. In Figure 5, the velocity magnitude of streamlines around the building for turbulence model is presented.

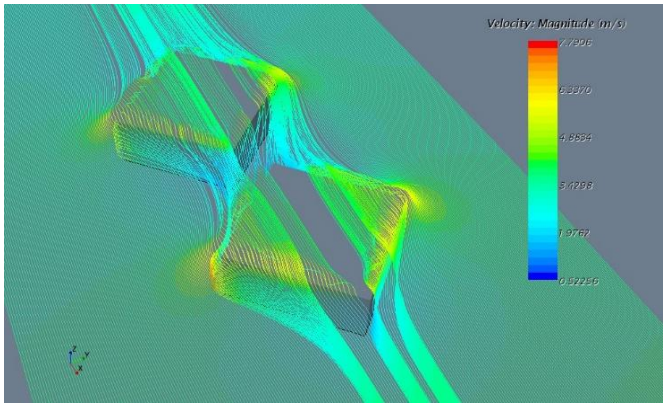

Figure 5: Streamlines with velocity magnitude.

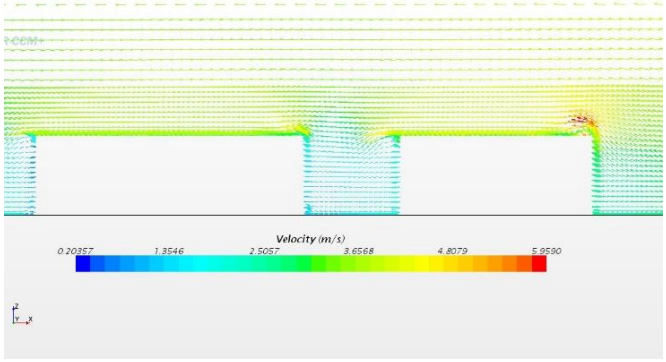

Figure 6: Velocity vector

In figure 6, velocity is shown as vector of a created plane from the middle of the computational domain, and as it is seen in the figure, when wind direction is defined from left to right, there is impinging on the up side of the wall where the wall has the first impact of the wind.

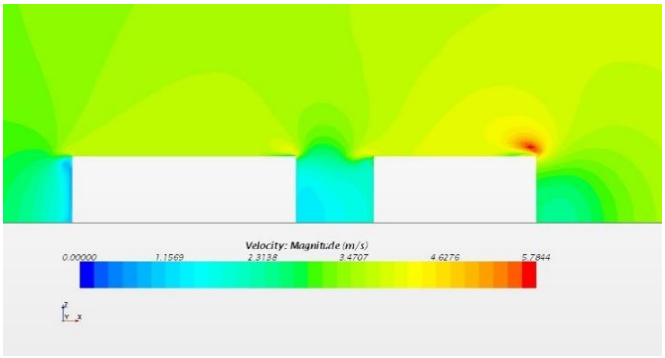

Figure 7: velocity contour

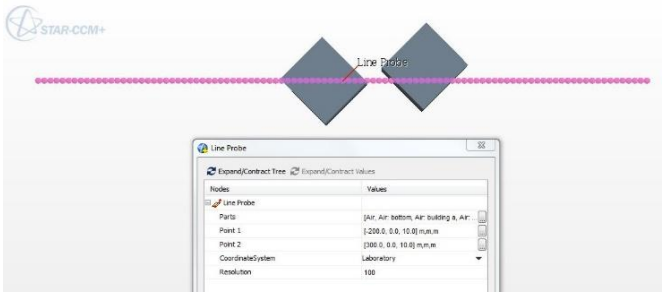

Figure 8: Probe line shown

Monitoring the vector and contour plots of velocity during calculation of the flow analysis are shown in figure 6 and 7. Also while figure 6 shows velocity vector and figure 7 shows velocity scalar, they have the same sense of velocity as expected.

In figure 8, a probe line was created along the flow direction in the middle of the computational domain. The purpose of the probe line is to plot some graphs along it. Also the probe line was located in 10 m height.

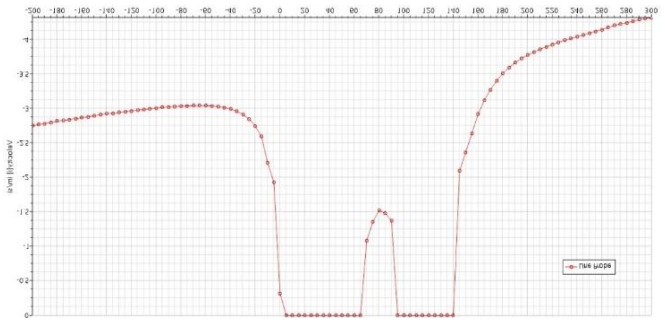

Figure 9:velocity graph along the probe line.

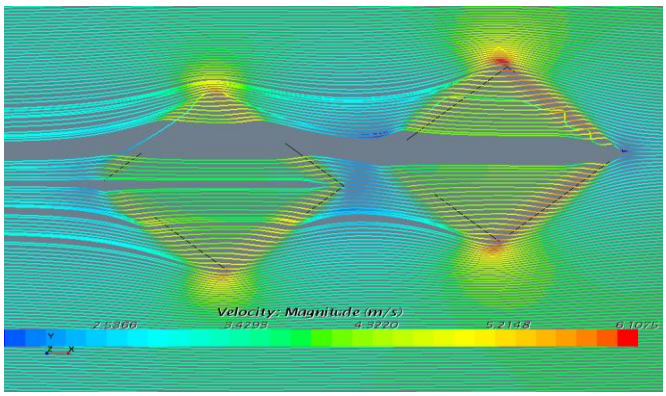

(a)

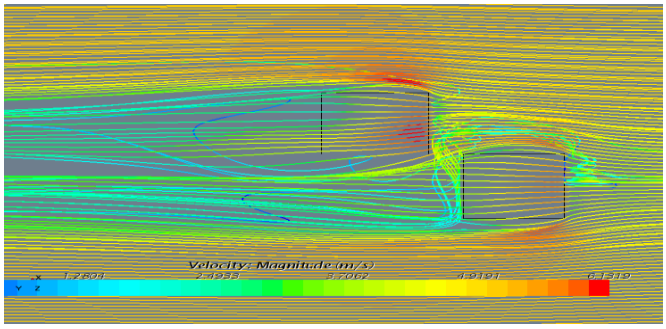

(b)

Figure 10: Flow direction with velocity magnitude; (a) Real direction (b) Imaginary direction.

In figure 9, velocity changes are plotted along the probe line which was created in figure 8. Also in figure 10, real flow direction with velocity magnitude is shown on the part A, and imaginary flow direction is shown on the part B. when they are compared according to flow directions. In part B, there is more and more turbulent and it needs to less and less. Thus the real flow can be considered as the optimum flow direction.

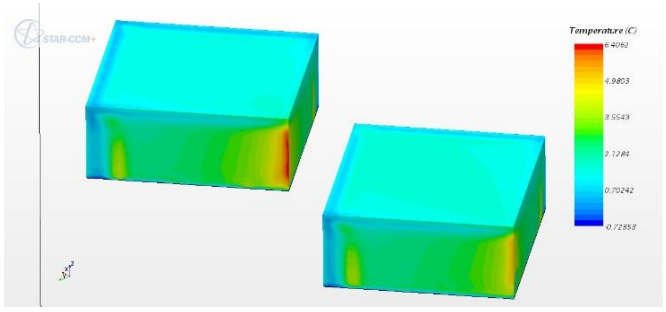

Figure 11: temperature field around the buildings.

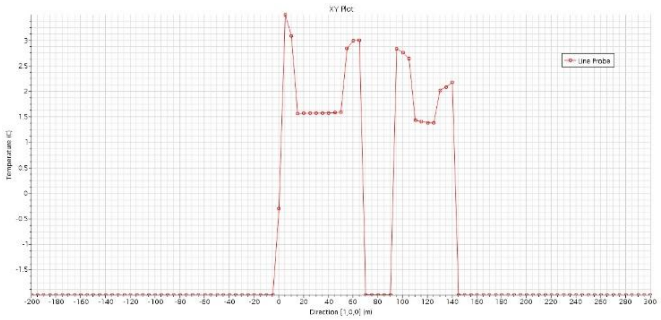

Figure 12: plotted graph of temperature along the probe line.

Temperature field around the buildings are represented in figure 11, and the graph of temperature along the probe line is plotted in figure 12. Also in figure 11, the highest temperature appears at back side of the first building when the flow is on –x direction.

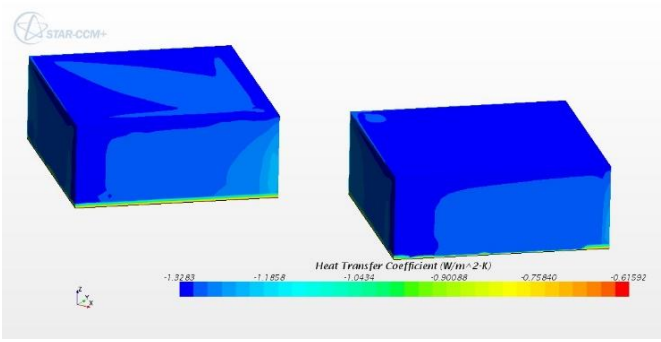

Figure 13: Heat transfer coefficient around the buildings.

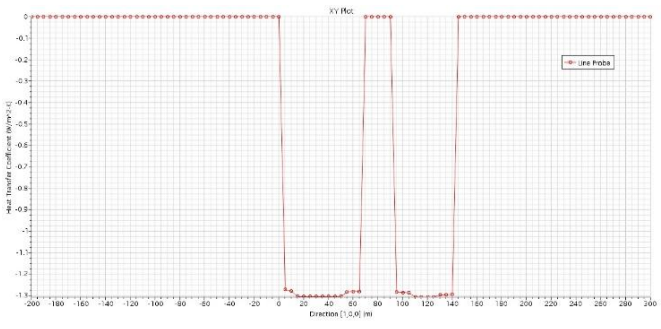

Figure 14: graph of heat transfer coefficient around the buildings.

Heat transfer coefficient around the buildings is shown in figure 13, and it is plotted along the probe line in figure 14. Heat transfer coefficient can be shown in formula as $h=q/\Delta T$, where q is amount of heat required (heat flux), h is heat transfer coefficient, and ΔT is difference in temperature between the solid and surrounding fluid area. The temperature differences bottom side of the buildings' wall is less, and thus heat transfer coefficient is high at that region as shown in figure13 and 14.

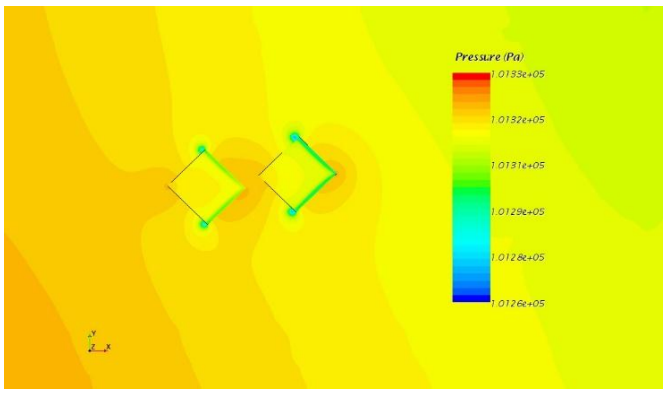

Figure 15: pressure distribution

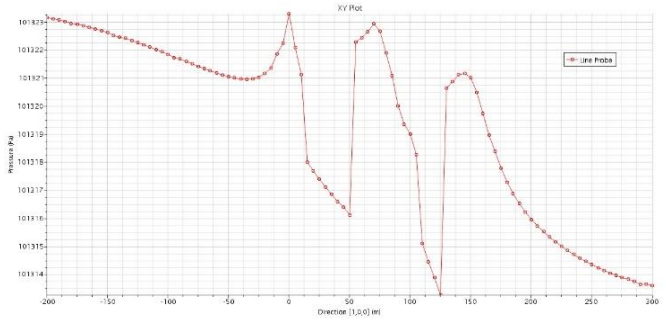

Figure 16: pressure graph along the probe line.

In addition, scalar of pressure distribution on the buildings is shown in figure 15, and also pressure drop is plotted as a graph along the probe line in figure 16.

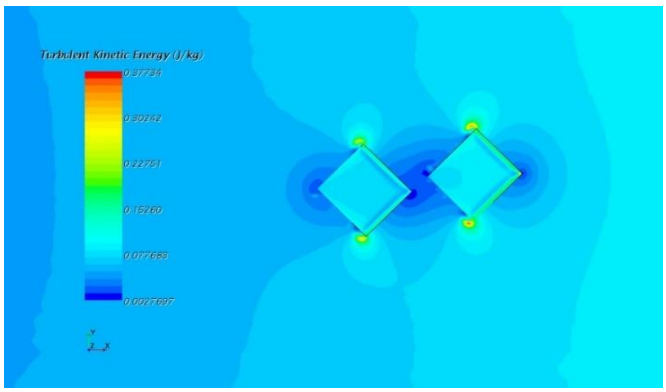

Figure 17: Turbulent kinematic energy

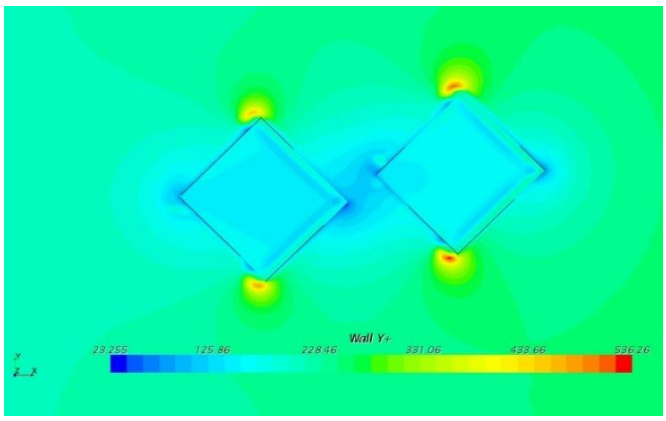

Figure 18: Wally+

A non-dimensional wall distance for a wall-bounded flow can be define as $y+=(u*y)/V$. Where $u*$ is the friction velocity at the nearest wall, $y$is the distance to the nearest wall and V is the local kinematic viscosity of the fluid. $y+$ is often referred to simply as *y plus* and is commonly used in boundary layer theory and in defining the law of the wall.

Figure 18 shows the turbulent kinetic energy, and figure 17 shows the non-dimensional wall distance. Also although their scalar fields are not the same, their senses are very similar as shown in those figure. Also their graphs can be compared. Figure 19 shows the graph of turbulent kinetic energy, and figure 20 shows the graph of wall y+.

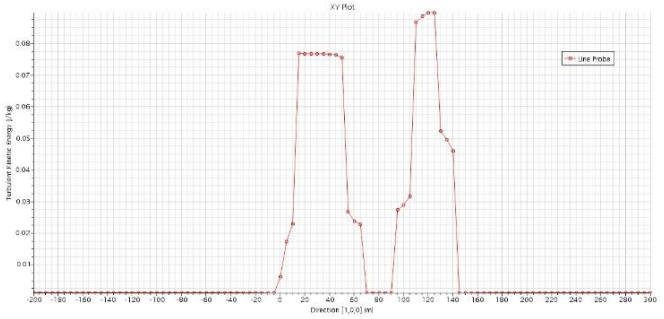

Figure 19: graph of turbulent kinetic energy

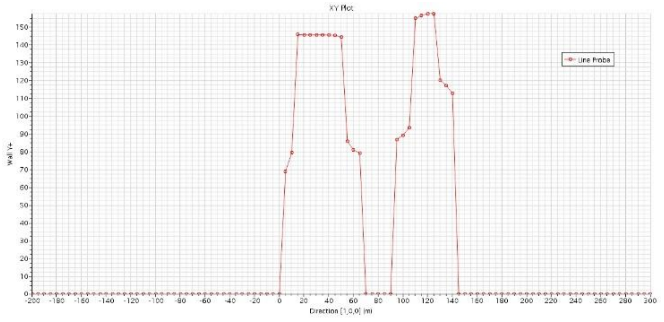

Figure 20: graph of wall y+

6 Conclusion

Turbulenceis a very important phenomenon that affects all atmospheric processes, but it is more important near the surfaces. Turbulence represents the irregularity or randomness of the flow. The *k-ε*turbulence model is used. The most unique measure for turbulence is kinetic energy of turbulent part of the flow. This variable depends on a variety of mechanisms. The most important are certainly buoyant production or consumption and shear production of turbulence kinetic energy (TKE). Both of these vary significantly in time and in space (especially in height). The third very important term is dissipation. This term provides

the reduction of turbulence with time which is the primary purpose of turbulence. This causes that the energy is dissipated from large vortices to small one.

Also the purpose of the case study was to compute flow around A and B buildings of IUS campus using CDF. The main focus of the case study was how heat is transferred by the forced convection which is natural wind. The computation was used to compute a heat transfer coefficient at the buildings wall for the winter season. For that purpose, velocity field, heat transfer coefficient distribution along the buildings, pressure distribution, wall y+, turbulent kinetic energy, and temperature distribution will be shown in scalar, vector and graph forms. The temperature of outside the buildings is declared as -2℃, and the wind flows at 21℃ with the velocity 5 m/s. Also it can be said that as a result of the analysis, the IUS buildings are located in the optimum position, actually it was the most important information of this study case.

References

1. http://www.windfinder.com/windstatistics/sarajevo_butmir
2. Wangda Zuo,"Introduction of Computational Fluid Dynamics", FAU Erlange-Nümberg, St. Petersburg, 2005.
3. Bradley S. Hurak, "Computational Fluid Dynamics Analysis of Air Flow and Temperature Distribution in Buildings".
4. Chanawat Nitatwichit, Yottana Khunatorn, and Nakorn Tippayawong, "Computational analysis and visualization of wind-driven naturally ventilated flows around a school building", Maejo international journal of science and technology, 2008.
5. Francis G.N.Li, A.Z.P. Smith, and Phillip Biddulph," Solid-wall U-values: heat flux measurements compared with standard assumptions", Routledge, London, 2015.
6. Matic Savli, "Turbulence Kinetic Energy (TKE)", University of Ljubljana, 2012.

ISSN 2303-4521
PERIODICALS OF ENGINEERING AND NATURAL SCIENCES
Vol. 4 No. 1 (2016)

Available online at: http://pen.ius.edu.ba

Validation of Stresses with Numerical Method and Analytical Method

Enes Akca

International University of Sarajevo, Department of Mechanical Engineering
Sarajevo, Bosnia and Herzegovina

enesakca@hotmail.com.tr, eakca@ius.edu.ba

ABSTRACT

In this study, the goal is to confirm stresses under kind of loads, with analytical and numerical methods. But each material is drawn in SolidWorks 3D design software, and exported to ANSYS. Also the other purpose is to give information about type of stresses and formulation of each stress with different loads.

Keywords:ANSYS, Stress, Shear stress, FEM, Analyticalsolution, Numerical solution

1. INTRODUCTION

Stress is defined as the strength of a material per unit area or unit strength. It is the force on a member divided by area, which carries the force, formerly express in N/mm^2or *MPa.* And there are types of stresses and component of stresses; normal stress, shear or transversal stress, maximum and minimum principle stresses. Besides, they will be defined in detail in chapter 2.

As computers have become more and more powerful, people have tended to use numerical approaches to develop theoretical models to predict the effect of whatever is studied. This has improved stress analysis and computer simulations. Numerical methods can potentially provide more accurate solutions since they normally require much less restrictive assumptions. The finite element method is very often used to analyze the stress state of an elastic body with complicated geometries.

The finite element method is capable of providing this information, but the time needed to create such a model is large. In order to reduce the modeling time, a 3D model created in solid

DOI: 10.21533/pen.v4i1.47

modeling software can be used. One such model is provided by SolidWorks. SolidWorks can generate models of three-dimensional members easily. In SolidWorks, the geometry is saved as a file and then it can be transferred from SolidWorks to ANSYS. ANSYS has pioneered the development and application of simulation methods to solve the most challenging product engineering problems. Simulation software enables organizations to confidently predict how their products will operate in the real world [1].

First of all, it should be emphasized that the "numerical approach" is not automatically equivalent to the "approach with use of computer", although we usually use numerical approach to find the solution with use of computers. That is because of the high computer performance incomparable to abilities of human brain. Numerical approach enables solution of a complex problem with a great number of very simple operations. It can be distinguished two main situations when numerical methods are used instead of analytical methods [2];

1. When analytical solution of the mathematically defined problem is possible but it is time-consuming and the error of approximation we obtain with numerical solution is acceptable. In this case the calculations are mostly made with use of computer because otherwise its highly doubtful if any time is saved. It is also indivually to decide what we mean by "time-consuming analytical solution". In my discipline even very simple mechanical problems are solved numerically simply.

2. When analytical solution is impossible, this means that we have to apply numerical methods in order to find the solution. This does not define that we must do calculations with computer although it usually happens so because of the number of required operations.

Hence in the next chapters, there will be results of both numerical and analytical solutions, also confirmation of 3 tests and one member is just consisting of numerical solution. On account of the fact that it will be proved that ANYS results are reliable if 3 tests are confirmed.

2. STRESSES

The purpose is to find the normal and shear stresses acting on any inclined section. For uniaxial load and pure shear, now the transformation relationships that give the stress components for any orientation is need to be derived. This is referred as *stress transformation*[3].

When an element is rotated from one orientation to another, the stresses acting on the faces of the element are different but they still represent the same state of stress, namely, the stress at the point under consideration.

Axial load $\sigma = P/A$

Torsional load in circular shaft $\tau = T_p/I_p$

Bending moment and shear force in beam $\sigma = M_y/I \qquad \tau = VQ/Ib$

Plane stress occurs when the material at a point is subjected to two normal stress components $\sigma_x$andσ_y and a shear stress τ_{xy}. Provided these components are known, then the stress components acting on an element having a different orientation θ can be determined using the two force equations of equilibrium or the equations of stress transformation [4].

$$\sigma_{x'} = \frac{\sigma_x + \sigma_y}{2} + \frac{\sigma_x - \sigma_y}{2} cos2\theta + \tau_{xy} sin2\theta$$

$$\tau_{x'y'} = -\frac{\sigma_x - \sigma_y}{2} sin2\theta + \tau_{xy} cos2\theta$$

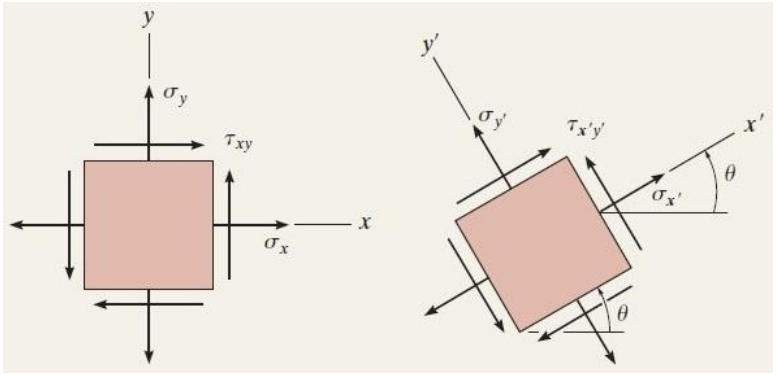

Figure 1: Plane stress

It is important to determine the orientation of the element that produces the maximum principal normal stresses and the maximum in-plane shear stress. Using the stress transformation equations, it is found that no shear stress acts on the planes of principal stress.The principal stresses are

$$\sigma_{1,2} = \frac{\sigma_x + \sigma_y}{2} \pm \sqrt{\left(\frac{\sigma_x - \sigma_y}{2}\right)^2 + {\tau_{xy}}^2}$$

The planes of maximum in-plane shear stress are oriented 45° from this orientation, and on these shear planes there is an associated average normal stress.

$$\tau_{\substack{max \\ in-plane}} = \sqrt{\left(\frac{\sigma_x - \sigma_y}{2}\right)^2 + {\tau_{xy}}^2}$$

$$\sigma_{avg} = \frac{\sigma_x + \sigma_y}{2}$$

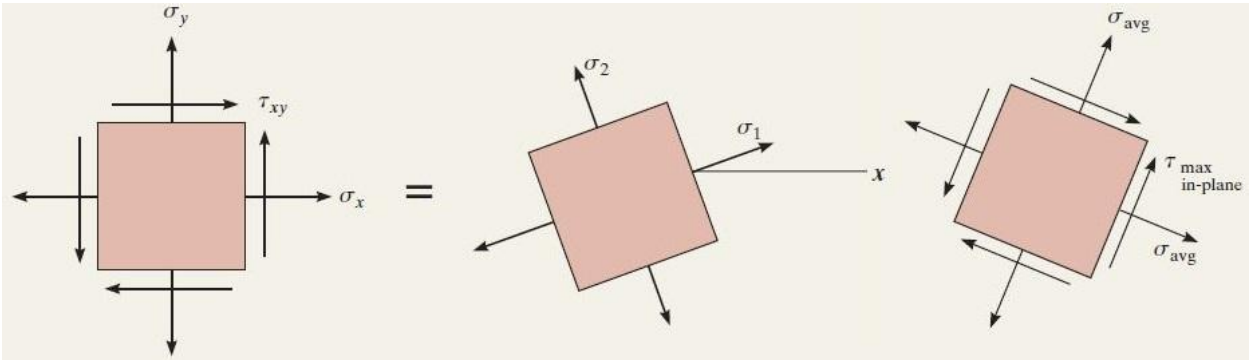

Figure 2: Planes of maximum in-plane shear stress

Mohr's circle provides a semi-graphical method for finding the stress on any plane, the principal normal stresses, and the maximum in-plane shear stress. To draw the circle, the σ and τ axes are established, the center of the circle *C* [(σ_x+σ_y)/2, 0]and the reference point *A* (σ_x,τ_{xy})are plotted.

The radius *R* of the circle extends between these two points and is determined from trigonometry [4].

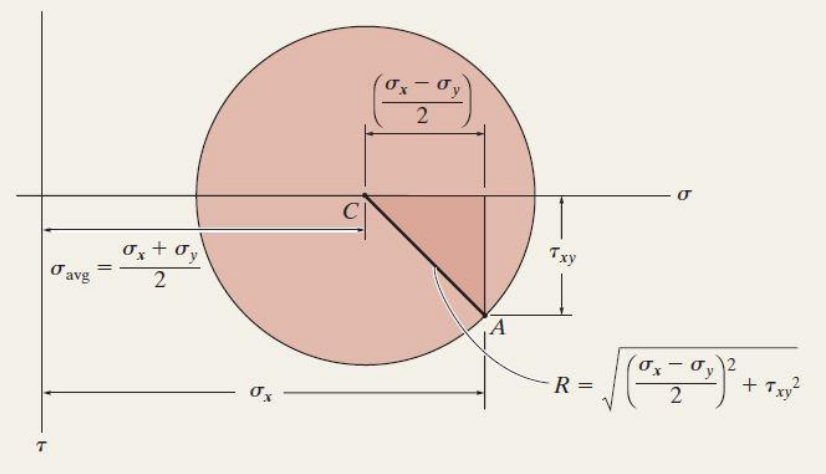

Figure 3: Mohr's circle explanation

If σ_1 and σ_2 are of the same sign, then the absolute maximum shear stress will lie out of plane.

$$\tau_{\substack{abs \\ max}} = \frac{\sigma_1}{2}$$

In the case of plane stress, the absolute maximum shear stress will be equal to the maximum in-plane shear stress provided the principal stresses σ_1 and σ_2 have the opposite sign [4].

$$\tau_{\substack{abs \\ max}} = \frac{\sigma_1 - \sigma_2}{2}$$

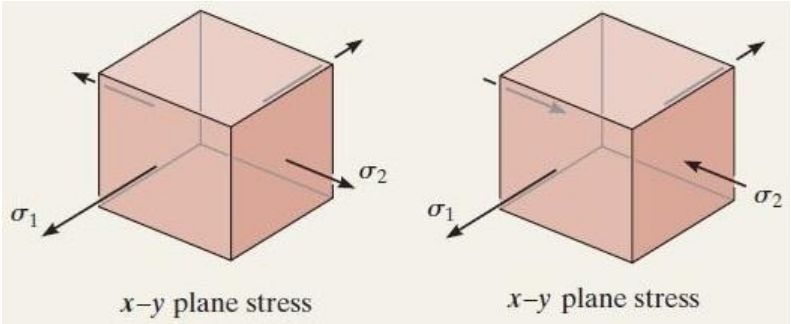

Figure 4: Absolute maximum shear stress

3. APPLICATION OF STRESSES

3.1.Tensile Test

Tensile testingis a fundamentalmaterials sciencetest in which a sample is subjected to a controlledtensionuntil failure. The results from the test are commonly used to select a material for an application, forquality control, and to predict how a material will react under other types offorces. Properties that are directly measured via a tensile test areultimate tensile strength, maximumelongationand reduction in area.From these measurements the following properties can also be determined:Young's modulus,Poisson's ratio,yield strength, andstrain-hardeningcharacteristics. And tension or tensile force will tend to lengthen the member [5].

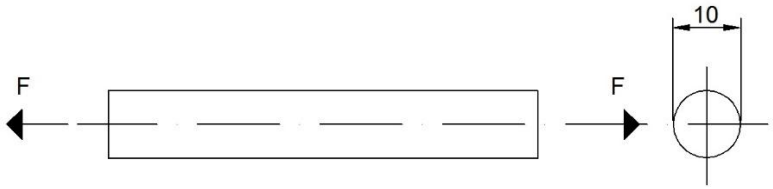

Figure 5: Drawing the bar

A bar that is applied the forces on the both edges of it.

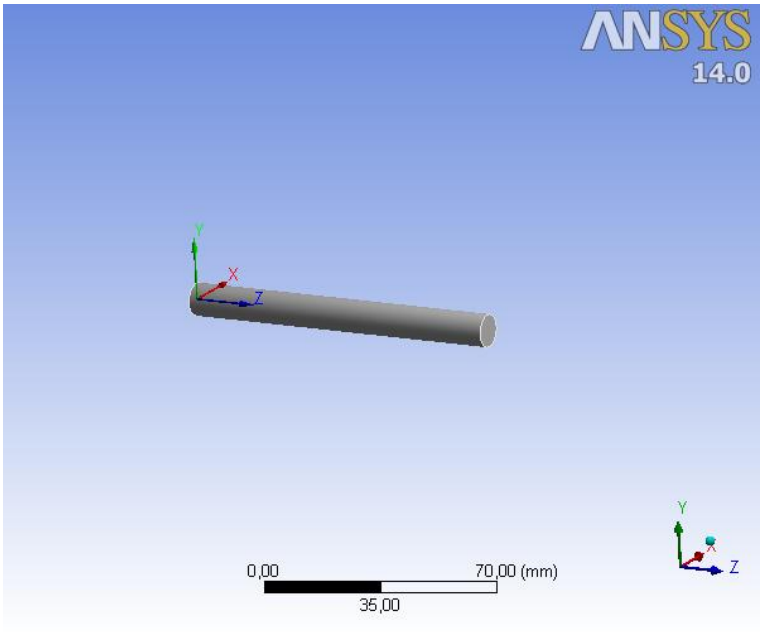

Figure 6: 3D drawing of the bar

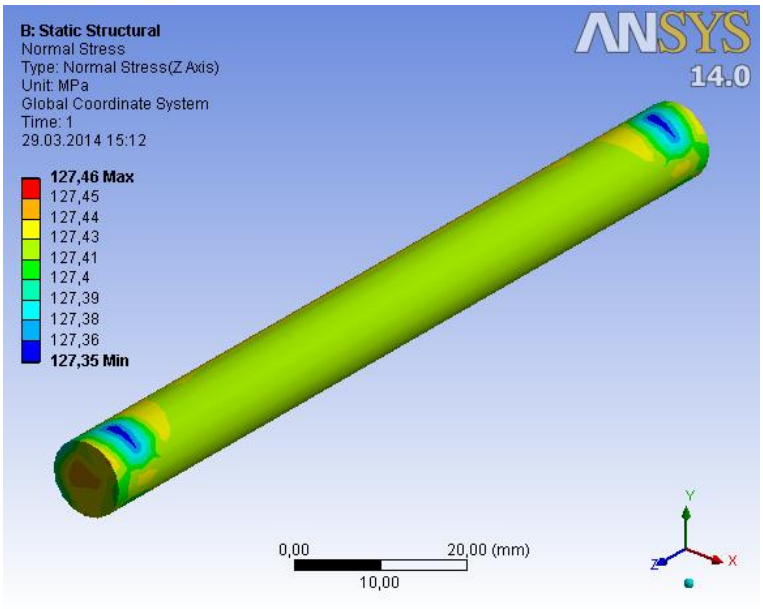

Figure 7: Stress distribution of the bar

Properties and dimensions of the member;

And numerical (ANSYS)result;

Material	Alloy steel
Tensile Yield Strength σ_y	250 MPa
Poisson's Ratio	0,3
Young's Modulus	210 GPa
Diameter	10 mm
F_n	10 kN
Normal Stress	127,46 MPa

Result from analytical calculation;

$$\sigma = \frac{F}{A}$$

$$\sigma = \frac{10x10^3}{\frac{\pi*(10*10^{-3})^2}{4}}$$

σ = 127 MPa

Hence, the results are close enough to confirm the analytical solution and numerical solution. It is shown in the table below;

Analytical Result	127 Mpa
Numerical (ANSYS) Result	127,46 MPa

3.2.Pressure Test

The pressure is applied inside of a pipe, and it is seen that maximum stress will occur inside of the pipe.

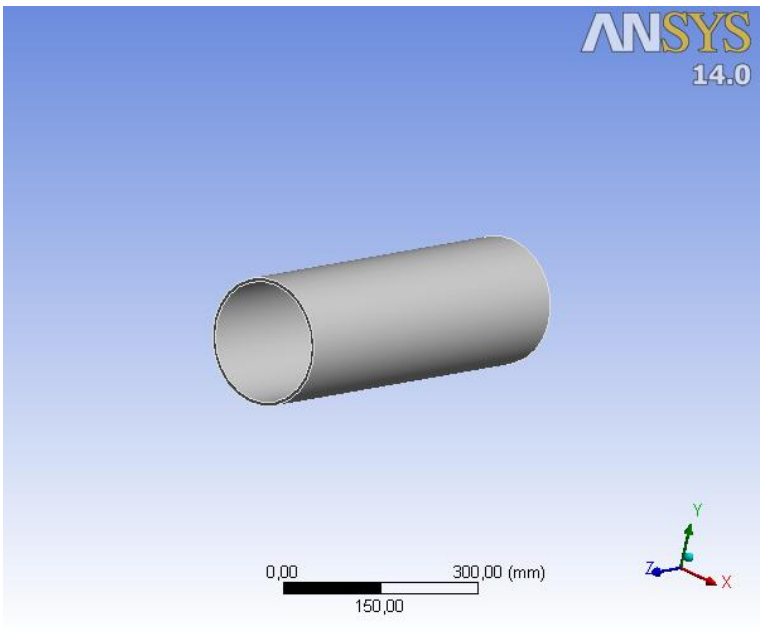

Figure 8: 3D model of the pipe

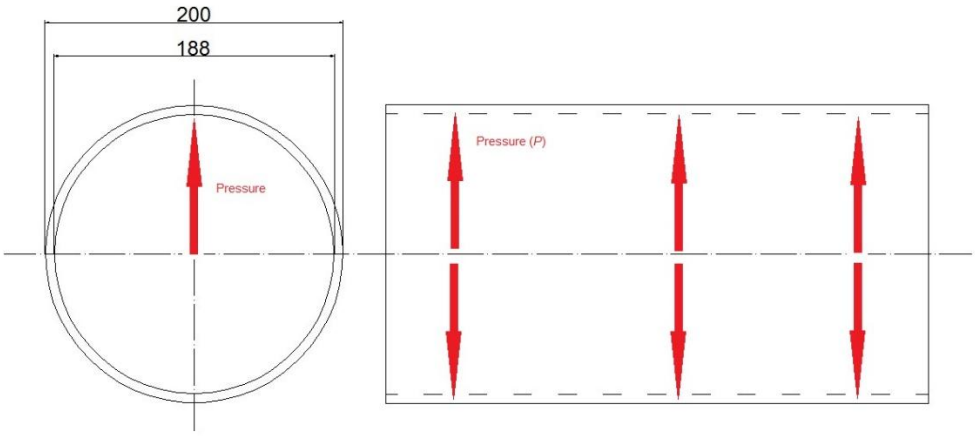

.

Figure 9: Drawing of the pipe (dimensions are in *mm*)

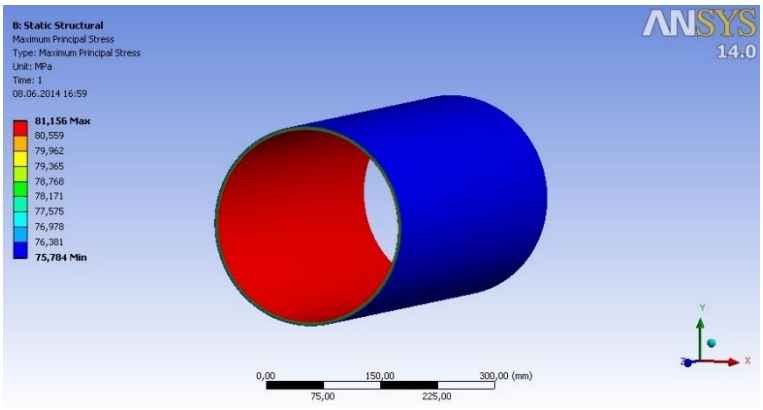

Figure 10: Stress distribution of the pipe

Properties and dimensions of the member;

And numerical (ANSYS)result;

Material	Alloy steel
Tensile Yield Strength σ_y	250 MPa
Poisson's Ratio	0,3
Young's Modulus	210 GPa
Out diameter	200 mm
Inner diameter	188 mm
Thickness	6 mm
Pressure	5 Mpa
Maximum Principal Stress	81.156 MPa

Result from analyticalcalculation;

OD = 200 mm

ID = 200-12= 188 mm

$R_i = \frac{188}{2} = 94$ mm

R_o = 100 mm

$t = \frac{200-188}{2} = 6$ mm

$\sigma_t = \frac{P\ x\ Ri}{t} \leq \sigma_{t,max}$

$\sigma_t = \frac{5\ x\ 94}{6} \leq \sigma_{t,max}$

$\sigma_{t,max}$ = 80 MPa

Hence, the results are close enough to confirm the analytical solution and numerical solution (ANSYS). It is shown in the table below;

Analytical result	80 MPa
Numerical (ANSYS) result	81.156 MPa

3.3.Combined Load

Force A, B and C are applied to the surface of the L and on the other surface of the L is fixed support with D that is shown in figure 11. Hence the purpose is to calculate the stresses on different forces [6].

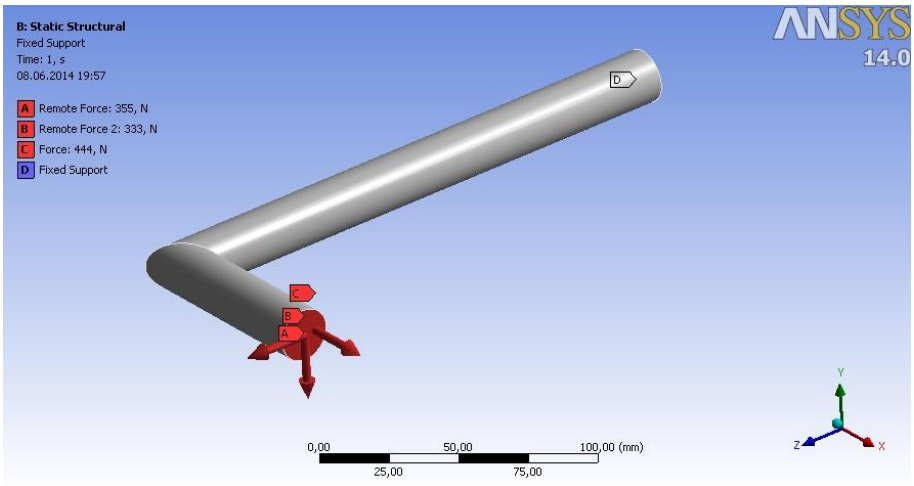

Figure 11: Forces on the L

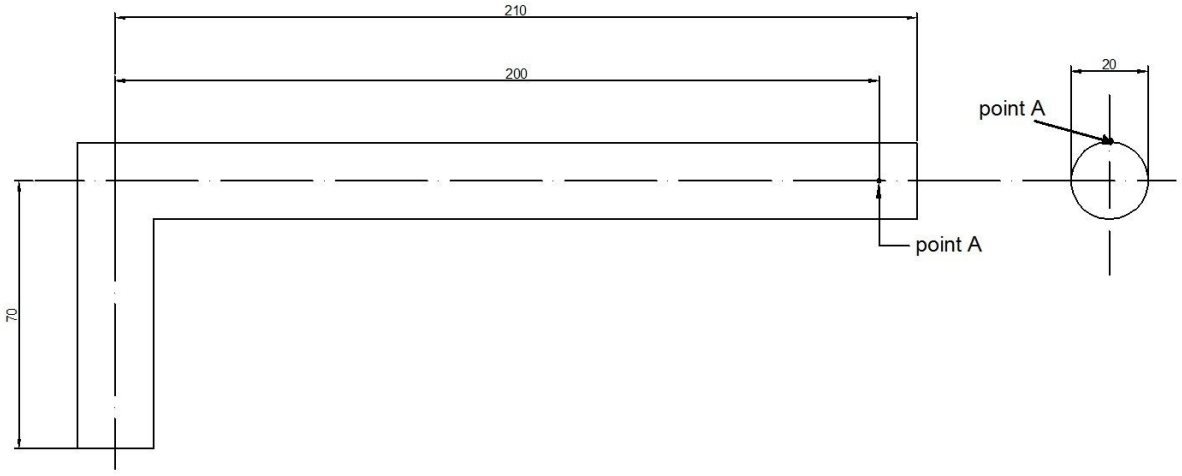

Figure 12: Dimension and the point of L (dimensions are in *mm*)

Properties of the member;

Material	Alloy steel
Tensile Yield Strength σ_y	250 MPa
Poisson's Ratio	0,3
Young's Modulus	210 GPa
Diameter	20 mm
Force A	355 N
Force B	333 N
Force C	444 N

All the calculations are made by manually in below, and each of it represents types of moment and type of forces that includes axial forces, transversal forces in 3D, torsion and bending moment in 2D.

F_x =333 N (axial tension)

F_y =355 N (transverse shear in y direction)

F_z =- 444 N (transverse shear in –z direction)

M_x=- ($7x10^{-2}$) x 355 = -24,85 Nm (torsion x-axis)

M_y=333 x 7 x 10^{-2}- 444 x 20 x 10^{-2}= -65,5 Nm (bending moment y-axis)

M_z= - 355 x 20 x 10^{-2} = -71 Nm (bending moment z-axis)

$A = \frac{\pi\, x\, d^2}{4} = 3{,}14\, x\, 10^{-4}$ m^2 (surface area)

$I = \frac{\pi\, x\, r^4}{4} = 7{,}854\, x\, 10^{-9}$ m^4 (moment of inertia)

$J = \frac{\pi\, x\, r^4}{2} = 1{,}57\, x\, 10^{-8}$ m^4 (polar moment of inertia)

$\sigma = \frac{F}{A} = \frac{333}{3{,}14\, x\, 10^{-4}} = 1{,}06\ MPa$ (Axial)

$\tau_{tor} = \frac{M_x\, r}{J} = \frac{24{,}85\, x\, 0{,}01}{1{,}57\, x\, 10^{-8}} = 15{,}82\ MPa$ (Torque)

$\tau_{xy} = \frac{4\,V}{3\,A} = \frac{4\, x\, 444}{3{,}14\, x\, 3\, x\, 10^{-4}} = 1{,}88\ MPa$ (Transversal shear)

$\sigma = \frac{M_z\, y}{I} = \frac{71\, x\, 0{,}01}{7{,}854\, x\, 10^{-9}} = 90{,}4\ MPa$ (Bending)

Thus, with those calculation, it will be calculated normal stress, shear stress, maximum principle stress, minimum principle stress in the next subtitles, and also the calculation of those stresses is explained in 2nd chapter as theory.

3.3.1. Normal Stress

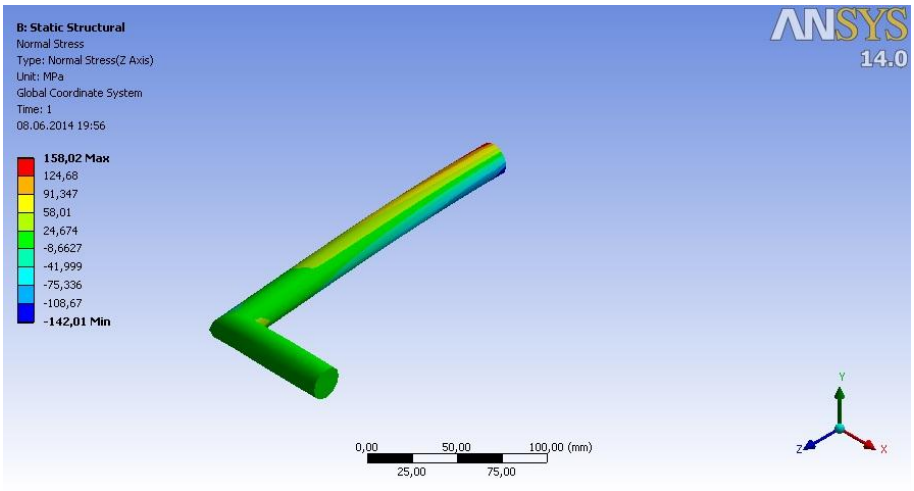

Figure 13: Normal stress

σ_x= 1,06 + 90,4 = 91,46 MPa

τ= 0

A stress is defined as the load divided by the area. For a normal stress, it is all loads perpendicular to the surface.

3.3.2. Shear Stress

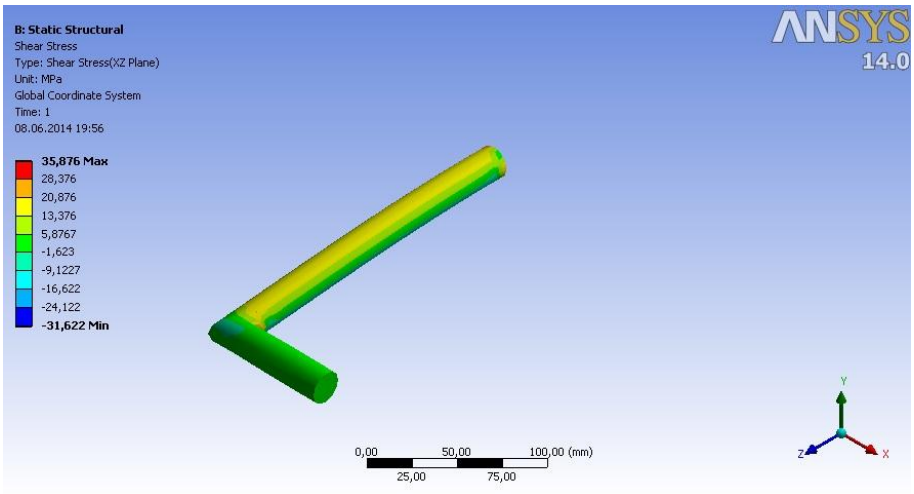

Figure 14: Shear stress

σ= 91,46 MPa

$\tau = \tau_{xy} + \tau_{tor}$ = 1,88 + 15,82 = 17,7 MPa

Shear stress is a stress state where the stress is parallel to the surface of the material, as opposed to normal stress when the stress is vertical to the surface.

3.3.3. Maximum Principle Stress

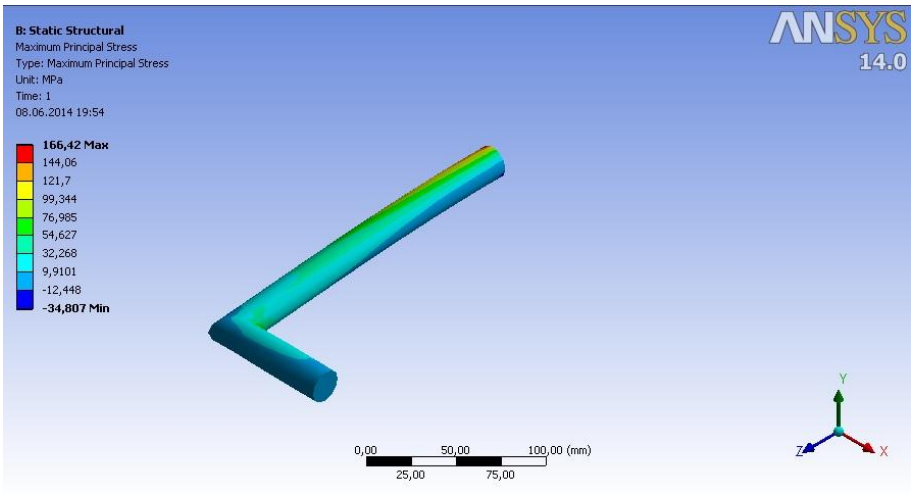

Figure 15: Max principle stress

$$R = \sqrt{(91{,}46/2)^2 + 17{,}7} = 45{,}92$$

$$\sigma_1 = \frac{91{,}46}{2} + 45{,}92 = 91{,}65\ MPa$$

3.3.4. Minimum Principle Stress

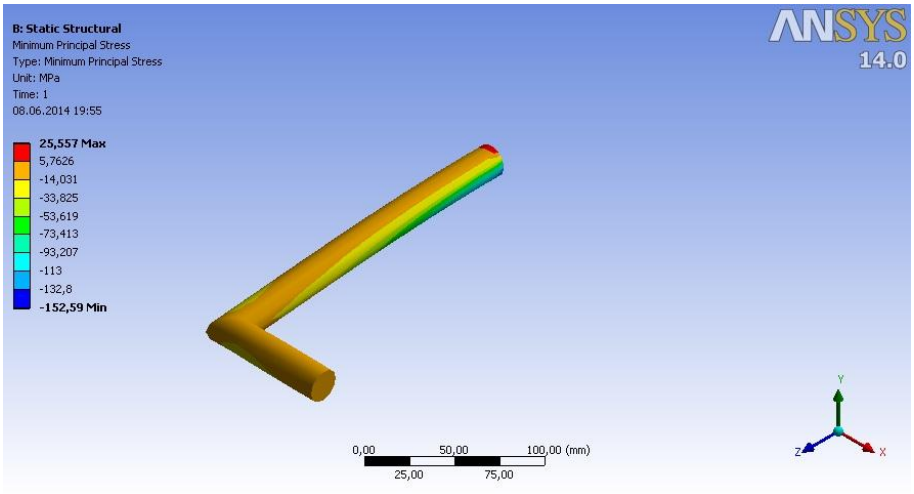

Figure 16: Min principle stress

$$R = \sqrt{(91{,}46/2)^2 + 17{,}7} = 45{,}92$$

$$\sigma_2 = \frac{91{,}46}{2} - 45{,}92 = -0{,}19\ MPa$$

3.3.5. Results

Analytical (manual) Results	
Normal Stress	91,46 Mpa
Shear Stress	17,7 MPa
Max Principle Stress	91,65 MPa

Min Principle Stress	-0,19 MPa

Numerical (Ansys) Results	
Normal Stress	91,347 Mpa
Shear Stress	13 $<\tau<$ 20 MPa
Max Principle Stress	76 $<\sigma_1<$ 99 MPa
Min Principle Stress	-14$<\sigma_2<$ 5 MPa

Hence, results which including analytical and numerical are compared, and it is confirmed in the tables above.

The mesh size must depend on the element size and it is an important topic in a finite element method because of its relationship to accuracy. As the element size increases, it is seen that the results become more accurate and almost constant in table above [7].

4. CONCLUSION

Finite element modelling of the members in some forces was examined in detail in chapter 3, and it is confirmed that the manual solutions and analytical solutions are verified. Hence it is proven that the software (ANSYS) is reliable,and it is considered that ANSYS results are true since the results approach each other and it is nearly constant. Also, in the chapter 4, it is tested only with numerical solution, it is seen that results are nearly constant and more accurate when element sizing is 40, 50 and 60 for both maximum principle stresses and minimum principle stresses.

REFERENCES

1. M.J.Fagan. Finite Element Analysis-Theory and Practices, Longman Group UK Ltd, 1992.
2. W. O. Jolley, J .J. Rencis, and H. T. Grandin, Jr., “A Module for Teaching Fundamentals of Finite Element , Theory and Practice Using Elementary Mechanics of Materials”, Proceedings of the 2003 American , Society for Engineering Education Annual Conference & Exposition, Nashville, Tennessee, June 2003.
3. B.J. Hamrock, B. Jacobson, S. R. Schmid, “Fundamentals of Machine Elements”, 1999.
4. R. C. Hibbeler, “Mechanics of Materials”, 8th edition in SI units, Prentice-Hall, 2011.
5. Budynas, R. G., & Nisbett, J. K., “Shigley's Mechanical Engineering Design”, New York: McGraw-Hill, 2008.
6. V.B.Bhandari, “Design of Machine Elements”, Tata McGraw Hill, New Delhi, 2010.
7. R. L. Norton, “Machine Design: An Integrated Approach”, 2nd edition, Prentice-Hall,New Jersey, 2000.

ISSN 2303-4521

PERIODICALS OF ENGINEERING AND NATURAL SCIENCES
Vol. 4 No. 1 (2016)
Available online at: http://pen.ius.edu.ba

Alcohol Modulation of Extra-synaptic Gamma-aminobutyric Acid Type A Receptors

Ayla Arslan

International University of Sarajevo, Faculty of Engineering and Natural Sciences, Department of Genetics and Bioengineering, Hrasnicka Cesta 15, Ilidža 71210 Sarajevo, Bosnia and Herzegovina

Abstract
Development of effective treatment agents for the alcohol use disorders requires the detailed understanding of molecular targets of alcohol in the brain. The gamma-aminobutyric acid type A receptors ($GABA_ARs$) are the major molecular targets of alcohol in the central nervous system. Mediating inhibitory neurotransmission upon GABA binding in the vertebrate central nervous system, $GABA_ARs$ are heteropentameric chloride channels, assembled from a large subunit pool encoded by 19 distinct genes. It is the subunit composition that determines the receptor's biophysical properties, neurotransmitter affinity, the pharmacology, and the position on the cell i.e., synaptic or extra-synaptic. This review paper briefly presents the alcohol modulation of a specific GABAAR subtype located at the extra-synaptic sites with a subunit composition of α, β and δ.

Keywords: Alcohol, GABA, extra-synaptic, GABA (A) receptors, δ (delta) subunit

1. Introduction

Affecting about 18 millions of adult Americans, alcohol abuse and alcohol dependence are classified as alcohol use disorders (AUD), which are not satisfactorily treatable. For example, Benzodiazepines (BZs), used for the treatment of symptoms of AUDs, cause addiction and Naltrexone, despite being an effective therapeutic agent, has severe side effects (Liang and Olsen, 2014). Thus, development of better treatment agents for the AUDs is essential which requires a detailed understanding of molecular targets of alcohol.

Accumulating evidence in the literature suggests that gamma-aminobutyric acid type A receptors ($GABA_ARs$) are the major target of alcohol in the brain (Mihic and Harris, 1997; Boehm et al., 2004; Kumar et al., 2009). $GABA_ARs$ are the member of "Cys-loop receptors" together with nicotinic acetylcholine receptors (nAChR), the 5- hydroxytryptamine type 3 ($5\text{-}HT_3$) receptors, the zinc-activated ion channel (ZAC) and the glycine receptors (GlyR) (reviewed in Sine and Engel, 2006). They are GABA-gated heteropentameric chloride channels responsible for the fast inhibitory synaptic transmission in the vertebrate central nervous system (CNS) (reviewed by Sieghart and Sperk 2002). The $GABA_ARs$ display a rich molecular and cellular diversity, which result in distinct functional roles. Assembled from a large subunit pool, receptor subunit composition affects the receptor gating, kinetics and the response to allosteric modulators (Haas and Macdonald, 1999; Lavoie, et al., 1997). Besides, subunit composition is a determinant of the cellular and subcellular localization of the receptor, i.e., synaptic or extra-synaptic sites (Jones et al, 1997; Brickley et al., 2001; Goetz et al., 2007).

2. The Subunit Composition of $GABA_ARs$: Synaptic and Extra-synaptic Receptors

One of the most distinguishing features of $GABA_ARs$ is the wide repertoire of subunits from which the receptor assembles (Seeburg et al., 1990). The $GABA_ARs$ are assembled from a pool of 19 subunits ($\alpha1-\alpha6$, $\beta1-\beta3$, $\gamma1-\gamma3$, δ, ε, θ, π, $\rho1-\rho3$) (Rudolph and Mohler, 2006). The expression of the subunit genes is age- and region dependent (Wisden et al., 1992; Laurie et al., 1992a, b; Fritschy and Mohler, 1995; Schwarzer et al., 2001). The most abundant $GABA_ARs$ in the mammalian brain seem to be the combination of $\alpha\beta\gamma2$ subunits with a subunit ratio of $2\alpha/2\beta/1\gamma$ (Ernst et al., 2003). These $\gamma2$ containing $GABA_ARs$ ($\gamma2\text{-}GABA_ARs$) mediate classical fast synaptic inhibition (phasic inhibition) and massively clustered in the synapses. On the other hand δ subunit containing $GABA_ARs$ receptors ($\delta\text{-}GABA_ARs$), typically in combination with $\alpha6$ and β subunits in the cerebellum (Jones et al, 1997; Brickley et al., 2001); and in combination with $\alpha4$ and β subunits (Patel et al., 2014) in the forebrain, are located extra-synaptically or perisynaptically (Nusser et al., 1998; Wei et al., 2003). Activated by GABA diffusing out of the synaptic cleft, these receptors mediate a special form of inhibition called the tonic inhibition characterized by a higher affinity for GABA and with a slower

DOI: 10.21533/pen.v4i1.48

Reviewed by Prof. Dr. Kemal Yelekci (Kadir Has University), Assoc. Prof. Dr. Tunç Çatal (Uskudar University)

desensitization rate (Nusser and Mody, 2002). Tonic inhibition is critical for the threshold for the action potential generation. It shunts the excitatory synaptic signals controlling neuronal excitability (Hamann, et al., 2002, Semyanov et al., 2004). Thus the extra-synaptic $GABA_A$Rs mediate a physiologically different form of GABAergic signaling than the synaptic receptors (Brickley and Mody 2012). The diversity of $GABA_A$R subunits with distinct physiological functions (Mody and Pearce, 2004) is also apparent at the level of its ligands. Benzodiazepines, barbiturates, alcohol and neurosteoids are the modulators of $GABA_A$Rs with differences in efficacy, potency and binding sites in a subunit dependent manner (Goetz et al, 2007). In this study we will present the alcohol modulation of extra-synaptic receptors containing $\alpha4\beta\delta$ or $\alpha6\beta\delta$ subunits (δ-$GABA_A$Rs).

3. The structure of the $GABA_A$Rs

Until last year, the molecular structure of a $GABA_A$R subunit complex was based on the studies of the muscle nAChR from the electric organ of the torpedo ray and the snail acetylcholine receptor binding protein (AChBP) (Brejc et al., 2001; Cromer et al., 2002; Ernst et al., 2003; Unwin, 2003, 2005; Sine and Engel, 2006). However, the recent work done by Miller and Aricescu (2014) reports the crystallized structure of homomeric $\beta3$ subunit containing $GABA_A$Rs ($GABA_A$R-$\beta3$cryst) at 3Å resolution which provides a direct overview for the receptor structure for the first time. Together with the recent structural data from $5HT_3$ receptors (Hassaine et al., 2014), these studies confirm the characteristics of eukaryotic Cys-loop receptors (reviewed by Lynagh and Pless, 2014).

$GABA_A$Rs are pentamers consist of five subunits arranged counterclockwise (i.e., $\gamma, \alpha, \beta,$) around a central pore. Each subunit comprises a long N- terminus located at the extracellular domain (ECD), followed by four transmembrane domains (TM1–TM4), and a short extracellular C-terminal. There is a large intracellular loop between the third and fourth transmembrane domains. According to Miller and Aricescu (2014) the receptor looks like a cylinder with a height of 110Å and with a diameter of 60 to 80Å. From the extracellular side, the receptor is surrounded by 15 N-linked glycans. Each extracellular domain (ECD) comprises an amino-terminal α-helix ($\alpha1$) followed by ten β–strands in parallel with the structure of other family members (reviewed in Lynagh and Pless, 2014). A second α–helix ($\alpha2$), between β-strands 3 and 4, is located under the $\alpha1$ helix. The pentameric transmembrane domain (TMD) is composed of four additional helices (M1–M4) from each subunit that come together to form a lining a pore with M2 segments. The subunit assembly is mediated by hydrogen bonds, van der Waals forces and salt bridges in the subunit ECDs, which also involve the neurotransmitter binding pocket.

When subunits are assembled in to the heteropentameric receptor, the neurotransmitter binding pocket, i.e., the GABA binding site, is located at the interface between N terminus extracellular domains of the β and α subunits, which constitutes a "principal face" and a "complementary face", respectively. As reported by Miller and Aricescu (2014), the principal face of human $GABA_A$R involves the $\beta4$ strand and residues Asp95-Leu99, Glu155-Tyr159, Phe200-Tyr205 in the β subunit. The complementary face corresponds to the residues Tyr62-Gln64 and Leu125-Arg129 in the α subunit. On the other hand, agonist sensitivity seems to be affected also by the motifs, which are not located in the neurotransmitter binding pocket (Korpi and Luddens, 1993; Böhme et al., 2004). For example a domain (S238-V264) in the δ subunit might be important for the high agonist affinity of the extra-synaptic $\alpha4\beta3\delta$ receptors (You and Dunn, 2007) compared to synaptic $\gamma2$ containing receptors. Thus, following the formation of receptor and agonist complex at the neurotransmitter binding site, the agonist affinity and efficacy might be affected by all subunits (see Unwin 2005).

4. Alcohol modulation $GABA_A$Rs

Alcohol has profound effects in the brain. Interacting with multiple neurotransmitter systems (Valenzuela CF., 1997), its impact is characterized by intoxicating, sedative, anxiolytic and addictive features in the behavioral level (Bayard et al., 2004). Ethanol affects many ion channels, including the NMDA glutamate receptors (Hanchar et al., 2005). In the CNS, $GABA_A$Rs are the major targets of alcohol (Mihic and Harris, 1997; Boehm et al., 2004; Hanchar et al., 2005; Kumar et al., 2009). In addition to direct allosteric effect of ethanol on $GABA_A$Rs (Deitrich et al., 1989), there are also indirect effects on the receptor due to ethanol mediated increase in the levels of presynaptic release of GABA (Yang et al., 2000; Roberto et al., 2003; Ming et al., 2006; Theile et al., 2008; Mameli et al., 2008) and neuroactive steroids (Caldeira et al., 2004; Mameli and Valenzula 2006; Izumi et al., 2007), which are the modulators of GABA receptors. Besides, ethanol affects the phosphorylation of $GABA_A$Rs, which in turn lead to an increase in the GABA sensitivity (Hodge et al., 1999, 2002; Kumar S., 2009). For allosteric effects, ethanol sensitivity depends on the $GABA_A$R subtypes. In general $\gamma2$- $GABA_A$R subtypes are sensitive to ethanol at doses attained by severe intoxication (Kumar S., 2009). The extra-synaptic δ–GABAARs are thought to be most

sensitive to ethanol, which will be discussed in the following section.

5. Alcohol and extra-synaptic $GABA_ARs$

In general, 1-3 mM blood ethanol levels can result from drinking half a glass of wine or less (Goetz et al 2007). This is especially important as the extra-synaptic δ–$GABA_ARs$ are thought to be most sensitive to ethanol at levels of social drinking, i.e., less than 30 mM (Sundstrom-Poromaa et al., 2002; Wallner et al., 2003, 2006; Wei et al., 2003; Hanchar et al., 2005; 2006; Santhakumar et. al., 2007; Glykys et al., 2007; Mody et al., 2007; Olsen et al., 2007). Studies of δ subunit knock out mice have shown the impact of extra-synaptic δ - $GABA_ARs$ for mediating the effects of ethanol (Mihalek et al., 2001). These mice show less responsiveness to the anticonvulsant effects of ethanol, a decreased response of excitability to ethanol withdrawal, and a less preference for ethanol compared to wild-type mice. This phenomenon is dependent on β subunit with β3 isoform providing maximal sensitivity to ethanol (Wallner et al., 2003).

A direct evidence of the effect of ethanol via δ-$GABA_ARs$ on cerebellar granule cells has been shown by the R100Q mutation in the α6 subunits of the alcohol non-tolerant rats. Cerebellar granule cells express the extra-synaptic receptors with a specific partnership of α6 and δ subunits together with the β subunit (Jones et al., 1997; Brickley et al., 2001). Rats homozygous for the mutation (α6-100QQ) have an increased alcohol-induced ataxia and they have an increased activity of α6βδ receptors enhanced by alcohol in cerebellar granule cells (Hanchar et al., 2005, 2006). On the other hand α6 knock-out mice do not show any distortion of alcohol sensitivity (Homanics et al., 1997). However, this may result from the adaptive responses of the cerebellar granule cells to the absence of α6 subunits, which could mask the relation of corresponding receptors (α6 and β subunits which has a specific partnership with δ subunit in the cerebellum) and ethanol actions. Indeed, the α6 subunit knock-out mice have increased expression of TASK-1 channel in these cells, which may impact on ethanol sensitivity. In line with this, TASK-1 knock-out mice are more sensitive to ethanol in behavioral level, which might explain the unchanged ethanol sensitivities of α6 knockout mice of $GABA_AR$ (reviewed by Korpi et al., 2007). Other experiments done with the recombinant expression systems have shown that 3-30 mM alcohol is enough to activate δα4β and δα6β subunit containing receptors (Wallner et al., 2003; 2006; Sundstrom-Poromaa et al., 2002). This effect is shown to increase the tonic inhibition (Wei et al., 2003; Hanchar et al., 2005; Glykys et al., 2007; Santhakumar et al., 2007; Liang et al., 2008), the specific form of inhibition mediated by the δ-$GABA_ARs$.

As a result, several lines of evidences from the studies of recombinant expression systems and electrophysiological recordings converge on the hypothesis that physiologically relevant, low dose (less than 50 mM) actions of ethanol is mediated by extra-synaptic δ- $GABA_ARs$. Thus, a glass of wine activating the extra-synaptic receptors could potentiate GABAergic tonic inhibition in the striatum and cerebellum via α4β3δ and α6βδ receptors respectively (Hanchar et al., 2005, 2006; Olsen et al., 2007).

On the other hand, these results generated some controversy in the field as the findings regarding the high alcohol affinity of the extra-synaptic receptors have not been replicated by some groups and presynaptic mechanisms have been proposed for the alcohol potentiation of GABAergic system (Carta et al., 2004; Borghese et al., 2006; Botta et al., 2007a, b; Korpi et al., 2007; Baur 2009). Several experimental errors or methodological issues may cause this contradiction. For example, in one of the studies who fail to replicate the physiologically relevant alcohol potentiation of extra-synaptic receptors (Botta et al., 2007), the magnitude of GABAergic tonic currents has been described as 55 pA, which is much higher than tonic currents (i.e., less than 30 pA) described in many other studies for the comparative age and cell types of rodents (cited in Otis, 2008). δ subunit is a rare isoform of GABA receptor subunits by means of its distribution in the brain: Its expression is restricted to cerebellar granule cells (Jones et al., 1997), dentate gyrus granule cells in the hippocampus (Sun et al., 2004) and ventrobasal nucleus of the thalamus and neocortex (Cope et al., 2005; Glykys et al., 2007). Thus, it is reasonable to expect some experimental caveats for the *in vitro* ectopic expression of δ- $GABA_ARs$ (Arslan et al., 2014). For example, in vitro expression of recombinant δ subunit is generated variable results by means of clustering on the cell membrane. Regarding this, one study reported that *in vitro* expression of recombinant δ subunit shows a diffusely distributed pattern on the cell membrane but *in vivo* studies show that δ subunit containing receptors form clusters (Sun et al., 2004). In parallel with the latter finding, Arslan et al., (2014) reported that recombinant δ subunit when expressed in the primary cultures of hippocampal neurons gave a punctate immunostaining on non-permabilized cells. Here it is important to consider many factors that could contribute to this discrepancy. For example Arslan et al. (2014) used N-terminus GFP tagged version of δ subunit where as Christie et al (2006) used the

C-terminus GFP tagged version of this subunit. Also, low *in vitro* expression profile of recombinant δ subunit (Arslan et al., 2014) and its restricted ability to form functional receptors *in vitro* may produce experimental failures (Olsen et al., 2007; Santhakumar et al., 2007; Otis, 2008). Moreover there are some possible effect of species differences in alcohol and alcohol antagonist responses (Wallner, et al., 2014). For example, a recent study suggests that there are some significant differences in the pharmacology of murine and human α4β1δ receptors (Villumsen et al., 2015). Therefore, it is clear that methodological issues should be carefully considered for studies with δ- $GABA_A$Rs in general and for the effects of alcohol on these receptors in particular.

6. Alcohol binding site

Perhaps a direct evidence for the ethanol enhancement of δ-$GABA_A$Rs would come from studies showing the alcohol binding site on the δ-$GABA_A$Rs. For the synaptic receptors like α1β2γ2 containing ones, mutagenesis and labeling studies have led to the identification of several amino acid residues in transmembrane domain critical for alcohol modulation. For example, site directed mutagenesis studies identified S270 and A291 on the second and third transmembrane domain of α subunit of $GABA_A$Rs critical for allosteric modulation by alcohol (and volatile anesthetics) (Mihic et al., 1997). Many of these residues are involved in the enhancement of receptor function by alcohol as positive allosteric modulator (Mihic et al., 1997; Jenkins et al., 2001; 2002; McCracken et al., 2010).

Regarding extra-synaptic δ-$GABA_A$Rs several studies have reported that a competitive antagonist of ethanol, Ro15-4513, prevents many of the behavioral aspects of ethanol intoxication (Suzdak et al., 1986; Lüddens et al., 1990; Hanchar et al., 2006, Wallner et al., 2006). Experiments utilizing the radiolabeled Ro15-4513 have shown that ethanol can displace Ro15-4513 on the δ subunit (Hanchar et al., 2006, Wallner et al., 2006). Addressing this, a new extracellular alcohol/imidazobenzodiazepine (Ro15-4513) site has been identified for the δ-$GABA_A$Rs (Wallner et al., 2014). By the use of site directed mutagenesis experiments and homology modeling, Wallner et al. (2014) have shown that this site, involving the residue Y76 in the β3 subunit, is located at the interface between the α4/α6 and β3 subunit of δ-$GABA_A$Rs and matches with the residue (γ2 T81) of benzodiazepine site of γ2 - $GABA_A$Rs. Thus the binding site of ethanol is likely located at a site on extra-synaptic δ-$GABA_A$Rs corresponding to benzodiazepine site of synaptic γ2 - $GABA_A$Rs.

7. Conclusion

The current pharmacotherapy for AUDs is not effective satisfactorily (Liang and Olsen 2014). Development of better treatment agents for the AUDs requires the detailed understanding of molecular targets of alcohol relevant to its effects in the brain. Accumulating evidences from the studies of recombinant expression systems, electrophysiological recordings from the neurons and labeling experiments converge on the hypothesis that physiologically relevant, low dose actions of ethanol is mediated by extra-synaptic δ-$GABA_A$Rs. This action is likely to occur by an allosteric mechanism corresponding to a BZ site in the ECD of the δ- $GABA_A$Rs (Wallner et al., 2014). But the ethanol action on $GABA_A$Rs does not seem to be limited to one site. Probably there are multiple sites, some of which are physiologically critical while others not (Mihic et al., 1997; Jenkins et al., 2001; 2002; McCracken et al., 2010; Wallner et al., 2014). Current developments in our understanding of the structure of $GABA_A$Rs (Miller and Aricescu, 2014) and related proteins from eukaryotic and prokaryotic organisms (reviewed by Lynagh and Pless, 2014) will likely answer these questions and initiate new opportunities addressing the alcohol actions on $GABA_A$Rs. Based on the available X-ray data, molecular dynamics (MD) simulations have the potential to offer an atomic level dynamics of the conformational changes on the receptor during the process of signal transmission, and the effect of allosteric modulators on this process. These opportunities will not only lead to the verification of present data and clarification of inconsistencies in the literature described so far but also elucidation of allosteric interactions of ethanol besides to other $GABA_A$R modulators at level of atomic scales for better perspectives of drug design. Thus, a significant progress is expected in the field to address the mechanism of allosteric modulation of various ligands besides to ethanol on different subtypes of $GABA_A$Rs, including extra-synaptic δ-$GABA_A$Rs.
subtypes.

References

Arslan A, von Engelhardt J, Wisden W. (2014) Cytoplasmic domain of δ subunit is important for the extra-synaptic targeting of GABAA receptor subtypes. J Integr Neurosci. Dec; 13(4):617-31.

Bayard M, McIntyre J, Hill KR, Woodside J Jr. (2004) Alcohol withdrawal syndrome. Am Fam Physician. 2004 Mar 15; 69(6):1443-50.

Boehm SL 2nd, Ponomarev I, Jennings AW, Whiting PJ, Rosahl TW, Garrett EM, Blednov YA, Harris RA. (2004) gamma-Aminobutyric acid A receptor subunit mutant mice: new perspectives on alcohol actions. Biochem Pharmacol. Oct 15;68(8):1581-602.

Borghese CM, Stórustovu Sí, Ebert B, Herd MB, Belelli D, Lambert JJ, Marshall G, Wafford KA, Harris RA. (2006) The delta subunit of gamma-aminobutyric acid type A receptors does not confer sensitivity to low concentrations of ethanol. J.
Pharmacol Exp Ther. Mar; 316(3):1360-8.

Botta P, Mameli M, Floyd KL, Radcliffe RA, Valenzuela CF. (2007a) Ethanol sensitivity of GABAergic currents in cerebellar granule neurons is not increased by a single amino acid change (R100Q) in the alpha6 GABAA receptor subunit. J Pharmacol Exp Ther. Nov; 323(2):684-91.

Botta P, Radcliffe RA, Carta M, Mameli M, Daly E, Floyd KL, Deitrich RA, Valenzuela CF. (2007b) Modulation of GABAA receptors in cerebellar granule neurons by ethanol: a review of genetic and electrophysiological studies. Alcohol. 2007 May; 41(3):187-99.

Bonnert, T.P., McKernan, R.M., Farrar, S., le Bourdelles, B., Heavens, R.P., Smith, D.W., Hewson, L., Rigby, M.R., Sirinathsinghji, D.J., Brown, N., Wafford, K.A., Whiting, P.J. (1999) A novel g-aminobutyric acid type A receptor subunit. Proc Natl Acad Sci U S A, 96:9891-9896.

Böhme I, Rabe H, Lüddens H. (2004) Four amino acids in the alpha subunits determine the gamma-aminobutyric acid sensitivities of GABAA receptor subtypes. J Biol Chem. 2004 Aug 20; 279(34):35193-200.

Brejc, K., van Dijk, W.J., Klaassen, R.V., Schuurmans, M., van Der Oost, J., Smit, A.B., Sixma, T.K. (2001) Crystal structure of an ACh-binding protein reveals the ligand-binding domain of nicotinic receptors. Nature, 411:269-276.

Brickley, S.G., Revilla, V., Cull-Candy, S.G., Wisden, W., Farrant, M. (2001) Adaptive regulation of neuronal excitability by a voltage-independent potassium conductance. *Nature*, 409:88-92.

Brickley SG, Mody I. (2012) Extrasynaptic GABA(A) receptors: their function in the CNS and implications for disease. Neuron. 2012 Jan 12;73(1):23-34.

Cromer BA, Morton CJ, Parker MW. Anxiety over GABA(A) receptor structure relieved by AChBP. Trends Biochem Sci. 2002 Jun; 27(6):280-7.

Caldeira JC, Wu Y, Mameli M, Purdy RH, Li PK, Akwa Y, Savage DD, Engen JR, Valenzuela CF. (2004) Fetal alcohol exposure alters neurosteroid levels in the developing rat brain. J Neurochem. Sep; 90(6):1530-9.

Carta M, Mameli M, Valenzuela CF. (2004) Alcohol enhances GABAergic transmission to cerebellar granule cells via an increase in Golgi cell excitability. J Neurosci. Apr 14; 24(15):3746-51.

Cope, D.W., Hughes, S.W., Crunelli, V. (2005) GABAA receptor-mediated tonic inhibition in thalamic neurons. J Neurosci., 25:11553-11563.

Deitrich RA, Dunwiddie TV, Harris RA, Erwin VG. Mechanism of action of ethanol: initial central nervous system actions. Pharmacol Rev. 1989 Dec;41(4):489-537.

Ernst, M., Brauchart, D., Boresch, S., Sieghart, W. (2003) Comparative modeling of GABAA receptors: limits, insights, future developments. Neuroscience, 119:933-943.

Fritschy, J.M., Mohler, H. (1995) GABAA-receptor heterogeneity in the adult rat brain: differential regional and cellular distribution of seven major subunits. J Comp Neurol., 359:154-194.

Glykys J, Peng Z, Chandra D, Homanics GE, Houser CR, Mody I. (2007) A new naturally occurring GABA(A) receptor subunit partnership with high sensitivity to ethanol. Nat Neurosci. Jan;10(1):40-8.

Goetz, T., Arslan, A., Wisden, W., Wulff, P., (2007) GABAA receptor structure and function in the basal ganglia. Prog. Brain Res. 160: 21-41.

Haas KF, Macdonald RL. (1999) GABAA receptor subunit gamma2 and delta subtypes confer unique kinetic properties on recombinant GABAA receptor currents in mouse fibroblasts. J Physiol. 1; 514 (Pt 1): 27-45.

Hamann, M., Rossi, D.J., Attwell, D., (2002) Tonic and spillover inhibition of granule cells control information flow through cerebellar cortex. Neuron 33(4): 625-33.

Hanchar, H.J., Wallner, M., Olsen, R.W. (2004) Alcohol effects on g-aminobutyric acid type A receptors: are extra-synaptic receptors the answer? Life Sciences, 76:1–8.

Hanchar, H.J., Dodson, P.D., Olsen, R.W., Otis, T.S., Wallner, M. (2005) Alcohol-induced motor impairment caused by increased extra-synaptic GABAA receptor activity. Nat Neurosci., 8:339-345.

Hanchar HJ, Chutsrinopkun P, Meera P, Supavilai P, Sieghart W, Wallner M, Olsen RW. (2006) Ethanol potently and competitively inhibits binding of the alcohol antagonist Ro15-4513 to alpha4/6beta3delta GABAA receptors. Proc Natl Acad Sci U S A. 103(22):8546-51.

Hassaine G, Deluz C, Grasso L, Wyss R, Tol MB, Hovius R, Graff A, Stahlberg H, Tomizaki T, Desmyter A, Moreau C, Li XD, Poitevin F, Vogel H, Nury H. (2014) X-ray structure of the mouse serotonin 5-HT3 receptor. Nature, 21; 512(7514):276-81. doi: 10.1038/nature13552.

Hausser, M. and Clark, B.A. (1997) Tonic synaptic inhibition modulates neuronal output pattern and spatiotemporal synaptic integration Neuron 19 (3) 665-78.

Hodge, C.W., Mehmert, K.K., Kelley, S.P., McMahon, T., Haywood, A., Olive, M.F., Wang, D., Sanchez-Perez, A.M., Messing, R.O. (1999) Supersensitivity to allosteric GABAA receptor modulators and alcohol in mice lacking PKC epsilon. Nat Neurosci., 2:997-1002.

Homanics GE, Ferguson C, Quinlan JJ, Daggett J, Snyder K, Lagenaur C, Mi ZP, Wang XH, Grayson DR, Firestone LL. Gene knockout of the alpha6 subunit of the gamma-aminobutyric acid type A receptor: lack of effect on responses to ethanol, pentobarbital, and general anesthetics. Mol Pharmacol. 1997 Apr; 51(4):588-96.

Homanics GE, Le NQ, Kist F, Mihalek R, Hart AR, Quinlan JJ. (1998) Ethanol tolerance and withdrawal responses in GABA(A) receptor alpha 6 subunit null allele mice and in inbred C57BL/6J and strain 129/SvJ mice. Alcohol Clin Exp Res. Feb; 22(1):259-65.

Izumi Y, Murayama K, Tokuda K, Krishnan K, Covey DF, Zorumski CF. (2007) GABAergic neurosteroids mediate the effects of ethanol on long-term potentiation in rat hippocampal slices. Eur J Neurosci. Oct; 26(7):1881-8.

Jones, A., Korpi, E.R., McKernan, R.M., Pelz, R., Nusser, Z., Makela, R., Mellor, J.R., Pollard, S., Bahn, S., Stephenson, F.A., Randall, A.D., Sieghart, W., Somogyi, P., Smith, A.J., Wisden, W. (1997) Ligand-gated ion channel subunit partnerships: GABAA receptor α6 subunit gene inactivation inhibits delta subunit expression. J Neurosci., 17:1350-1362

Korpi ER, Lüddens H. (1993) Regional gamma-aminobutyric acid sensitivity of t-butylbicyclophosphoro[35S]thionate binding depends on gamma-aminobutyric acid A receptor alpha subunit. Mol Pharmacol. Jul; 44(1):87-92.

Korpi ER, Debus F, Linden AM, Malécot C, Leppä E, Vekovischeva O, Rabe H, Böhme I, Aller MI, Wisden W, Lüddens H. (2007) Does ethanol act preferentially via selected brain GABAA receptor subtypes? the current evidence is ambiguous. Alcohol. 2007 May;41(3):163-76.

Kumar S, Porcu P, Werner DF, Matthews DB, Diaz-Granados JL, Helfand RS, Morrow AL. (2009)The role of GABA(A) receptors in the acute and chronic effects of ethanol: a decade of progress. Psychopharmacology (Berl). Sep; 205(4):529-64.

Laurie, D.J., Seeburg, P.H., Wisden, W. (1992a) The distribution of 13 GABAA receptor subunit mRNAs in the rat brain. II. Olfactory bulb and cerebellum. J Neurosci., 12:1063-1076.

Laurie DJ, Wisden W, Seeburg PH. (1992b) The distribution of thirteen GABAA receptor subunit mRNAs in the rat brain. III. Embryonic and postnatal development. J Neurosci., 12:4151-4172.

Lavoie AM, Tingey JJ, Harrison NL, Pritchett DB, Twyman RE (1997) Activation and deactivation rates of recombinant GABA(A) receptor channels are dependent on alpha-subunit isoform. Biophys J. 1997 Nov;73(5):2518-26.

Liang J, Suryanarayanan A, Chandra D, Homanics GE, Olsen RW, Spigelman I.(2008) Functional consequences of GABAA receptor alpha 4 subunit deletion on synaptic and extrasynaptic currents in mouse dentate granule cells. Alcohol Clin Exp Res. Jan;32(1):19-26.

Liang J, Olsen RW. (2014) Alcohol use disorders and current pharmacological therapies: the role of GABA(A) receptors. Acta Pharmacol Sin. 2014 Aug;35(8):981-93. doi: 10.1038/aps.2014.50.

Luddens, H., Pritchett, D.B., Kohler, M., Killisch, I., Keinanen, K., Monyer, H., Sprengel, R., Seeburg, P.H. (1990) Cerebellar GABAA receptor selective for a behavioural alcohol antagonist. Nature, 346:648-651.

Lynagh T, Pless, S.A., Principles of agonist recognition in Cys-loop receptors Front Physiol. 2014 Apr 24;5:160. doi: 10.3389/fphys.2014.00160. eCollection 2014.

Macdonald, R.L., Haas, K.F. (2000) Kinetic Properties of GABAA Receptor Channels. In Martin, D.L., Olsen, R.W. (Eds.), GABA in the Nervous System: The View at Fifty Years, Lippincott Williams and Wilkins, Philadelphia, pp. 141-165.

Mameli M, Valenzuela CF. (2006) Alcohol increases efficacy of immature synapses in a neurosteroid-dependent manner. Eur J Neurosci. Feb;23(3):835-9.

Mameli M, Botta P, Zamudio PA, Zucca S, Valenzuela CF. Ethanol decreases Purkinje neuron excitability by increasing GABA release in rat cerebellar slices. J Pharmacol Exp Ther. 2008 Dec; 327(3):910-7.

Meera P, Olsen RW, Otis TS, Wallner M. (2010) Alcohol- and alcohol antagonist-sensitive human GABAA receptors: tracking δ subunit incorporation into functional receptors. Mol Pharmacol. Nov; 78(5):918-24.

Mihalek RM, Bowers BJ, Wehner JM, Kralic JE, VanDoren MJ, Morrow AL, Homanics GE. (2001) GABA(A)-receptor delta subunit knockout mice have multiple defects in behavioral responses to ethanol. Alcohol Clin Exp Res. 2001 Dec; 25(12):1708-18.

Mihic SJ, Ye Q, Wick MJ, Koltchine VV, Krasowski MD, Finn SE, Mascia MP, Valenzuela CF, Hanson KK, Greenblatt EP, Harris RA,

Harrison NL. (1997) Sites of alcohol and volatile anaesthetic action on GABA(A) and glycine receptors. Nature, 389(6649):385-9.

Mihic SJ, Harris RA. (1997) GABA and the GABAA receptor. Alcohol Health Res World. 21(2):127-31.

Miller PS, Aricescu AR. (2014) Crystal structure of a human GABAA receptor. Nature. 2014 Aug 21;512(7514):270-5. doi: 10.1038/nature13293. Epub 2014 Jun 8.

Ming Z, Criswell HE, Yu G, Breese GR. (2006) Competing presynaptic and postsynaptic effects of ethanol on cerebellar purkinje neurons. Alcohol Clin Exp Res. 2006 Aug;30(8):1400-7.

Mirheydari P, Ramerstorfer J, Varagic Z, Scholze P, Wimmer L, Mihovilovic MM, Sieghart W, Ernst M. (2014) Unexpected Properties of δ-Containing GABAA Receptors in Response to Ligands Interacting with the α+ β- Site. Neurochem Res. Jun; 39(6):1057-67.

Mody, I., Pearce, R.A. (2004) Diversity of inhibitory neurotransmission through GABAA receptors. Trends Neurosci., 27:569-575.

Mody I, Glykys J, Wei W (2007) A new meaning for "Gin & Tonic": tonic inhibition as the target for ethanol action in the brain. Alcohol (41)145-53.

Nusser, Z., Sieghart, W., Benke, D., Fritschy, J.M., Somogyi, P. (1996) Differential synaptic localization of two major g-aminobutyric acid type A receptor a subunits on hippocampal pyramidal cells. Proc Natl Acad Sci U S A. Oct 15;93(21):11939-44.

Nusser Z, Mody I. (2002) Selective modulation of tonic and phasic inhibitions in dentate gyrus granule cells. J Neurophysiol. 87(5):2624-8.

Nusser, Z., Sieghart, W., Somogyi, P. (1998) Segregation of different GABAA receptors to synaptic and extra-synaptic membranes of cerebellar granule cells. J Neurosci., 18:1693-1703.

Olsen, R.W., Chang, C.S., Li, G., Hanchar, H.J., Wallner, M. (2004) Fishing for allosteric sites on GABAA receptors. Biochem Pharmacol., 68:1675-1684.

Olsen RW, Hanchar HJ, Meera P, Wallner M. GABAA receptor subtypes: the "one glass of wine" receptors. Alcohol. 2007 May; 41(3):201-9.

Otis TS. (2008) Comments on "Ethanol sensitivity of GABAergic currents in cerebellar granule neurons is not increased by a single amino acid change (R100Q) in the alpha6 GABA(A) receptor subunit". J Pharmacol Exp Ther. 2008 Jan; 324(1): 399-400; author reply 401-3.

Patel B, Mortensen M, Smart TG. (2014) Stoichiometry of δ subunit containing GABA(A) receptors. Br J Pharmacol. 2014 Feb;171(4):985-94.

Roberto M, Madamba SG, Moore SD, Tallent MK, Siggins GR. (2003) Ethanol increases GABAergic transmission at both pre- and postsynaptic sites in rat central amygdala neurons. Proc Natl Acad Sci U S A. 2003 Feb 18; 100(4):2053-8.

Rudolph, U., Moehler, H. (2006) GABA-based therapeutic approaches: GABAA receptor subtype functions. Current Opinion in Pharmacology, 6:18–23.

Santhakumar V, Wallner M, Otis TS. (2007) Ethanol acts directly on extra-synaptic subtypes of GABAA receptors to increase tonic inhibition. Alcohol. May;41(3):211-21.

Schwarzer, C., Berresheim, U., Pirker, S., Wieselthaler, A., Fuchs, K., Sieghart, W., Sperk, G. (2001) Distribution of the major gamma-aminobutyric acid(A) receptor subunits in the basal ganglia and associated limbic brain areas of the adult rat. J Comp Neurol., 433:526-549.

Seeburg, P.H., Wisden, W., Verdoorn, T.A., Pritchett, D.B., Werner, P., Herb, A., Luddens, H., Sprengel, R., Sakmann, B. (1990) The GABAA receptor family: molecular and functional diversity. Cold Spring Harb Symp Quant Biol., 55:29-40.

Semyanov, A., Walker, M.C., Kullmann, D.M., Silver, R.A. (2004) Tonically active GABAA receptors: modulating gain and maintaining the tone. Trends Neurosci., 27:262-269.7.

Sieghart, W., Sperk, G. (2002) Subunit composition, distribution and function of GABAA receptor subtypes. Curr Top Med Chem., 2:795-816.
Sine, S.M., Engel, A.G. (2006) Recent advances in Cys-loop receptor structure and function. Nature 440: 448-455

Sine, S.M., Engel, A.G. (2006) Recent advances in Cys-loop receptor structure and function.
Nature 440: 448-455

Sun C, Sieghart W, Kapur J. (2004) Distribution of alpha1, alpha4, gamma2, and delta subunits of GABAA receptors in hippocampal granule cells. Brain Res. 17;1029(2):207-16.

Sundstrom-Poromaa, I., Smith, D.H., Gong, Q.H., Sabado, T.N., Li, X., Light, A., Wiedmann, M., Williams, K., Smith, S.S. (2002) Hormonally regulated alpha(4)beta(2)delta GABAA receptors are a target for alcohol. Nat Neurosci., 5:721-722.

Suzdak PD, Glowa JR, Crawley JN, Schwartz RD, Skolnick P, Paul SM. (1986) A selective imidazobenzodiazepine antagonist of ethanol in the rat. Science. Dec 5;234(4781):1243-7.

Theile JW, Morikawa H, Gonzales RA, Morrisett RA. (2008) Ethanol enhances GABAergic transmission onto dopamine neurons in the ventral tegmental area of the rat. Alcohol Clin Exp Res. Jun;32(6):1040-8.

Unwin, N. (2003) Structure and action of the nicotinic acetylcholine receptor explored by electron microscopy. FEBS Lett., 555:91-95.

Unwin, N. (2005) Refined structure of the nicotinic acetylcholine receptor at 4 Å resolution. J. Mol. Biol., 346:967–989.7.

Valenzuela CF. (1997) Alcohol and neurotransmitter interactions. Alcohol Health Res World. 21(2):144-8.

Villumsen IS, Wellendorph P, Smart TG. (2015) Pharmacological characterisation of murine α4β1δ GABAA receptors expressed in Xenopus oocytes. BMC Neurosci. 2015 Mar 5;16(1):8.

Wallner, M., Hanchar, H.J., Olsen, R.W. (2003) Ethanol enhances a4 b3 d and a6 b3 d gammaaminobutyric acid type A (GABAA) receptors at low concentrations known to affect humans. Proc Natl Acad Sci U S A., 100:15218-15223.

Wallner M, Hanchar HJ, Olsen RW. (2006) Low-dose alcohol actions on alpha4beta3delta GABAA receptors are reversed by the behavioral alcohol antagonist Ro15-4513. Proc Natl Acad Sci U S A. 103(22):8540-5.

Wallner M, Hanchar HJ, Olsen RW. (2014) Alcohol selectivity of β3-containing GABAA receptors: evidence for a unique extracellular alcohol/imidazobenzodiazepine Ro15-4513 binding site at the α+β- subunit interface in αβ3δ GABAA receptors. Neurochem Res. 2014 Jun;39(6):1118-26.

Wei, W., Zhang, N., Peng, Z., Houser, C.R., Mody, I. (2003) Perisynaptic localization of delta subunit-containing GABAA receptors and their activation by GABA spillover in the mouse dentate gyrus. J Neurosci., 23: 10650-10661.

Wisden, W., Laurie, D.J., Monyer, H., Seeburg, P.H. (1992) The distribution of 13 GABAA receptor subunit mRNAs in the rat brain I: Telencephalon, diencephalon, mesencephalon. J Neurosci., 12:1040-1062.

Yang X, Criswell HE, Breese GR. Ethanol modulation of gamma-aminobutyric acid (GABA)-mediated inhibition of cerebellar Purkinje neurons: relationship to GABAb receptor input. Alcohol Clin Exp Res. 2000 May;24(5):682-90.

You H, Dunn SM. (2007) Identification of a domain in the delta subunit (S238-V264) of the alpha4beta3delta GABAA receptor that confers high agonist sensitivity. J Neurochem. Nov; 103(3):1092-101.

ISSN 2303-4521

PERIODICALS OF ENGINEERING AND NATURAL SCIENCES
Vol. 4 No. 1 (2016)
Available online at: http://pen.ius.edu.ba

Potential of Algae for Biofuel Production

Ćamil Duraković
International University of Sarajevo,
Faculty of Engineering and Natural Sciences,
Genetics and Bioengineering Program,
Hrasnička cesta 15, 71000 Sarajevo,
Bosnia and Herzegovina
cdurakovic@ius.edu.ba

Abdulrezzak Memon
Usak University
Faculty of Science and Arts,
Department of Molecular Biology and Genetics
1 Eylul Campus, 6420 Usak,
Turkey
armemon@usak.edu.tr

Abstract
A non-renewable fuel like petroleum has been used from centuries and its usage has kept on increasing day by day. This also contributes to increased production of greenhouse gases contributing towards global issues like global warming. In order to meet environmental and economic sustainability, renewable, carbon neutral transport fuels are necessary. To meet these demands microalgae are one of the key sources for the production of biodiesel. These green microalgae synthesise lipids by using sunlight like plants do but in a much more efficient manner. Biodiesel provides more environmental benefits, and being a renewable resource it has gained lot of attraction. However, the main obstacle for commercialization of biodiesel is its cost and feasibility. Biodiesel is usually used by blending with petro diesel, but it can also be used in pure form. Biodiesel is a sustainable fuel, as it is available throughout the year and can run any engine. It will satisfy the needs of the future generation to come. It will meet the demands of the future generation to come.

Keywords: algae, biofuel production, biodiesel

1. Introduction

A 2010 study published in the journal, Energy Policy by researchers from Oxford University, predicted that demand for crude oil would surpass supply by 2015, unless forced by strong recession pressures caused by reduced supply or government interference. On an average, human utilizes fossil fuels which results in the release of 29 giga tonnes CO each year. This critical situation has led to the emergence of an eco-friendly, alternative fuel like biodiesel. According to United States Environmental Protection Agency, the volume requirement of the biomass based on diesel in 2013 is 1.28 million gallons which accounts for 1.13% of the total renewable fuels. This, combined with growing demand, significantly increases the worldwide prices of petroleum derived products. Most important concerns are the availability and price of liquid fuel for transportation [1-3].

Energy shortage refers to the crisis of energy resources to an economy. There has been a massive uplift in the global demand for energy in recent years as a result of industrial development and population growth. Since the early 2000s, the demand for energy, especially from liquid fuels, and limits on the rate of fuel production have created such a stage leading to the current energy crisis. The cause may be overconsumption, aged infrastructure, choke point disruption or crisis at oil refineries, and port facilities that confine fuel supply.

1.1. Microalgae as a source of biofuel

Microalgae are unicellular and simple multicellular microorganisms, including prokaryotic microalgae that are cyanobacteria (chloroxybacteria) and eukaryotic microalgae for example, green algae (chlorophyta), and diatoms (bacillariophuta). These microalgae are beneficial as they are capable of all year production; they grow in aqueous media and hence need less water than terrestrial crops. Unlike other biodiesel corps microalgae does not require herbicides or pesticides, microalgae also produce beneficial co-products such as proteins and residual biomass after oil extraction, which can be used as feed or fertilizer or can be fermented to produce ethanol or methane; the oil yield, can be significantly increased by varying growth conditions to modulate biochemical composition of algal biomass [4-5].
The algal biofuel technology includes selection of specific species for production and extraction of valuable co-products. Algae are bioengineered for achieving advanced photosynthetic efficiencies through continued development of production system. Challenges include,

DOI: 10.21533/pen.v4i1.50.g66

only single species cultivation techniques which are developed so far and are recommended to follow globally, but mixed culture may yield more algae oil than mono culture. The cost of producing oil from algae is economically cheaper than extracting oil from other sources which includes techniques such as water pumping, CO2 transmission, harvesting and extraction [6-7]. This review focuses on microalgae as a potential source of biodiesel.

1.2. Macroalgae for biofuel production

Other algae like macroalgae are generally fast growing and are able to reach sizes up to 60 m in length. Growth rates of macroalgae far exceed those of terrestrial plants. For example, brown algae biomass of the average productivity was approximately 3.3 to 11.3 kg dry weight m^{-2} yr^{-1} for non-cultured algae and up to 13.1 kg dry weight m^{-2} over 7 month for cultured algae compared with 6.1 to 9.5 kg fresh weight m^{-2} yr^{-1} for sugar cane, a most productive land plant. They are seasonally available in the natural water basins. Cultivation of macroalgae at sea, which does not require arable land and fertilizer, offers a possible solution to the energy crisis. Macroalgal biomass contains high amounts of sugars (at least 50%), which can be used in ethanol fuel production [8].

2. Algal fuel

Algae fuel or algal biofuel is another form of fossil fuel that uses microalgae as its source of natural deposits. Some of the unique characteristics of algal fuels are as follows: they can be grown with negligible impact on fresh water resource, they can be synthesized using ocean and wastewater, and they are biodegradable and relatively harmless to the environment if spilled. Algae cost more per unit mass due to the high capital and production costs. [9]

The US Department of Energy's Aquatic Species Program final report recommended that biodiesel could be the only feasible method to produce enough fuel to change current world diesel consumption. Algal fuel is highly favourable and feasible related to other biofuels, as they do not have to produce structural compounds and they can convert higher fractions of biomass to oil compared to other cultivated crops [10].

Studies display that some species of algae have the ability to produce up to 60% of their dry weight in the form of oil. Because the cells grow in aqueous suspension, where they have more effective access to water, CO_2 and nutrients are capable of producing large amounts of biomass and usable oil in either high rate algal ponds or photo bioreactors.

Figure 1. Advantages of algal fuel

2.1. Macroalgae

Notoya, 2010 says that macroalgae's are the most important component in the marine ecosystems that serve for the marine bioresources preservation by preventing eutrophication and pollution. Macroalgae belong to the lower plants, in that they do not have roots, stems, and leaves. They can grow very fast and in sizes of up to tens of meters in length. Based on their pigmentation, they are classified into Phaeophyta (brown), Rhodophyta (red), and Chlorophyta (green) algae [11]. In their natural environment, macro-algae grow on rocky substrates and form stable, multilayered, perennial vegetation, capturing almost all available photons. Approximately 200 species of macroalgae are used worldwide, about ten of them are intensively cultivated, such as the Phaeophyta, Laminaria japonica and Undaria pinnatifida, the Rhodophyta, Eucheuma, Gracilaria, Porphyra and Kappaphycus, and the Chlorophyta, Enteromorpha and Monostroma [12]. Figure 2 shows examples of some commercially exploited macroalgae.

Advantages of algal biofuel production are shown below:

- Production of biofuel from the macroalgae cultivation in seawater is a new approach, and since macroalgae have a unique life cycle in one productive year more than five harvests can be made.
- Macroalgae can succeed in salty water with only sunlight and available nutrients from the seawater.
- Production of bioethanol has a large impact on the environment in general due to eutrophication, acidification, and ecotoxicity.

• With the advancement of genetic engineering, it is now possible to develop a suitable species of macroalgae for bioethanol production [13]. Genetically engineered macroalgae would need to be cultivated in enclosed bioreactors.

• Converting the macroalgal biomass to ethanol rather than using terrestrial plant biomass have some important benefits, i.e., no negative impact on the food security. The relatively high sugar content and lower lignin content than lignocelluloses facilitates high mass production. [14]

• Apart from bioethanol production, algal biomass can be used for the production of an enormous variety of supplementary products i.e., protein, pigments, plastics, etc. [15]

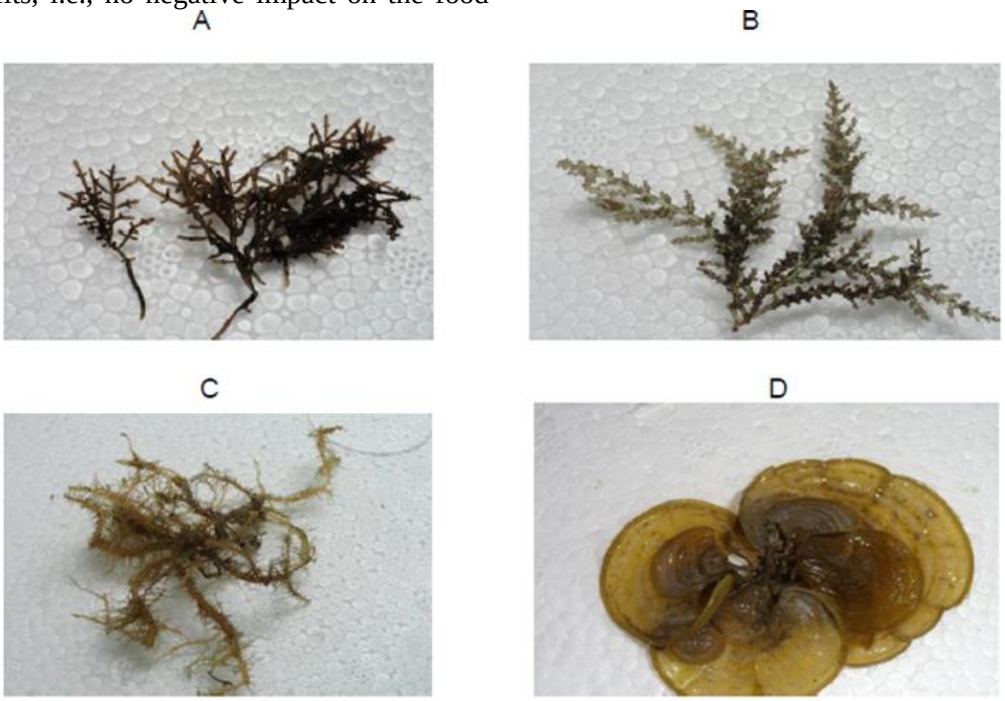

Figure 2. Some commercially exploited macroalgae A) Gracilaria dura B) Acanthophora spicifera C) Hypnea esperi D) Padina pavonica (Rajkumar et al. 2014)

There are some species of macroalgae which gather a high amount of carbohydrates that are capable in the processes of microbial conversion as substrate, i.e., production of biofuels or the other desirable and attractive chemicals with high product price.

Recently it is discovered that triglycerides from a number of macroalgae such as *Ascophyllum nodosum, Codium tomentosum, Enteromorpha intestinalis, Fucus spiralis, Saccorhiza polyschides, Sargassum muticum, Ulva rigida,* and *Pelvetia canaliculata,* etc. could be used to produce biodiesel by a transesterification process. Macroalgae such as Sargassum spp., *Gracilaria spp., Prymnesium parvum, Gelidium amansii,* and *Laminaria spp*. are promising candidates for bioethanol production. [16]

Table 1 Carbohydrate Contents of Macroalgae (Dhargalkar and Pereira 2005)

Species	Carbohydrates (%)
Ulva	42.0
Enteromorpha	64.9
Monostroma	63.9
Laminaria	39.3
Alaria	39.8
Sargassum	33.0
Padina	31.6
Porphyra	45.1
Rhodymenia	44.6
Gracilaria	61.75

2.2. Microalgae

Microalgae are photosynthetic microorganisms that are found in both marine and freshwater habitats. Microalgae species at present, are divided into four groups, namely

diatoms (Bacillariophyceae), green algae (Chlorophyceae), blue green algae (Cyanophyceae), and golden algae (Chrysophyceae) [17]. The dominating species of microalgae in commercial production include Isochrysis, Chaetoceros, Chlorella, Arthrospira (Spirulina), and Dunaliella. As heterotrophs, the algae rely on glucose or other utilizable carbon sources for carbon metabolism and energy. The biomolecules such as carbohydrates, proteins, lipids, and nucleic acids are the common constituents in microalgae.

Commercial applications of microalgae have gained interest during the last few years. Owing to their rapid growth rate, i.e., 100 times faster than the land based plants which can double their biomass in less than 1 day, microalgae appear to be an attractive renewable energy source [18]. This is mostly due to their simple cellular system and big surface to quantity ratio that gave them the facility to utilize more amounts of nutrients from the source of water and hence, supporting their algae growth rate.

Biofuel production using microalgal farming offers the following advantages [19]:

- Increased efficiency or decrease in the cost. The sum of harvesting and transportation of microalgae costs can be relatively low compared to those of the other plant biomass resources.
- Generally, microalgae can grow in fresh, brackish, or salt water environments or non-arable lands that are incompatible for growing other crops and conventional agriculture. Microalgae produce a greater yield per hectare with superior environmental attributes.
- The most common microalgae contain oil ranges between 20 and 50% by dry weight of biomass, but superior productivities can be attained. [20]
- Microalgae are able to fix carbon dioxide in the atmosphere, assisting the reduction of atmospheric carbon dioxide levels, which is recently considered a global crisis. In addition, production of microalgal biomass can affect the biofixation of waste carbon dioxide, reducing the releases of a major greenhouse gas (1 kg of dry microalgal biomass requires about 1.8 kg of carbon dioxide). [21]

Table 2 Oil Content of Microalgae by Chisty (2007)

Feedstock	Oil content (% dry wt)
Botryococcus braunii	25-75
Chaetoceros calcitrans CS178	39.8
Nannochloropsis sp.	31-68
Schizochytrium sp.	50-77
Skeletonema sp. CS252	31.8
Tetraselmis suecica	15-23

The green algae *Chlorococum spp*. and *Spirogyra spp*. have been revealed to accumulate high contents of polysaccharides together in their complex cell walls and as starch. This accumulation of starch can be used in the bioethanol production. Bioethanol has the prospect of being an alternative fuel, but it is highly important to ensure that the expansion of this fuel is not hindered by the raw material constraints. In this context, the harvesting cycle of microalgae cells has a very short period (1 to 10 days) compared with the other feedstock (harvesting time once or twice per year), and thus can provide enough supplies to meet demands for the ethanol production. [22]

Table 3 Bioethanol Production from Various Strains of Microalgae

Feedstock	Ethanol yield (g ethanol/g substrate)
Chlorococcum humicola	0.52
Chlorococcum infusionum	0.26
Chlamydomonas reinhardtii	0.24

3. Production

3.1. Algae cultivation

Algae are typically found growing in ponds, waterways, or other wetlands which receive sunlight and CO_2. Growth varies on many factors and can be enhanced for temperature, sunlight utilization, pH control, fluid mechanics, and more. Man-made production of algae tends to replicate the natural environments to achieve ideal growth conditions. Algae production systems can be organized into two distinct categories: open ponds and closed photo bioreactors. Open ponds are simple expanses of water sunken into the ground with some mechanism to deliver CO_2 and nutrients with paddle wheels to mix with the algal broth. Closed photo bioreactors are a broad category referring to systems that are bounded and which allow more precise control over growth conditions and resource management. [23].

3.2. Algae biofilm

Biofilm formed by algae can be harvested easily using unit operations like filtering, scraping, size, reduction, and drying. Photoreactors are used to produce high quality algae in either sessile form or mainly biofilm. Attached algae have produced more oil than planktonic form. The reason for high lipid content is due to alteration in the lipid metabolic pathway of attached algae resulting in change in the membrane fluidity of

algae to make them attached to a substratum. For small-scale as well as large-scale production, the photoreactors are used wherein natural or synthetic light can be used to grow algae.

3.3. Algae harvesting and oil extraction

Production of oil from algae is a straight forward process that consisted of growing the algae by providing necessary inputs for photosynthesis, harvesting, dewatering, and oil extraction. Energy in the form of photons is absorbed by the algae cells, which convert the inorganic compounds of CO_2 and water into sugars and oxygen. The sugars are eventually converted into complex carbohydrates, starches, proteins, and lipids within the algae cells. In order to extract the valuable lipids, a series of steps must be undertaken to isolate the algae cells and oil (see Figure 3).

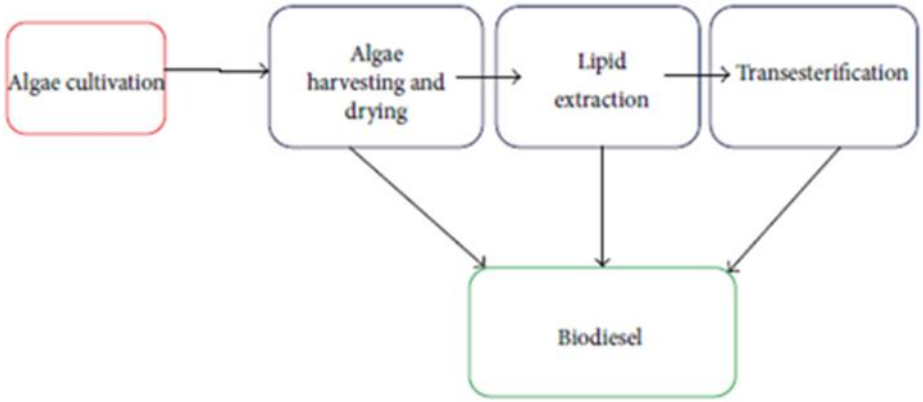

Figure 3. Algae growth and harvesting process

3.4. Trans-esterification

Biodiesel from algae is commonly produced by the transesterification. There are several procedures for carrying out this transesterification reaction including the collective batch process, supercritical processes, ultrasonic methods, and even microwave methods.

Chemically, trans-esterified biodiesel comprises a mix of mono-alkyl esters of long chain fatty acids. The most conjoint form uses methanol (converted to sodium methoxide) to produce methyl esters (commonly referred to as fatty acid methyl ester (FAME) as it is the cheapest alcohol available; though ethanol can be used to form an ethyl ester (commonly referred to as fatty acid ethyl ester (FAEE), biodiesel and higher alcohols such as isopropanol and buthanol have also been used. Using alcohols of higher molecular weights improves the cold flow properties of the resulting ester, at the cost of a less efficient transesterification reaction. A lipid transesterification production process converts the base oil to the desired esters. Any free fatty acids (FFAs) in the base oil are either converted to soap or removed from the process, or they are esterified (yielding more biodiesel) using an acidic catalyst. After this processing, biodiesel has combustion properties very similar to those of petroleum diesel and can be replaced fully or partially for petroleum.

4. Use of algae for biofuel production and waste water treatment

In general, the algal biomass grown with the industrial wastewaters can also be converted into bio crude oil using a thermochemical liquefaction process. Hence, growing algae in wastewaters for biofuel and bioenergy production seems a viable and eco-friendly option for the future. Two main culture systems are available for algal production. An open system generally combines waste treatment with algal production. This system employs the use of ponds, which range from the oxidation ponds to the high rated algae ponds. An oxidation pond recycles nutrients through a bacteria-algae symbiotic process. The pond is one to two meters deep and unmixed. The algal yield in such a pond is thus low. In contrast, the high-rate algae pond (HRAP), which consists of an open raceway mixed by paddle-wheels, is very shallow and is capable of producing very high yields. High-rate algae ponds are suitable for the generation of algal biomass for high-quality animal feed and extraction of useful compounds such as protein and pigments. Research on the combined algal production and waste-treatment systems has been done in Israel, India, Thailand, the United States, and some other countries.

As fresh water sources are scarce, utilization of poor quality wastewaters such as treated municipal sewage

wastewater as low-cost nutrient growth medium for mass cultivation of biofuel algae appears a viable option for the future. In recent times, research into microalgal cultivation has gained importance because of application of this resource in the production of biofuels. Cultivation of microalgae in the open pond systems has been used since the 1950, and raceway ponds are the most commonly used artificial systems. Open ponds provide a very efficient method of cultivating algae, but they become contaminated with the algal species very easily.

The major advantage of the open ponds is that they are very easy to construct and operate; in comparison to most closed systems, they are easy to clean up after cultivation and are ideal for mass cultivation of microalgae. This should be given consideration in view of the escalating equipment costs, particularly the use of the reactor-style systems that lack a reliable scale-up method. While considering the economic and the environmental aspects, a raceway pond coupled with a low cost harvesting technique would be a preferable choice to produce biodiesel.

While the demand for the production of biofuel is in part driven by ecological concerns, there is no doubt that constructing and operating an HRAP dedicated to producing algal biomass for biofuels can have an ecological impact. Production of algal biomass using wastewater HRAPs, by contrast, offers a far more interesting proposition from an ecological point of view. The impacts of the HRAP construction and operation are a necessity of providing the treatment of wastewaters and hence, the subsequent algal production represents a biofuel feedstock free of this ecological issue. [24]

Among the various cultivation systems involved in producing algal biomass, the aspect of harvesting biomass is an important economic issue. It was estimated that harvesting algae biomass can account for 20 to 30% of the total production cost. When, the algae grow phototrophically, their concentration is about 0.5 to 1.0 g L-1 for open ponds and around 5 to 10 g L-1 biomass concentration for closed systems. For the production of 1 g L-1 algal biomass, 1000 kg of water must be used to capture 1 kg of biomass. [25]

Methods of algal biomass harvesting, such as filtration, centrifugation, sedimentation and flocculation, and floatation are being practiced either individually or in any combination. Several literature reviews have provided for the algae harvesting techniques. Among the various methods, centrifugation is a possible method suitable for higher-value products but is very expensive in an integrated system producing lower-value products, such as algal oils (http://www.ecs.umass.edu/biofuels). In the case of algal-derived biofuels, the low-cost promising method is gravity settling enhanced by flocculation, without benefit of chemical flocculants. Other mechanisms exist, including the auto flocculation process, and it depends on the coprecipitation of calcium carbonate with microalgal cells and other precipitates that form in hard waters subject to high pH. Apart from settling, in some cases the biomass will float, either due to high oil content or by using a dissolved air flotation (DAF) process.

Employing minor amounts of flocculants to assist in such a process could be cost effective, depending on the amount used. In general, the harvesting method of choice depends on algal species, the cultivation conditions, and the application of the product. For biofuels applications, low-cost algal harvesting techniques are still in process of development. Significant research efforts are needed to develop the cost-effective techniques for harvesting and for production of low cost biofuels from algae. [26]

5. Conclusion

As justified here, microalgal biodiesel is technically feasible. It is the only renewable biodiesel that can potentially and methodically displace liquid fuels obtained from petroleum. Economics of producing microalgal biodiesel need to be improved substantially in order to be competitive with petro diesel, but the level of improvement necessary appears to be possible. Producing low-cost microalgal biodiesel requires primarily improvements to algal biology through genetic and metabolic engineering. Use of the biorefinery concept and advances in photobioreactor engineering will further reduce the cost of production. In view of their much greater productivity than raceways, tubular photobioreactors are likely to be used in producing most of the microalgal biomass required for making biodiesel. Algae biofilm grown in photobioreactors provide a controlled environment that can be tailored to the specific demands of highly productive microalgae to attain a consistently good annual yield of oil.

Nevertheless, diversified biofuels production from algae biomass is very important to improve overall energy balance. For example, higher net value could be achieved by using a combined operation in which algae-produced lipids are converted to diesel fuel and the cellulosic part of the algal biomass (after lipid extraction) is enzymatically converted to glucose, which is fermented to produce bioethanol and other by-products. Apart from that, biofuel contributes to energy security and helps reduce CO2 emissions. A thorough understanding of the past may serve to overcome the past lapses toward building a better future. These recent biofuel discussions demonstrate two issues. First, they show the wide potential utility of these organisms that are capable of producing multiple products ranging from energy, chemicals, and materials to exploitation in the sequestration of carbon and remediation of wastewater. Second, they show the need for energetic support based on factual information to confirm decisions

for the strategic improvement of algae and to counter those declarations made on a solely tentative basis to promote commercial investment.

References

[1] N. A. Owen, O. R. Inderwildi, and D. A. King, "The status of conventional world oil reserves—hype or cause for concern?" Energy Policy, vol. 38, no. 8, pp. 4743–4749, 2010.

[2] M. K. Hubbert, Nuclear Energy and the Fossil Fuels. Published in Drilling and Production Practice, American PetroleumInstitute, 1956.

[3] T.Therramus, "Oil Caused Recession, NotWall Street," January 2010, http://www.oil-price.net/

[4] K. B. Cantrell, T. Ducey, K. S. Ro, and P. G. Hunt, "Livestock waste-to-bioenergy generation opportunities," Bioresource Technology, vol. 99, no. 17, pp. 7941–7953, 2008.

[5] L. Rodolfi, G. C. Zittelli, N. Bassi et al., "Microalgae for oil: strain selection, induction of lipid synthesis and outdoor mass cultivation in a low-cost photobioreactor," Biotechnology and Bioengineering, vol. 102, no. 1, pp. 100–112, 2009.

[6] E. Ono and J. L. Cuello, "Feasibility assessment of microalgal carbon dioxide sequestration technology with photobioreactor and solar collector," Biosystems Engineering, vol. 95, no. 4, pp. 597–606, 2006.

[7] C. U. Ugwu, H. Aoyagi, and H. Uchiyama, "Photobioreactors for mass cultivation of algae," Bioresource Technology, vol. 99, no. 10, pp. 4021–4028, 2008.

[8] Wi, S. G, Kim, H. J, Mahadevan, S. A, Yang, D., and Bae, H. (2009) "The potential value of the seaweed Ceylon moss (Gelidium amansii) as an alternative bioenergy resource," Bioresour. Technol. 100, 6658-6660.

[9] "Low Cost Algae Production System Introduced," Energy-Arizona, August 2007.

[10] T. Shirvani, X. Yan, O. R. Inderwildi, P. P. Edwards, and D. A. King, "Life cycle energy and greenhouse gas analysis for algaederived biodiesel," Energy & Environmental Science, vol. 4, no. 10, pp. 3773–3778, 2011.

[11] Chan, C. X., Ho, C.L., and Phang, S.M. (2006). " The trends in seaweed research," Trends in Plant Science 11, 165-166.

[12] Luning, K., and Pang, S.J. (2003)."Mass cultivation of seaweeds: Current aspects and approaches," J. Appl. Phycol. 15, 115-119.

[13] Goh, C. S., and Lee, K.T. (2010). "A visionary and conceptual macroalgae-based third generation bioethanol (TGB) biorafinery in Sabah, Malaysia as an underlay for renewable and sustainable development, Renew. Sust. Energy Rev. 14, 842-848.

[14] Adams, J.M., Gallagher, J. A., and Donnison, I. S. (2009). "Fermentation study on Saccharina latissima for bioethanol production considering variable pre-treatments," J. Appl. Phycol. 21(5), 569-574.

[15] Wijffels, R. (2009). "Microalgae for production of bulk chemicals and biofuels, "The 3rd Congress of Tsukuba 3E Forum, Tsukuba International Conference Centre, Tsukuba, Japan.

[16] Maceiras, R., Rodriguez, M., Cancela, A., Urrejola, S., and Sanchez, A. (2011). Macroalgae: Raw material for biodiesel production," Appl. Ener. 88, 3318-3323.

[17] Khan, S. A., Rashmi., Hussain M. Z., Prasad, S., and Banerje, U. C. (2009). "Prospects of biodiesel production from microalgae in India," Renew. Sust. Energy Rev. 13, 2361-2372.

[18] Tredici, M. R. (2010). "Photobiology of microalgae mass cultures: Understanding the tools for the next green revolution," Biofuels 1,143-162.

[19] Ahmad, A. L., Mat Yasin, N. H., Derek, C. J. C., and Lim, J. K. (2011). "Microalgae as a sustainable energy source for biodiesel production: A review" Renew. Sust. Energy Rev. 15, 584-593.

[20] Mata, T. M., Martins, A. A.m and Caetano, N. S. (2010). "Microalgae for biodiesel production and other applications: A review," Renew. Sust. En. Rev. 14(1), 217-232.

[21] Rodolfi, L., Zitteli, G. C., Bassi, N., Padovani, G., Biondi, N., and Bonnini, G. (2008). "Microalgae for oil: Strain selection, induction of lipid synthesis and outdoor mass cultivation in a low cost photobioreactor," Biorechnol. Bioeng. 102(1), 100-112.

[22] Schenk, P. M., Thomas-Hall, S. R., Stephens, E., Marx, U. C., Mussgnug J. H., Posten, C., Kruse, O., and Hankamer, B. (2008). "Second generation biofuels: High-efficiency microalgae for biodiesel production," Bioener. Res. 1, 20-43.

[23] I. Perner-Nochta and C. Posten, "Simulations of light intensity variation in photobioreactors," Journal of Biotechnology, vol. 131, no. 3, pp. 276–285, 2007.

[24] Park, J. H., Yoon, J. J., Park, H. D., Kim, Y. J., Lim, D. J., and Kim, S. H. (2011). "Feasibility of biohydrogen production from Gelidium amansii," Int. J. Hydrogen Energy 36, 13997-14003.

[25] Chisty, Y. (2007). "Biodiesel from microalgae" Biotechnol. Adv. 25, 294-306.

[26] Mutanda, T., Ramesh, D., Karthikeyan, S., Kumari, S., Anandraj, A., and Bux, F. (2011). "Bioprospecting for hyper-lipid producing microalgal strains for sustainable biofuel production," Bioresour. Technol. 102, 50-57.

ISSN 2303-4521
PERIODICALS OF ENGINEERING AND NATURAL SCIENCES
Vol. 4 No. 1 (2016)
Available online at: http://pen.ius.edu.ba

Complex Ecological System Modeling

Migdat Hodzic
International University of Sarajevo
Sarajevo, Bosnia and Herzegovina

Suvad Selman
International University of Sarajevo
Sarajevo, Bosnia and Herzegovina

Mirsad Hadzikadic
University of North Carolina
Charlotte, N. Carolina, USA

Abstract

In this paper we extend our previous results in dual approach to analysis and simulation of a complex ecological system of preys and predators. We first define nonlinear dynamic equations Lotka-Volterra Model (LVM) with three preys and three predators and then simulate the equivalent situation with an Agent Based Model (ABM) which models a variety of species attributes and behaviors using NetLogo simulation environment for ABM model. The idea is that the LVM and ABM methods reinforce each other as the predator-prey models become more complex and their dimensionality rises. In particular LVM's parameters, components of community matrix, can be fine tuned using ABM simulations. Dual approach may be able to answer and qualify some of the long standing ecological paradoxes.

1. INTRODUCTION

In analysis and simulation of complex ecological systems, we often start with a nonlinear Lotka Volterra Model (LVM) of predator-prey dynamic system [1, 2]. The problem with this approach is that the LVM is very simplified model and apart from a detailed stability analysis [2], there are no real life complex ecological dynamic system models which are flexible and useful enough. Some of the reasons are (i) Lack of any general model build up methodology, (ii) Lack of any structural analysis of complex dynamical ecological models, and (iii) Very few results explaining some well know ecological paradoxes. In our earlier paper [1] very simple single prey and single predator system was modeled and analyzed by using both LVM and ABM. In this paper we extend the results in [1] and define two main paper goals:

(i) Define mathematical details of a dynamic system with three aquatic predators and three prays (3+3 model) using a notion of community matrix and classic Lotka-Volterra predator-prey nonlinear model. This serves as a mathematical background which will be used in later research to reconcile two models, LVM and ABM, with the idea that two models reinforce each other. In particular we plan to use ABM to fine tune LVM and community matrix parameters which is at its heart.

(ii) Next we simulate ABM 3+3 model using NetLogo simulation tool where we can define ABM parameters, in particular related to various properties of preys and predators. These properties include their total numbers, consumption rates, how they are "born" and how they "die" in simulation cases, and several other tuning "knobs" allowed by NetLogo environment.

The results of this paper can be extended to higher number of species as well. Our goal is also to gain further insight into predator-prey population dynamics, structural properties of the models, understanding of stability in multispecies communities, and improve rigor, usability, robustness and adaptivity of both LVM and ABM models. We believe that the dual approach can bring about very usable but complex predator-prey ecological models which are also mathematically tractable.

2. SINGLE PREY SINGLE PREDATOR MODELS

General ecological nonlinear model is described by [2]:

$$S: \; dX/dt = A(t,X)\, X \qquad (1)$$

where X is a species vector. The model has an appearance of a linear system. The vector X may be a 2-dimensional vector, i.e. one pray, one predator [1], or it could consist of many more species arranged in tropical levels of preys and predators. Matrix A(t,X) is a "community" matrix with nonlinear elements, time-dependent functions $a_{ij}=a_{ij}(t,X)$, where "ij" indicates position in the matrix. In 2-dimesional X, matrix A is 2 by 2, with the elements a_{11}, a_{12}, a_{21}, and a_{22}, which describe self and cross interactions among the two species. A special case of (1) is well known nonlinear Lotka-Volterra Model (LVM). For purposes of this paper, we review briefly what was covered in [1] for Single Prey Single Predator (SPSP) model.

DOI: 10.21533/pen.v4i1.9

2.1 LVM Basic Mathematics

Let us assume $X = [X_1, X_2]^T$, X_1 is prey species, X_2 is predator species. The classic LVM [2] is:

$$dX_1/dt = X_1 (A_1 + A_{12} X_2) = A_1X_1 + A_{12}X_2X_1$$
$$dX_2/dt = X_2 (A_2 + A_{21} X_1) = A_2X_2 + A_{21}X_1X_2 \quad (2)$$

which can also be written in a compact form as:

$$dX_i/dt = X_i (A_i + A_{ij} X_j) \quad (3)$$

where i,j=1,2 and $i \neq j$, A_1 is the growth rate of the prey. With $A_{12} = 0$ (no predator X_2) the prey population X_1 increases exponentially,. With $A_{12} < 0$, predator X_2 controls prey population from growing exponentially. For the predator population, growth is dependent on $A_2 < 0$, the rate of predator removal from the system (death or migration), and A_{21}, the positive growth rate for predators. The solution to Equations 2 and 3 is periodic, with the predator population always following the prey. Figure 1 gives an example with constant values of positive coefficients A_1 and A_{21}, and negative growth rates A_{12} and A_2. The other SPSP models can be defined, such as positive A_2 and negative A_{21} for the predator, depending on the model. The interest is to keep the basic model stable. General LVM stability results are given in [2].

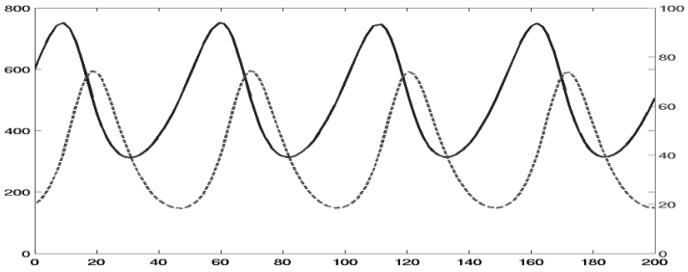

Figure 1. SPSP LVM Population Levels (Prey Solid, Predator Dashed)

In terms of (1) and, the community matrix A is:

$$A(X) = \quad (4)$$

$a_{11}(X)$	$a_{12}(X)$
$a_{21}(X)$	$a_{22}(X)$

with:

$$a_{11} = A_1,\ a_{12} = A_{12} X_1,\ a_{21} = A_{21} X_2,\ a_{22} = A_2 \quad (5)$$

The LVM can be extended to incorporate crowding effect:

$$dX_i/dt = X_i (A_i + \sum A_{ij} X_j) \quad (6)$$

where i = 1,2 and sum is over j = 1,2. This would be equivalent to prey self multiplication without predator. In this case community matrix elements are:

$$a_{11}=A_1+A_{11}X_1,\ a_{12}=A_{12} X_1,\ a_{21}=A_{21} X_2,\ a_{22}=A_2+A_{22}X_2 \quad (7)$$

In this model, A_{12} and A_{21} are negative, with positive A_{11} and A_{22}. Next LVM feature could be time varying community matrix:

$$dX_i/dt = X_i [A_i(t,X) + \sum A_{ij}(t,X) X_j] \quad (8)$$

or in compact form:

$$dX/dt = A(t,X) X \quad (9)$$

with:

$$A(t,X) = \quad (10)$$

$a_{11}(t,X)$	$a_{12}(t,X)$
$a_{21}(t,X)$	$a_{22}(t,X)$

For example:

$$a_{11}(t,X) = A_1(t,X) + A_{11}(t,X) X_1 \quad (11)$$

and similarly for the rest of the coefficients in (10). We can also add environmental effects [2] into LVM by:

$$S: \quad dX/dt = A(t,X) X + B(t,X) \quad (12)$$

where B(t,X) models external environmental effects (food, space, temperature), and it can be considered as a model control vector. More details can be found in [1],[2].

2.2 ABM and LVM Combined

The Equations 2 and 3 present a very simple ecological model, where unlimited food available to the prey is assumed, and so the prey (and predator) growth rates are limited by corresponding "growth" coefficients. The prey growth coefficient is A_1 and A_{21} for the predator. On the other hand, in ABM, the growth rate for both populations can be determined by how successful they are at finding food. This can be modeled as a stochastic process which averages out to a stable rate across populations, hence corresponding practically to LVM model, in the limit. Various effects/ model attributes can be incorporated in ABM. As an example, the predators disappear from the simulation at a constant rate by reaching the end of their programmed lifetime. This parallels negative A_2 in LVM. The predator population increases linearly based on the prey consumption. This is proportional to the number of both populations, and thus represented by $A_{21}X_1X_2$ in LVM. Within the ABM various LVM features can be accommodated by simply adding new features into the ABM. Hence LVM coefficients can be estimated using ABM simulations. Figure 2 gives a typical agent based snapshot of NetLogo simulation control window. Let us also note that the initial ABM is not intended to include all the properties of an existent ecosystem, but rather to indicate the most fundamental properties of the predator–prey relationship as a general model. For example, the environment is assumed homogeneous with no variations in sea temperature, depth, or ocean currents. This can be changed as more complex models are developed. One of the ABM parameters is the amount of food available to prey and predator. This corresponds to B(t,X) in LVM given by (12). When the food is increased initially, both A_1 and A_{21}, increase initially. In the steady state, the prey growth rate A_1 remains constant with their population growth offset by increased predator population.

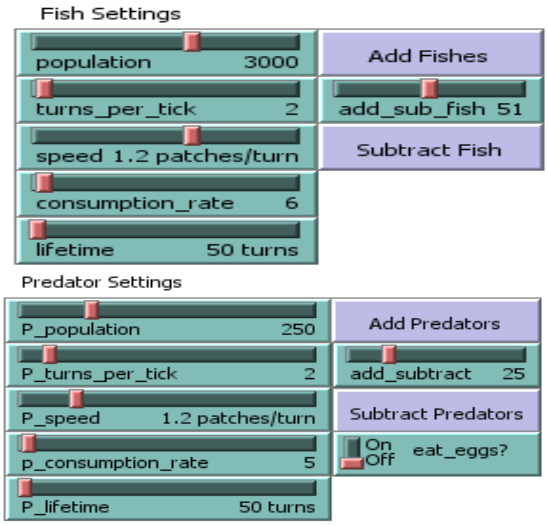

Figure 2. Typical NetLogo ABM simulation control

The rate of predator removal A_2, by death or migration, is determined by the predator ABM attribute age and a limited lifetime for each individual. The prey also has an attribute for age, but in practice, very few fish die of old age. This is particularly true at higher levels of resources, because their average age drops as a consequence of fish being born faster while their population remains stable. It is this last fact that may cause the system instability, at very high levels of resources. Analytical LVM stability results are discussed in details in [2]. In [1] we described one specific ABM SPSP in details.

Per Figure 2, ABM gives lots of flexibility to model the system, but essentially gives no analytical insight and the solution such as the case with LVM. That is the essence of our dual approach here, i.e.

(i) Use ABM for its flexibility and intuitiveness, and

(ii) LVM for its mathematical elegance and rigor.

This way we can use ABM to improve LVM, and vice versa as complexity of the model increases. As we develop more complex predator-prey models, the approach is to rely on the LVM formulas and feature based ABM to reiterate each other findings. This will require a very disciplined research work, so we will be able to precisely interpret every step of the two models.

3. MULTIPLE PREY-PREDATOR MODEL

As described in details in [1], Multiple Prey Multiple Predator (MPMP) model is described in LVM by:

$$dX_i/dt = X_i [A_i(t,X) + \sum A_{ij}(t,X) X_j] \qquad (13)$$

where i = 1,2, ... , n, and sum $\sum$ is over j = 1,2, ... , n. We can model 2 preys 1 predator, 4 preys 2 predators, 10 preys 3 predators, etc., hence building up complexity of the LVM's. Some examples of (6x6) community matrix are repeated here from [1] as references. More details are given in a specific example of Section 4 where we model 3+3 scenario, i.e. three preys and three predators.

(i) Four preys (species 1,2,4,5) and two predators (3,6) produce the following (6x6) community matrix:

A(t,X) = (14)

a_{11}	a_{12}	a_{13}	0	0	0
a_{21}	a_{22}	a_{23}	0	0	0
a_{31}	a_{32}	a_{33}	0	0	0
0	0	0	a_{44}	a_{45}	a_{46}
0	0	0	a_{54}	a_{55}	a_{56}
0	0	0	a_{64}	a_{65}	a_{66}

which consists of two decoupled predator-prey systems. Any of the zero coefficients a_{ij} indicates lack of influence of j-th specie to i-th specie. This type of model is advantageous due to decoupling which simplifies any species estimation and control algorithms [2].

(ii) Assuming that predators can prey on all of the species, but not on each other, we have:

A(t,X) = (15)

a_{11}	a_{12}	a_{13}	0	0	a_{16}
a_{21}	a_{22}	a_{23}	0	0	a_{26}
a_{31}	a_{32}	a_{33}	0	0	0
0	0	a_{43}	a_{44}	a_{45}	a_{46}
0	0	a_{53}	a_{54}	a_{55}	a_{56}
0	0	0	a_{64}	a_{65}	a_{66}

(iii) If predators prey on each other, then we have:

A(t,X) = (16)

a_{11}	a_{12}	a_{13}	0	0	a_{16}
a_{21}	a_{22}	a_{23}	0	0	a_{26}
a_{31}	a_{32}	a_{33}	0	0	a_{36}
0	0	a_{43}	a_{44}	a_{45}	a_{46}
0	0	a_{53}	a_{54}	a_{55}	a_{56}
0	0	a_{63}	a_{64}	a_{65}	a_{66}

(iv) Two almost decoupled specie communities share a common four (**boldfaced**) elements:

A(t,X) = (17)

a_{11}	a_{12}	a_{13}	0	0	0
a_{21}	a_{22}	a_{23}	0	0	0
a_{31}	a_{32}	**a_{33}**	**a_{34}**	0	0
0	0	**a_{43}**	**a_{44}**	a_{45}	a_{46}
0	0	0	a_{54}	a_{55}	a_{56}
0	0	0	a_{64}	a_{65}	a_{66}

Any estimation and control for this model can be handled by an approach in [6], where the model is "expanded" into a larger species vector space to decouple it effectively. Note that the shape of the community matrix will also depend on how the prey and predators are ordered in the species vector X. As the community matrices become larger, we note that there are certain structural properties in the way "0" elements are placed. This is calling for "structural"

approaches described in [3,5,6] which take advantage of special structure of system matrices to (i) simplify calculations and (ii) expose key structural properties of the models. As the number of species grow, smart shuffling of the position of species in the vector X may produce hierarchical (or almost hierarchical) structure of community matrix A(t,X) [5], producing much simpler controls and stability analysis, as the overall community matrix is split into subsystems hierarchically interconnected. We will address estimation and control aspect of ecological system models in future research.

4. THREE PREYS THREE PREDATORS MODEL

Before we illustrate one specific 3+3 example, few comments are in order related to general model assumptions.

4.1 General Assumptions

The ABM is not intended to include all the properties of an existent ecosystem, but rather to expose the most fundamental properties of the predator–prey-resource relationship as a general model. As such, the environment is largely homogeneous: that is, there are no variations in sea temperature, depth, or ocean currents. Furthermore, each tropic level is represented by a single species. Important refinements such as species growth over time, variable predation strategies, environmental heterogeneities and dynamics, more complex food web networks, and different functional responses can be selectively added to future models in an iterative process to ensure that one understands the basic dynamics at each level before proceeding to the next level of complexity.

Other simplifying assumptions include: all species are of the same size, produce the same amount of resources when consumed, and share the same set of simple strategic rules. For the fish these rules are: if there is one or more predators on the current patch, pick one and move in the opposite direction; if no predators are present and there is food on the current patch, eat one unit; otherwise, move randomly. For the predators the rules are: if there is one or more fish on the current patch, eat one. After eating (or not, if no fish are present), move randomly.

The fishes and predators all have a limited lifetime. Also, the patches grow food (resources for the fish) stochastically, based on an operator controlled setting that defines the percentage chance of growth for each individual patch. Food is simulated as units per patch, from zero (no food) to a maximum, such that if food is present a fish can eat one unit per turn. Specifically, a 0.20 food growth rate translates into a 20% chance for each patch to add one unit of food, during each simulation time step. Aggregated across the 22,801 patches in the simulation, this rate becomes a linear, but still stochastic, rate of growth for food. In all experiments reported here the maximum number of food units per patch is set to ten.

The population of fish eggs is included to provide another step towards a more realistic simulation; however, all major results listed here exhibit LV like oscillations. The majority of experiments are run with a baseline model from which any experimental deviations are made. As with classic LV oscillations of Figure 1, ABM models are inherently volatile where certain parameter settings can be adjusted to emphasize or de-emphasize certain system behavior and produce a desirable system from which to experiment. This allows us to compare results under the following settings to produce desired scenarios, such as:

(i) Stable model
(ii) Oscillating-but stable model
(iii) Unstable model

as well as expose which settings produce each.

4.2 LVM (3+3) Model Details

In this paper we focus on a specific 3+3 model with:

$$X = [X_1, X_2, X_3, X_4, X_5, X_6]^T \quad (18)$$

where the first three vector components are preys and the last three are predators. We assume that each predator preys on each prey but not on each other. The preys are not affecting each other. The community matrix is then:

$$A(t,X) = \quad (19)$$

a_{11}	0	0	0	0	0
0	a_{22}	0	0	0	0
0	0	a_{33}	0	0	0
a_{41}	a_{42}	a_{43}	a_{44}	0	0
a_{51}	a_{51}	a_{53}	0	a_{55}	0
a_{61}	a_{62}	a_{63}	0	0	a_{66}

where the community matrix main diagonal coefficients are:

$$a_{ii}(t,X) = A_i(t,X_i) + A_{ii}(t,X_i)\, X_i \text{ , } i=1,2,3,4,5,6 \quad (20)$$

and off diagonal (lower left corner) coefficients are:

$$a_{ik}(t,X) = A_{ik}X_i \quad i=4,5,6 \text{ and } k=1,2,3 \quad (21)$$

Typically A_{ii} are positive (crowding effect), or it could be 0 for the predators X_4,X_5, and X_6. The A_{ik} are negative, and A_i could be positive or negative, depending on what we want to simulate. To illustrate the ABM model behavior, some initial values for various prey/predator parameters were chosen. In this example prey species are represented by three fish populations, i.e. X_1, X_2, and X_3. The predators are fish eating species (dolphins, sharks).

4.3 NetLogo ABM (3+3) Stable Model Simulation

To set the scene, we use NetLogo modeling and have Figure 3 which shows initial (left) and final (right) prey/predator distribution in a certain area after a number of simulation turns. The following Figures show more details for this generic oscillatory model between preys and predators. Figure 4 shows cumulative count of predators and prays (fish in this

simulation) which exhibits general LVM type of equations oscillatory behavior (such as Figure 1) confirming LVM validity in general. Figure 5 shows more details on three types of predators, and similarly Figure 6 has the counts for three types of prays. They all indicate typical oscillatory behavior between number of preys and predators. This corresponds to community matrix in (19) which indicates how species interact in general. In Figure 7 we have an indication of number of fish eggs which "produce" fish in simulation, as well as number of fish and predators. Figure 8 summarizes predators elimination rate set by the ABM model. Finally, Figure 9 indicates preys consumption rate by predators. All of these parameters can be set in NetLogo ABM control window (Figure 2).

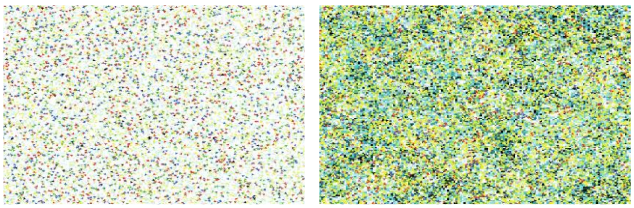

Figure 3. Initial and Final Prey/Predator Distribution

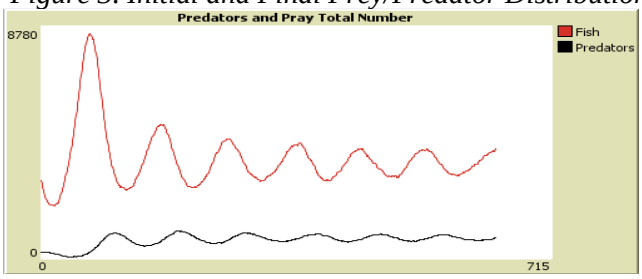

Figure 4. Total 3 predators and 3 preys count

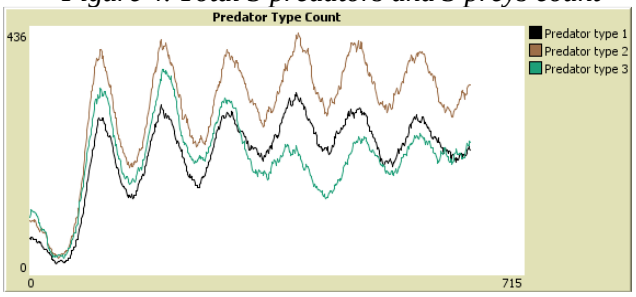

Figure 5. Detailed three predators count

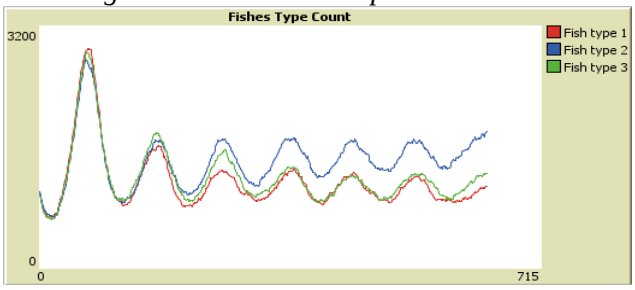

Figure 6. Detailed three preys count

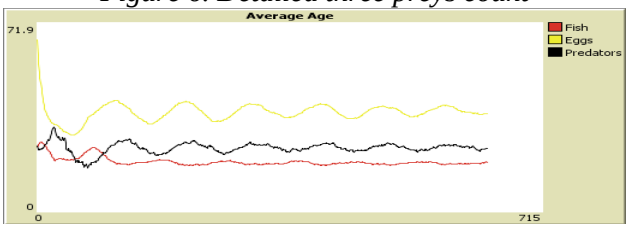

Figure 7. Eggs, fish and predator numbers

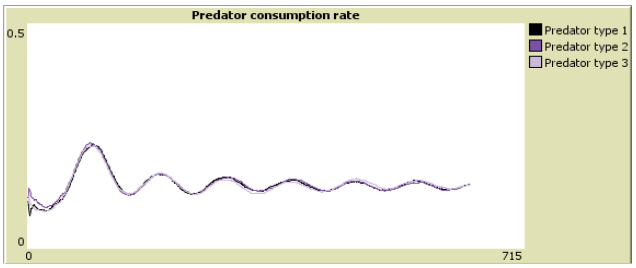

Figure 8. Predators eliminating rate

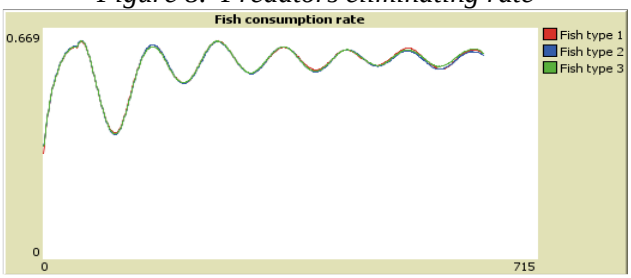

Figure 9. Preys consumption rate by predators

Next two Figures, 10 and 11, indicate parameters used to generate Figures 5-9 using NetLogo simulation control window. One can set many different parameters and create very complex ABM model. This is an advantage of ABM compareed to simpler mathematical LVM. On the flip side, we have no essential insight into what is happening "inside" ABM, whereas we do with LVM. Their combination, our Dual Approach, may be a winning strategy in general. Figure 10 shows rate of food consumption by fish population, and Figure 11 rate of fish consumption by predators.

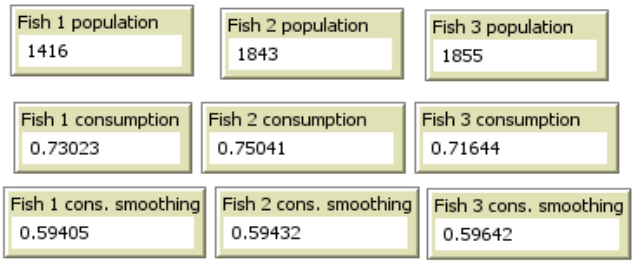

Figure 10. Rate of food consumption by fish population

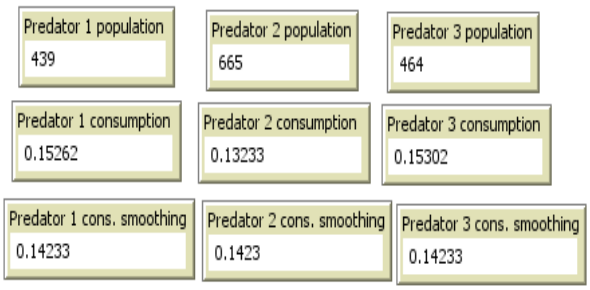

Figure 11. Rate of fish consumption by predators

4.4 NetLogo ABM (3+3) Unstable Model Simulation

One of the key features of predators-prey system is its stability properties. In the next set of Figures we have predator and prey numbers for an unstable system.

Example 1. In Figures 12 and 13 we have a summary of parameters used to generate unstable system of Figure 14. At first it appears as if the system is stable.

When we look into specific prey numbers shown in Figure 15, we see that one of the prey species indeed goes into instability, i.e. its numbers are rising steadily. One prey species is unstable and two are stable. That is hidden in Figure 14 which shows total prey and predator numbers.

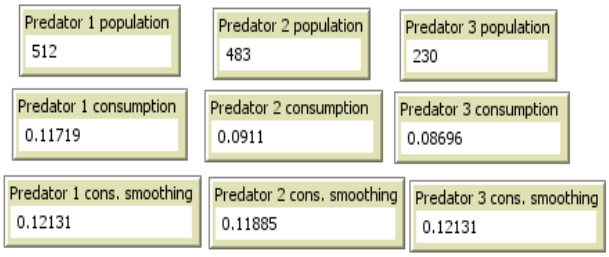

Figure 12. Unstable system predator parameters

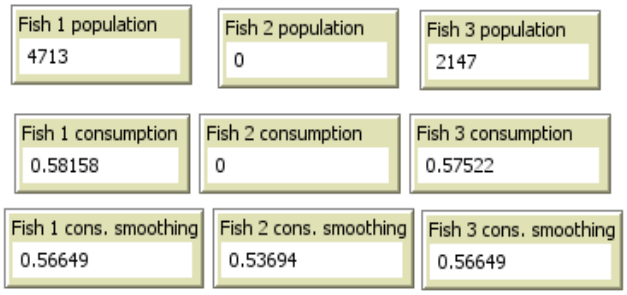

Figure 13. Unstable system pray parameters

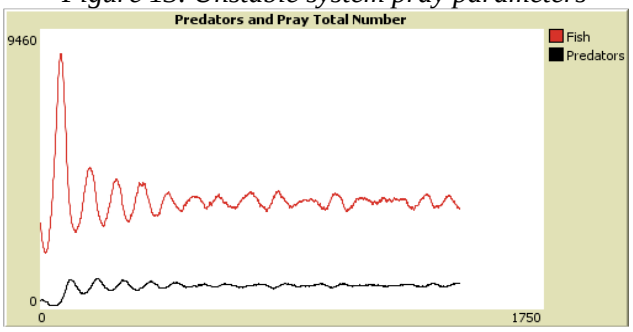

Figure 14. Unstable predator-prey system

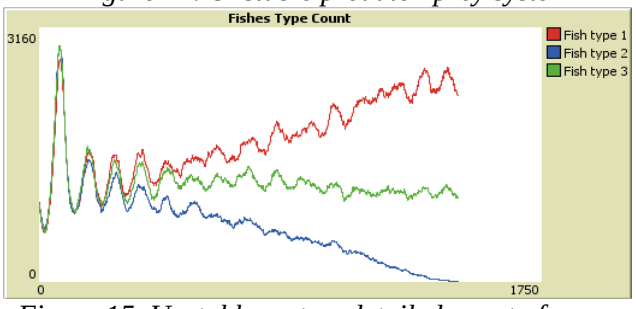

Figure 15. Unstable system detailed count of preys

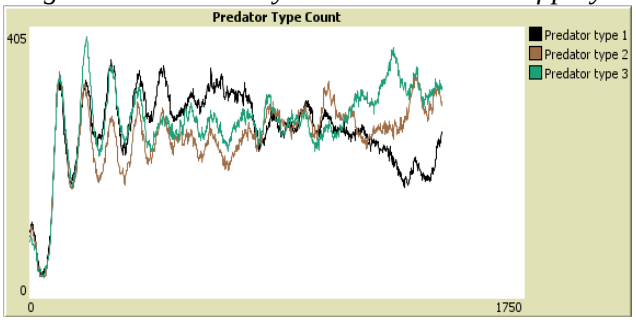

Figure 16. Unstable system detailed count of predators

Finally, in Figures 17 and 18 we summarize predators elimination rate and preys consumption by predators rate, respectively, for the unstable system. All figures in Example 1 indicate how various ABM features can be set and played With. Eventually in our follow up work we will use this for the benefit of LVM model, in particular to fine tune various Community Matrix parameters. As the number of species and complexity of the models grow this will be important to get reliable and predictable mathematically tractable LVM formulas.

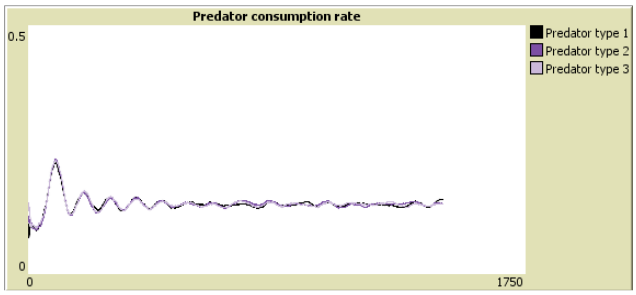

Figure 17. Predators elimination rate, unstable system

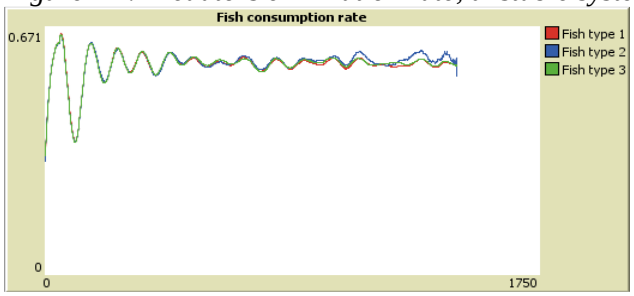

Figure 18. Preys consumption rate by predators

Example 2. In this example number of preys and predators are changed, as well as other parameters, per Figure 19. All other figures grouped together into Figure 20 summarize various details similar as in Example 1.

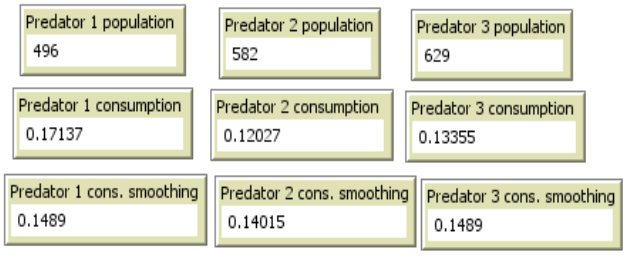

Figure 19. Unstable system predator parameters

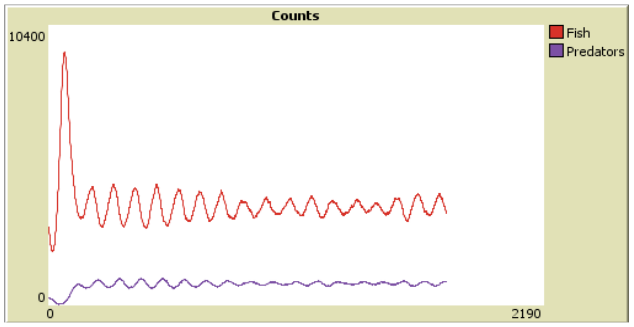

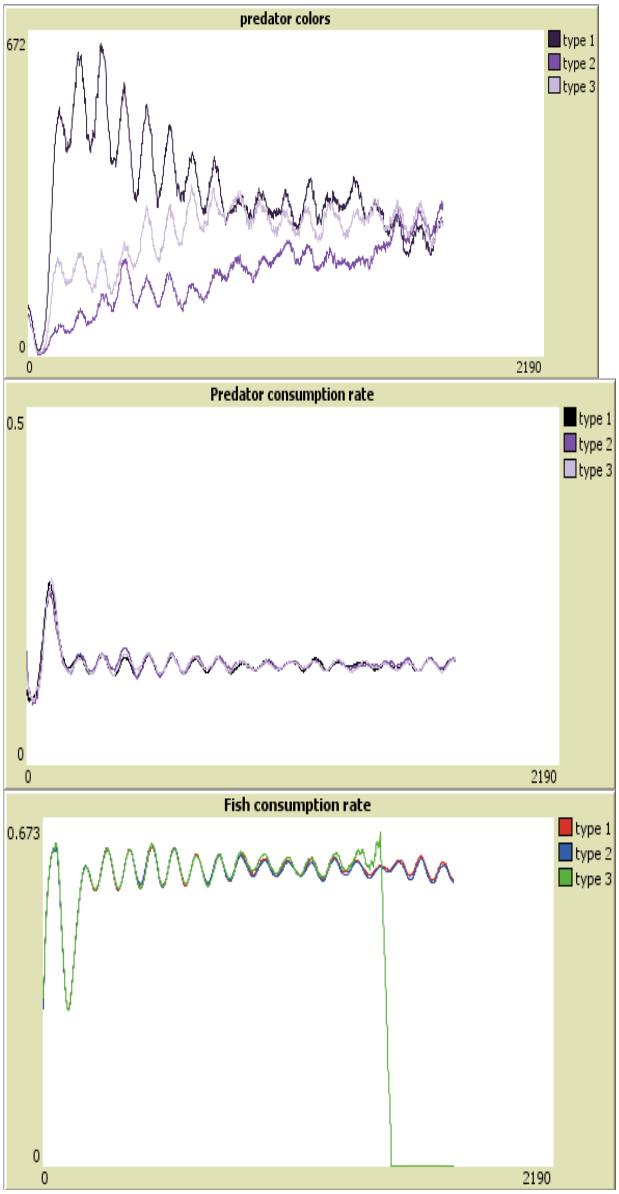

Figures 20. Results for Example 2 unstable system

We conclude Example 2 with Figure 21 which has average age of preys, predators and "eggs" which "produce" preys.

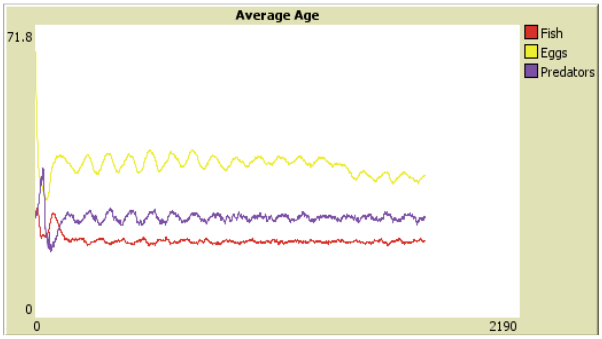

Figures 21. Example 2 average age, preys, predators

5. CONCLUSION

In this paper we continue research started in [1] on dual model approach for complex predator-prey models. We present Single Prey Single Predator as well as Multiple Prey Multiple Predator LVM models. ABM simulation using NetLogo environment illustrates three predator-prey examples, one stable and oscillatory, the other two unstable with different count of 3+3 species involved. Our main goal is to show how ABM can mimic LVM formulas which allows to fine tune LVM. ABM can produce very complex simulations. On the other hand, LVM, which is based on mathematical equations models predator-prey behavior via its Community Matrix with certain number of elements. In this paper we used 6 species which results in 6x6=36 parameters. Typically not all the species are connected hence there are less than 36 parameters to consider. Once we establish reliable ABM, we can use it to fine tune these LVM parameters. With this paper we made another step in that direction with building complex ABM. This approach aims to produce results which can be used in practical ecological problems, and potentially assist in better understanding of classic multi-species issues, as (i) Paradox of the Plankton and of the Enrichment, (ii) Oksanen's description and tropic levels, and other general paradigms such as (iii) Adaptivity and (iv) Emergence.

6. REFERENCES

[1] M. Hodzic at all, Dual Approach to Complex Ecological Dynamic System Modeling and Control, INASE MMSSE 2015, Volume 42, Edited by N. Mastorakis, P.A. Pardalos, R. P. Agarwal, Vienna, Austria, March 16-18, 2015.

[2] D. D. Siljak, Large–Scale Dynamic Systems, Stability Structure, North Holland, New York, 1978.

[3] M. I. Hodzic, "Some Extensions to Classic Lotka - Volterra Modeling For Predator Prey Applications", SEJSC, Vol. 3/1, 2014.

[4] A. I. Zecevic and D. D. Siljak, Control of Complex Systems, Structural Constraints and Uncertainty, Springer, Berlin, 2010.

[5] M. I. Hodzic, Estimation of Large Sparse Systems, Chapter 3, Stochastic Large-Scale Engineering Systems, edited by Spyros G. Tzafestas, and Keigo Watanabe, Marcel Dekker, N. York, 1992.

[6] M. I. Hodzic, R. Krtolica and D. D. Siljak, A Stochastic Inclusion Principle, Chapter 30, Differential Equations, Stability and Control, Edited by Saber Elaydi, Marcel Dekker, New York, 1991.

[7] D. D. Siljak, Decentralized Control of Complex Systems, Academic Press, San Diego, 1991.

[8] M. Hadzikadic, T. Carmichael and C. Curtin, "Complex Adaptive Systems and Game Theory: An Unlikely Union", Wiley, 2010.